Centre for Maintenance Optimization & Reliability Engineering

Director

Chi-Guhn Lee

Semi-annual report

June 2022

Mechanical & Industrial Engineering
UNIVERSITY OF TORONTO

cmore.mie.utoronto.ca | 416·946·7867

Table of Contents

C-MORE progress meeting agenda

Thursday June 9, 2022

Opening remarks, executive summary 9:00-9:30		Chi-Guhn Lee
Member presentation UK MOD DSTL		
9:30-10:00	Designing in-service support to meet multi-dimensional requirements	Tim Jefferis
10:00-10:15	15-minute break	
KPI featured cluster		
10:15-10:35	Eliminate the Communication Gaps: A Holistic Approach to Developing KPIs within the Mining Industry	Blair Cui Beishi He Gabriel Merisanu
10:35-10:55	Dashboard design for KPIs in maintenance and operations	Ariana Duan Hamza Garib
10:55-11:10	15-minute break	
Collaborations with industry partners		
11:10-11:30	Physical Asset Management (PAM): An Economical Asset Replacement Problem for Mining Industry	Sean He
11:30-11:50	A reinforcement learning approach for maintenance of multi-unit systems: Kinross fleet case study	Vahid Najafi
11:50-12:35	45-minute break	
12:35-12:55	TTC: Ongoing updates to NDT projects	Janet Lam
12:55-1:15	Fault Detection for Wind Turbine Under Varying Operational Conditions.	Mohamed Hassan
1:15-1:30	15-minute break	
1:30-2:15	An Encoder-Decoder Perspective of Deep Learning	Scott Sanner
2:15-2:30	15-minute break	
Student research projects		
2:30-2:50	Predictive Quality Assessment for 3D Printing	Katie Xu
2:50-3:10	Time Series Classification for Combustion Analysis in Freight Fires	Sophie Tian
3:15-3:30	Adversarial perturbation based latent reconstruction for domain-agnostic self-supervised learning	Kuilin Chen
Closing remarks		Chi-Guhn Lee

Executive summary

Chi-Guhn Lee, C-MORE Director

Introduction

We are now working seamlessly in both real and virtual worlds. In effect, C-MORE has become a hybrid entity, with a foot in two worlds and capitalizing on the benefits of both. Among other things, our consortium members have benefited from more frequent and logistically simpler status updates made possible by our online presence. As conferences return to pre-pandemic and hybrid modes, C-MORE is continuing to participate virtually while taking steps towards in-person participation in local conferences, such as MainTrain. Our next PAM2 course, scheduled for June 20-24, will be delivered online; another is planned for international audiences later this summer. In short, our online proficiency will continue to complement our work and research at C-MORE well into the future.

The past six months have featured work as usual. We have continued to seek opportunities to leverage our work with external funding. For example, we recently submitted a proposal to the Ministry of Transportation of Ontario's Highway Infrastructure Innovations Funding Program. Outreach is another major focus. We are seeking new collaborators at multiple levels. C-MORE was a featured research group at the University of Toronto's Engineering Research Day. Having a booth at this event enabled us to network with future students and other researchers in the community with whom we may work in the future. Beyond our ongoing work with consortium members, TTC, DSTL, and Kinross Gold, we have engaged with industry partners on an ad-hoc basis, including Titan Technologies and Unilever. Last, but by no means least, we have discussed possible collaboration and/or shared the C-MORE portfolio with a number of interested companies. Research is obviously a main thrust of our work, and this too is business as usual. The June meeting will feature some of what we've been doing, including Tim Jefferis's (DSTL) work on designing in-service support to meet multi-dimensional requirements and research on KPIs conducted with Vatsal Agarwal (Kinross). The remainder of the executive summary gives more details of C-MORE's recent work, with attention to individual contributors. More information on individual projects is provided in the main body of the Report.

The C-MORE team

Chi-Guhn Lee, Director
In the past six months, Chi Guhn has supervised a large research group of 31, including 2 post-doctoral fellows and 29 graduate students (10 PhD, 5 MASc, and 14 MEng students). He has also worked with international partners: Professor Lee at KAIST in South Korea on multi-agent reinforcement learning and Professor Subimal at IIT-Bombay in India on an irrigation management problem. Due to the pandemic travel restrictions, the international collaboration was exclusively online. As always, he has worked with international partners via C-MORE. In particular, the Centre completed a project with the Technical University of Denmark (DTU) on a maintenance workload forecasting problem, and he served as an external examiner of a PhD student participating in the collaboration at DTU. Since the last progress meeting, his main focus has been teaching and research.

Janet Lam, Assistant Director
Janet has been working with graduate and undergraduate students to push on with various industry-sponsored research projects. In particular, she worked with Gabe, Blair, and Beishi on the mining KPIs project. She is now working with summer interns on a project to generate synthetic data to support the mining KPIs project. She worked directly with Jennifer Lu and Farhan Wadia from TTC on extensions and updates to the TTC track inspection projects. Janet met virtually with several potential collaborators to discuss ways to combine forces, and she renewed contact with current members to keep projects fresh. She will be teaching one day of the 5-day Physical Asset Management 2 course, with Chi-Guhn, Ali and Jim Reyes-Picknell in June, and she presented a talk at MainTrain, the annual conference by PEMAC.

Andrew K. S. Jardine, Professor Emeritus
Andrew's main activities during the past six months have been serving as an external examiner for a doctoral thesis at the University of Queensland, Australia and evaluating an academic promotion submission at the University of Portsmouth, England. In addition, he taught an on-line graduate class at University of the West Indies, Trinidad and Tobago and continued his participation as a member of PEMAC's Awards Committee.

Dragan Banjevic, C-MORE Consultant
Dragan continued to collaborate with C-MORE on projects with consortium members, mostly with Kinross Gold, TTC, and DSTL. He also provided help in other projects with C-MORE students, as well as in their research.

Fae Azhari, University of Toronto
Fae's research group now consists of four doctoral students, three MASc students, and two undergraduate students. Her group works on a range of projects in the field of structural health monitoring and smart materials. Her students have submitted/published nine journal and conference papers in the past year.

Scott Sanner, University of Toronto
Scott's research group continued work on a range of applied projects covering data-driven control systems with particular emphasis in the past six months on multi-intersection traffic signal control; a number of papers are currently under review or in preparation. Scott's group also continued fundamental AI research on the topics of optimal sequential decision-making, leveraging recent computational architectures for deep learning (two conference papers published at AAAI-22), recommender systems (conference papers published at WWW-22 and SIGIR-22),

semantic type safety in data science (conference paper published at RCIS-22), and conditional inference in generative deep learning models (journal article accepted by *Machine Learning Journal*).

Jue Wang, Affiliate Professor
Since March, Jue has been working on a new paper about actively learning to balance the performance and deterioration of system under dynamic environment and condition monitoring. The idea is to adjust the workload or stress of the system in real time while learning about the deterioration rate under different workloads. This paper is close to completion and will be submitted in the summer. Roozbeh Yousefi, a PhD student under Jue's supervision at Smith School of Business, successfully defended his PhD thesis on optimal control of stochastic system with applications in revenue management and online learning.

Ali Zuashkiani, Director of Educational Programs
Ali has continued to provide consulting services to various industries, including oil and gas, power generation and distribution, mining, and petrochemical, and to teach courses all over the Middle East. He remains an excellent international ambassador for C-MORE.

C-MORE graduate students and postdoctoral fellows

Postdoctoral fellows
Danial Khorasanian started his postdoctoral fellowship in the Department of Mechanical and Industrial Engineering in September 2021. His main research interest is dynamic routing in the transportation of hazardous materials. He is presently co-leading a group of MEng students in a project in cooperation with Unilever. The Unilever project is in the areas of forecasting and supply chain management.

Doctoral students
Mohamed Abubakr is a first-year PhD student whose primary interest is domain adaptation for continuously evolving environments, with a current focus on failure detection under varying operating conditions.

Kuilin Chen is a fourth-year PhD student. His current research interests are few-shot learning and representation learning. He submitted two papers on representation learning to NeruIPS 2022.

Michael Gimelfarb continued his work on knowledge transfer in reinforcement learning and has been a postgraduate affiliate of the Vector Institute since April 2020. His research focuses on transferring skills robustly and safely in a risk-aware setting. His current work leverages robust and risk sensitive MDPs, representation learning and planning under uncertainty.

Scott Koshman continued his research on equipment health monitoring (EHM) for Halifax Class Frigates, under the supervision of Fae Azhari. His recent focus has been data conditioning, the optimum application of parallel assets to the analysis of large datasets (40+ billion transactions), and the fusion of data across databases. He works with data from diverse sources including EHM systems, an ERP, internal reporting, and external public environmental data. This research will inform approaches for the development of maintenance optimization models given certain types of imperfect data inputs. In his workplace, he has been the lead in the development of graduate courses and the transition to a virtual delivery model in global strategic security studies.

Yang Li is currently working towards his PhD with the school of Mechanical Engineering, Southeast University, Nanjing, China, and is a visiting doctoral student in Mechanical and Industrial Engineering, University of Toronto. His main research interests are intelligent monitoring and fault diagnosis, artificial intelligence, and acoustic emission signal processing. He is working on the application of deep learning in fault diagnosis of hoisting machinery.

Seyedvahid (Vahid) Najafi is a PhD student under the supervision of Chi-Guhn Lee and is focused on developing reinforcement learning algorithms to solve large-scale asset management problems. He recently proposed an optimal policy for joint optimization of inspection intervals and maintenance actions of a hydroelectric plant and is extending the model to deal with more complex systems. Before joining the University of Toronto, Vahid worked as a project management officer and business analyst in telecommunication and logistics companies.

Avi Sokol is a flex-time doctoral student and a full-time employee. Avi continues to research the integration of reinforcement learning and inventory control to reduce waste in supply chains and the benefits of reward decomposition. He recently applied reward decomposition in Q-learning and SARSA models to solve inventory control problems. Both models produced the expected results and converged to the near-optimal solution. Avi is currently exploring the application of reward decomposition in deep Q-learning models.

Baoxiang Wang is a fourth year doctoral candidate in Mechanical Engineering and is working on the fault diagnosis of rolling bearings. Her research focuses on the exploration of new algorithms or the improvement of existing algorithms to extract fault features caused by bearing defects. She is currently studying the application of the sparse representation algorithm in bearing fault diagnosis.

Master's students

Xiangzi Chen is an MEng student in Mechanical and Industrial Engineering with an emphasis on data analytics. She is currently working on the dynamic safe routing for the transportation of hazardous materials and aims to develop a dynamic routing solution that can minimize the travel time and also reduce the risk during transportation.

Blair Cui is an MEng student in Mechanical and Industrial Engineering with an emphasis on data analytics and healthcare engineering. She is currently working on the development of KPIs for a project in the mining sector. Her work is focused on evaluating the factors affecting maintenance effectiveness and verifying the KPIs' appropriateness for mining using machine learning models.

Beishi He is a first-year MEng student in Mechanical and Industrial Engineering, with an emphasis on data analytics. Her research focuses on the design of a new KPI framework for the mining industry. She aims to figure out the KPIs relevant for each core functional group and deliver data-driven insights through machine learning models.

Sean He is an MEng student in Mechanical and Industrial Engineering, with an emphasis on data analytics. He has two+ years of professional experience in the financial industry. He is working on a project with Kinross Gold Corporation to develop a model to determine the optimal economic life of various mining equipment and determine when such assets need to be replaced.

Gabriel Merisanu is a first-year MEng student in Mechanical and Industrial Engineering, with an emphasis on data science and ELITE. With three years of professional experience in consulting and project management, Gabriel is passionate about leveraging his past industry

knowledge while exploring greater meaning within his career and the overall positive impact engineering can have on society at large. Gabriel's research is primarily focused on developing a new KPI framework and toolset to bridge the communication gaps between maintenance teams and strategic leadership within the mining industry. Given his experience in consulting and his passion for management, Gabriel is focused on delivering end-to-end solutions that successfully integrate technology and human factors. In September 2022, Gabriel will be joining Guidehouse as a consultant on the Energy, Sustainability and Infrastructure team.

Dhavalkumar (Dhaval) Patel started his MEng program in the Department of Mechanical and Industrial Engineering in September 2021. Dhaval's work at C-MORE is focused on the exploration and application of machine learning algorithms for predictive maintenance. He is currently working on a hybrid prognostic framework for modelling a stochastic degradation process with a deep learning-driven trajectory.

Hazel Shi is a first-year MEng student in Mechanical and Industrial Engineering, with an emphasis on data analytics. She is currently working on the toy signal generation for a machine learning model to detect the faulty state of wind turbine bearings.

Rutvik Solanki is pursuing his MEng with an emphasis on ELITE. Before starting his graduate studies, he worked as a business analyst at Vedanta Resources Ltd, stationed at the Hindustan Zinc head office. Rutvik's work is mainly focused on developing a machine learning-backed data-driven business intelligence dashboard that caters to maintenance managers, operational leaders, and senior management, with a major focus on reliability.

Sophie Tian is a second-year MASc student working on the combustion signature analysis project in collaboration with NRC. She has been applying time series classification and augmentation methods to the combustion signature dataset and aims to submit a paper to a decision support related journal in the next few months. In addition, Sophie has been working with Kuilin on proposing an adversarial perturbation-based domain-agnostic self-supervised learning method; they submitted a paper to NeurIPS 2022.

Katie Xu is a second-year MASc student working on the use of machine learning for process monitoring and control in 3D printing. Since the meeting in December 2021, she has finished data collection and is working on building machine learning models for predictive quality assessment of 3D printed parts.

C-MORE activities with consortium members

Defence Science and Technology Laboratory (DSTL)
Tim Jefferis took an interest in the KPI projects presented at the December 2021 meeting and has joined the project as one of the advisors. He will be making a presentation at the June meeting on designing in-service support to meet multi-dimensional requirements.

Kinross Gold Corporation
Vatsal Agarwal from Kinross has been working closely with C-MORE on several projects. In one project, Sean He began to develop a model that defines the optimal life of an asset, incorporating many different variables. In another, Vahid Najafi incorporated a model for selecting optimal components to be replaced together under a constrained budget at a company-wide level as part of his PhD thesis. Vatsal has also provided tremendous support to our KPI teams, looking for non-

financial KPIs and other trackers for the KPI cluster. All of these projects will be presented at the June meeting.

Toronto Transit Commission (TTC)
TTC discussed the potential of independently computing the linetest interval updates by learning the methods used in the reports presented to date. Together with C-MORE, TTC explored the possibility of computing re-inspection intervals for defects disaggregated by failure mode and defect priority. We worked on harmonizing the definition of some priority levels, as they have changed in the recent past. C-MORE's relationship with the TTC was recently highlighted in a faculty-wide newsletter; the NDT linetest project was the project of interest.

C-MORE educational programs

In the past six months, education has continued to represent one of the main pillars of C-MORE. We are taking advantage of the possibilities inherent to online instruction while gradually opening up in-person learning.

April 7: Chi-Guhn presented a seminar on machine learning for the Gwangju Institute of Science and Technology (GIST) graduate seminar series

March 5-6, April 2-3: Andrew Jardine taught MENG6704: Maintenance Analysis and Optimization at the University of the West Indies. This course was delivered online

June 20-24: A one-week course titled Machine Learning and Artificial Intelligence Applications in Physical Asset Management (PAM2) will be offered through the School of Continuing Studies at the University of Toronto. Chi-Guhn Lee, Janet Lam, Ali Zuashkiani, and James Reyes-Picknell will form the teaching team.

Ongoing: Ali Zuashkiani continues to offer courses throughout the Middle East region.

Summer 2022: Another PAM2 course is planned for international audiences in summer 2022.

Conclusion

Although this Report is supposed to deal only with the past six months, and even though our "new normal" is so normal that it seems not worth mentioning, I want to take a moment to reflect and thank everyone. At this point, two years into the pandemic, we may start to forget precisely what we have accomplished since 2020. All of us at C-MORE – industry collaborators, staff and academics, students, and collaborating researchers – are now working effortlessly in both the actual and the virtual worlds. As I review the past two years, I think the pandemic presented an opportunity to broaden our methods of collaboration, and as time goes on, we will continue to pursue alternative methods in our instruction, formal and informal meetings, informal get-togethers, and conference presentations. Thank you, one and all. It continues to be an honour and a pleasure to work with you!

Chi-Guhn Lee

June 2022

C-MORE leadership activities

Chi-Guhn Lee, Director

In the past six months I have supervised a large research group of 31 including 2 post-doctoral fellows and total of 29 graduate students (10 PhD, 5 MASc, and 14 M.Eng students). I have also worked with international partners. Professor Lee at KAIST of South Korea on multi-agent reinforcement learning and Professor Subimal at IIT-Bombay of India on irrigation management problem. Due to the travel restriction during the pandemic, the international collaboration has been done exclusively online. I have also worked with international partner via C-MORE. In particular, the centre has completed a project with DTU on maintenance workload forecasting problem and I served as an external examiner of a PhD student participating in the collaboration at DTU. Since the last progress meeting, my main focus has been teaching and research.

Janet Lam, Assistant Director

Janet has been working with graduate and undergraduate students to push on with various industry-sponsored research projects. In particular, she worked with Gabe, Blair and Beishi on the Mining KPIs project. She is now working with summer interns on a project to generate synthetic data to support the Mining KPIs project. She worked directly with Jennifer Lu and Farhan Wadia from TTC on extensions and updates to the TTC track inspection projects.

She met virtually with several potential collaborators to discuss ways to combine forces, as well as renewed contact with current members to keep projects fresh.

She will be teaching one day of the 5-day Physical Asset Management 2 course, with Chi-Guhn, Ali and Jim Reyes-Picknell in June. She presented a talk at MainTrain, the annual conference by PEMAC.

Andrew K. S. Jardine, Professor Emeritus

Andrew's main activities during the past six months have been serving as an external examiner for a doctoral thesis at the University of Queensland, Australia and evaluating an academic promotion submission at the University of Portsmouth, England.

In addition, he taught an on-line graduate class at University of the West Indies, Trinidad and Tobago and continued his participation as a member of PEMAC's Awards Committee.

Dragan Banjevic, C-MORE Consultant

Dragan continued to collaborate with C-MORE on projects with consortium members, mostly with Kinross Gold, TTC, and UKMOD. He also provided help in other projects with C-MORE students, as well as in their research.

Fae Azhari, University of Toronto

Fae's research group now consists of 4 doctoral students, 3 MASc students, and 2 undergraduate students. Her group works on a range of projects in the field of structural health monitoring and smart materials. Her students have submitted/published 9 journal and conference papers in the past year.

Scott Sanner, University of Toronto

Scott's research group continues work on a range of applied projects covering data-driven control systems with particular emphasis in the past six months on multi-intersection traffic signal control with a number of papers currently under review or in preparation. Scott's group also continues fundamental AI research on the topics of optimal sequential decision-making leveraging recent computational architectures for deep learning (two conference papers published at AAAI-22), recommender systems (conference papers published at WWW-22 and SIGIR-22), semantic type safety in data science (conference paper published at RCIS-22), and conditional inference in generative deep learning models (journal article accepted at the Machine Learning Journal).

Jue Wang, Affiliate Professor

Since March, Jue is working on a new paper about actively learning to balance the performance and deterioration of system under dynamic environment and condition monitoring. The idea is to adjust the workload or stress of the system in real time while learning about the deterioration rate under different workloads. This paper is close to completion and will be submitted in the summer.

Roozbeh Yousefi, a PhD student under Jue's supervision at Smith School of Business, has successfully defended his PhD thesis on optimal control of stochastic system with applications in revenue management and online learning.

Ali Zuashkiani, Director of Educational Programs

Ali has continued to provide consulting services to various industries, including oil and gas, power generation and distribution, mining, and petrochemical, and to teach courses all over the Middle East. He remains an excellent international ambassador for C-MORE.

Overall project direction

Janet Lam, Assistant director

Goals and retrospectives

This section highlights the some of the main achievements in C-MORE for the period January 2022 – June 2022. The C-MORE team has embraced the changes emerging from the pandemic; the paradigm shift of virtual meetings has lowered the barrier to meetings. Our consortium members have benefited from more frequent and logistically simpler status updates.

As conferences return to pre-pandemic and hybrid modes, C-MORE is taking steps towards in-person participation in local conferences, such as MainTrain. Our next PAM2 course is scheduled for June 20-24, to be delivered online. Another is planned for international audiences later this summer.

We continue to seek opportunities to leverage our work with external funding. We submitted a proposal to the Ministry of Transportation of Ontario's Highway Infrastructure Innovations Funding Program.

Beyond our continuous work with consortium members, we have engaged with other industry partners on an ad-hoc basis, including Titan Technologies.

Activities

Collaboration with companies and site visits

This section gives details on progress in research conducted with consortium members

Member	Collaborations
Defence Science and Technology Laboratory	Tim Jefferis took an interest in the KPI projects that were presented in the December 2021 meeting, and have joined the project as one of the advisors for the project. He will be making a presentation on Designing in-service support to meet multi-dimensional requirements.
Kinross	Vatsal Agarwal from Kinross has been working closely with C-MORE on several projects, which will all be featured today.

Member	Collaborations
	Sean He began a project to develop a model that defines the optimal life of an asset, incorporating many different variables. Vahid Najafi incorporated a model for selecting optimal components to be replaced together under a constrained budget at a company-wide level as part of his Ph.D. thesis. Vatsal has provided tremendous support to our KPI teams, looking for non-financial KPIs and other trackers for the KPI cluster. All of these projects will be presented today.
Toronto Transit Commission	TTC discussed the potential of independently computing the linetest interval updates, by learning the methods used in the reports presented to date. We explored the possibility of computing re-inspection intervals for defects disaggregated by failure mode and defect priority. We worked on harmonizing the definition of some priority levels, as they have changed in the recent past.

Theoretical work

This section on theoretical work is oriented toward students' and postdoctoral fellows' research topics.

Name	Activity
Mohamed Abubakr, Ph.D. student	Mohamed is a first year PhD student. His current research interest is domain adaptation for continuously evolving environments with focus on failure detection under varying operating conditions.
Kuilin Chen, Ph.D. candidate	Kuilin is a fourth-year Ph.D. student. His current research interest is few-shot learning and representation learning. He submitted two papers on representation learning to NeruIPS 2022.
Xiangzi Chen, M.Eng student	Xiangzi is an M.Eng student in Mechanical and Industrial engineering with an emphasis in data analytics. She is currently working on the dynamic safe routing for hazardous materials transportation and aims to develop a dynamic routing solution that can minimize the travel time and, in the meantime, reduce the risk during the transportation.
Blair Cui, M.Eng. student	Blair is an M.Eng student in Mechanical and Industrial Engineering program with an emphasis in data analytics and healthcare engineering. She is currently working on development of KPI (Key Performance Indicator) for mining sector project. Her work is focused on evaluating the factors affecting the maintenance effectiveness and verify the indicators' appropriateness for mining industries through machine learning models.
Michael Gimelfarb, Ph.D. candidate	Michael has continued his doctoral work on knowledge transfer in reinforcement learning and has been a postgraduate affiliate of the Vector Institute since April 2020

Name	Activity
Beishi He, M.Eng student	Blair is an M.Eng student in Mechanical and Industrial Engineering program with an emphasis in data analytics and healthcare engineering. She is currently working on development of KPI (Key Performance Indicator) for mining sector project. Her work is focused on evaluating the factors affecting the maintenance effectiveness and verify the indicators' appropriateness for mining industries through machine learning models.
Sean He, M.Eng student	Sean is a M.Eng student in Mechanical and Industrial engineering with emphasis in data analytics. He has two+ years of professional experience in the financial industry. He is working on a project with Kinross Gold Corporation to develop a model to determine the optimal economic life of various mining equipment and find out when such assets need to be replaced.
Scott Koshman, Ph.D. student	Scott continues his research on equipment health monitoring (EHM) for Halifax Class Frigates, under the supervision of Professor Fae Azhari
Danial Khorasanian, postdoctoral fellow	Danial Khorasanian has started his postdoc in MIE department of UofT since Sep 2021. His main research is about dynamic routing in hazardous materials transportation. He is also co-leading a group of M.Eng students in a project in cooperation Unilever company. The Unilever project is in the areas of forecasting and supply chain management.
Yang Li, visiting Ph.D. student	Yang Li is currently working toward the Ph.D. degree with the school of Mechanical Engineering, Southeast University, Nanjing, China. And he is also as a visiting PhD. Student in the Department of Engineering Mechanical & Industrial Engineering, University of Toronto, St. George, Canada. His main research interests are intelligent monitoring and fault diagnosis, artificial intelligence and acoustic emission signal processing. He is working on the application of deep learning in fault diagnosis of hoisting machinery.
Gabriel Merisanu, M.Eng student	Gabriel is a first year M.Eng student in Mechanical and Industrial Engineering pursuing an emphasis in Data Science and ELITE. With 3 years of professional experience in consulting and project management, Gabriel is passionate about leveraging this past industry knowledge while exploring greater meaning within his career and the overall positive impact engineering can have on society at large. Gabriel's research is primarily focused on developing a new KPI framework and toolset used to bridge the communication gaps between maintenance teams and strategic leadership within the mining industry. Due to his experience in consulting and passion for management, Gabriel is focused on delivering end-to-end solutions that successfully integrate technology and human factors. As of September 2022, Gabriel will be joining Guidehouse as a Consultant within the Energy, Sustainability and Infrastructure team.

Name	Activity
Seyedvahid Najafi, Ph.D. student	Vahid is a Ph.D. student under the supervision of Professor Chi-Guhn Lee and is focused on developing reinforcement learning algorithms to solve large-scale asset management problems. He proposed an optimal policy for joint optimization of inspection intervals and maintenance actions of a hydroelectric plant and is extending the model to deal with more complex systems. Before joining the University of Toronto, Vahid worked as a project management officer and business analyst in telecommunication and logistics companies.
Dhavalkumar Patel, M.Eng. student	Dhaval started his M.Eng program in the Department of Mechanical and Industrial Engineering in September 2021. Dhaval's work at the centre is focused on the exploration and application of Machine Learning algorithms for predictive maintenance. Currently, he is working on the hybrid prognostic framework for modeling stochastic degradation process with deep learning driven trajectory.
Hazel Shi, M.Eng. student	Hazel is a first year M.Eng student in Mechanical and Industrial Engineering with emphasis in data analytics. She is currently working on the toy signal generation for the machine learning model to detect the faulty state of wind turbine bearings.
Avi Sokol, Ph.D. student	As a flex-time Ph.D. student and a full-time employee, Avi continues to research integration of Reinforcement Learning and Inventory Control to reduce waste in supply chains and the benefits of Reward Decomposition. Avi applied Reward Decomposition in Q-learning and SARSA models to solve Inventory Control problems. Both models produced the expected results and converged to the near-optimal solution. Currently Avi explores the application of Reward Decomposition in Deep Q-Learning models. In the past 6 months Avi passed his qualifying exam and is expected to have first annual meeting in the beginning of 2021.
Rutvik Solanki, M.Eng student	Rutvik is a graduate student pursuing a Master of Engineering alongwith and ELITE Emphasis. Before starting grad studies, he worked as a Business Analyst at Vedanta Resources Ltd, stationed at the Hindustan Zinc head office. Rutvik's work is primarily focused on developing a Machine Learning backed Data Driven Business Intelligence Dashboard that caters to the Maintenance managers, operational leaders and the senior management, with a major focus on reliability.
Sophie Tian, M.ASc. student	Sophie is a second year M.ASc. student working on the combustion signature analysis project in collaboration with the NRC. She has been applying time series classification and augmentation methods to the combustion signature dataset and aims to submit to a decision support related journal in the next few months. In addition, Sophie has been working with Kuilin on proposing a adversarial perturbation-based domain-agnostic self-supervised learning method, and they submitted the paper to NeurIPS 2022.

Name	Activity
Baoxiang Wang, visiting Ph.D. student	Baoxiang Wang is a fourth year of Ph.D student in Mechanical Engineering and works on the fault diagnosis of rolling bearings. The specific research is to explore new algorithms or improve existing algorithms to extract fault features caused by bearing defects. She is studying the application of sparse representation algorithm in bearing fault diagnosis.
Katie Xu, M.ASc. student	Katie is a second year M.ASc. student working on the use of machine learning for process monitoring and control in 3D printing. Since the last meeting she has finished data collection and is working on building machine learning models for predictive quality assessment of 3D printed parts.

Visits and interactions with consortium members and others

January 2022 – June 2022

Biweekly throughout **National Research Council of Canada**
Sophie Tian, Prof. Chi-Guhn Lee, Nour Elsagan, Yoon Ko, Dexen Xi, Hamed Mozaffari, Danial Khorasanian held research progress update meetings between the fire safety team at NRC and the team at the University of Toronto on combustion signature analysis project and safe routing project. A progress update will be presented today.

Biweekly throughout **Kinross**
Sean He and Vatsal Agarwal from Kinross met biweekly throughout to discuss progress on his economic asset replacement project. The progress update will be presented today.

Monthly throughout **TITAN Technologies**
Prof. Chi-Guhn Lee, Mohamed Hassan, Hazel Shi and Qiang Zhao from Titan technologies met on a monthly basis to discuss data requirements, sensor configuration and data format. The results of this research will be presented today.

January 2022 **West Indian Journal of Engineering**
Andrew was re-appointed as a member of the International Editorial Advisory Committee for three years.

January 18, 2022 **Jeonju University, South Korea**
Chi-Guhn served as a reviewer of the AI curriculum at Jeonju University of South Korea

January 19, 2022 **Sofina Foods**
Chi-Guhn and Janet met with Ryan McMinn of Sofina Foods to discuss potential collaborations.

January 21, 2022 **Ford**
Chi-Guhn presented research ideas at the Ford Workshop

Feburary 11, 2022 **Cameco**
Chi-Guhn and Janet presented C-MORE's research portfolio the NEXT Committee at Cameco. The objective was to inspire the committee with a wide range of possibilities of data analytics in Cameco. This committee is tasked with forward-looking technologies in mining. The committee

members are from a wide range of departments in Cameco, including operations, human resources, and marketing.

Feburary 17, 2022 **Universidade Federal de Pernambuco**
Chi-Guhn met with Professor Cristiano Cavalcante, Director of RANDOM to share C-MORE's research portfolio and discuss potential synergies. RANDOM is a research group on risk and decision analysis in operations and maintenance.

Feburary 22, 2022 **Kinross**
Vahid met with Vatsal Agarwal from Kinross to discuss the main objectives of the project on multi-unit systems.

Feburary 24, 2022 **Universidade Federal de Pernambuco**
Chi-Guhn gave a presentation to the RANDOM group on C-MORE's research portfolio.

March 4, 2022 **TITAN Technologies**
Chi-Guhn and Janet met with Joe Xu and this team to discuss a new project involving the safety of railway turnouts.

March 5, 6; April 2, 3, 2022 **University of the West Indies**
Andrew taught MENG6704: Maintenance Analysis and Optimization at the University of the West Indies. This course was delivered online

March 8, 2022 **Sofina Foods**
Chi-Guhn and Janet met with Ryan McMinn to discuss in more detail the type of data required for a computer vision system that would integrate with robots to apply lard to hams.

March 8, 2022 **Kinross**
Vahid met with Vatsal to share more details, and to discuss the raw data for the project on multi-unit systems.

March 21, 2022 **Defence Science and Technology Lab, UKMOD**
Janet, Blair Cui, Beishi He and Gabe Merisanu met with Tim Jefferis to talk about how the KPI project can be refocussed to provide valuable information to maintenance managers. Tim advised the team to consider "but why?" so many of the technical details we were developing so that we could clearly communicate the value of the project results to members.

March 22, 2022
Katie presented her research work to Professor Yu Zou's group: Laboratory for Extreme Mechanics & Additive Manufacturing, in the Department of Material Science and Engineering.

March 22, 2022 **Kinross**
Vahid met with Vatsal to present the visualization of Kinross' haul truck feet data, and discussed Kinross' maintenance policy for various components.

March 25, 2022
Chi-Guhn served as a moderator for an industry seminar by Unilever for Centre for Analytics and Artificial Intelligence Engineering group at the University of Toronto.

March 29, 2022
Katie presented "Towards Autonomous Additive Manufacturing" with Jiahui Zhang at the Centre for Analytics and Artificial Intelligence Engineering seed projects seminar series.

April, 2022 **University of Portsmouth**
Andrew served as an external assessor of a candidate's suitability for promotion to Reader and the University of Portsmouth, England

April 7, 2022 **Gwangju Institute of Science and Technology**
Chi-Guhn met presented a seminar on machine learning for the GIST graduate seminar series.

April 12, 2022 **Kinross**
Vahid met with Vatsal to discuss data requirements, specifically failure information and maintenance types.

May, 2022 **University of Queensland**
Andrew served as an external examiner for the Ph.D. thesis titled "A study of the selection and rigour of forensic analysis methodology affecting the accuracy and expediency of the decision-making process."

May, 2022 **Mogulinker**
Jue Wang had multiple virtual meetings with Mogulinker, an IoT startup on condition-based maintenance based in Shenzhen, China.

May 5, 2022 **Toronto Transit Commission**
Chi-Guhn, Janet and Dragan met with Tauqeer and his team at TTC to discuss progress on the NDT project as well as next steps. A need to clarify the defect priority levels, and to re-set the data was identified.

May 6, 2022 **Toronto Transit Commission**
C-MORE's relationship with the TTC has highlighted in a faculty-wide newsletter. The NDT linetest project was the project of interest.

May 9, 2022 **Electricity Canada**
Chi-Guhn and Janet met with Dan Gent and others to create a committee for Electricity Canada's awards. A rubric for adjudication, and governance documents were discussed.

May 17, 2022 **Fleetway**
Chi-Guhn and Janet met with Ken Drapeau and his team at Fleetway to discuss potential collaborations.

May 19, 2022
C-MORE was a featured research group in the University of Toronto's Engineering Research Day. Having a booth at this event enabled us to network with future students, and other researchers in the community who we may work with in the future.

June 16, 2022 **KOMIR**
C-MORE will host a delegation from Korea Mine Rehabilitation and Mineral Resources Corporation (KOMIR) to share our research portfolio, and to discuss potential collaborations.

June 20-24, 2022
A one-week course titled: Machine Learning & AI Applications in Physical Asset Management will be offered through the School of Continuing Studies at the University of Toronto. Chi-Guhn, Janet, Ali and James Reyes-Picknell form the teaching team.

Unsupervised Continuous Domain Adaptation.

Mohamed Hassan

Introduction

Although computer vision-based machine learning algorithms have experienced large advancements in recent years, developing and deploying such algorithms for real-life or engineering applications is still far from trivial. Most machine learning algorithms learn through examples (supervised machine learning algorithms). These machine learning algorithms are extremely data-hungry, which means these machine learning algorithms require a lot of examples to learn from before having any reasonable performance [1].

The general methodology we intend to use to tackle such a problem is focused on overcoming the problem of machine learning models' limited generalization capability. Boosting the machine learning generalization (generalization to unseen domains or Out-of-Distribution (OOD) data) can be formulated and tackled in different strategies, including domain adaptation, meta-learning, and multi-task learning [2]. Each of these approaches contains several sub-approaches that are designed for different problem settings.

Domain adaptation has proved its effectiveness in different fields. It was initially developed for natural language processing and was later successfully applied for object detection [3] and other practical applications, such as mechanical systems condition monitoring [4], medical diagnosis [5], and remote sensing [6], to name a few.

More specifically, it deals with the case where few limited labeled data sampled from a particular source distribution, or domain ($D_0 = \{(x, y) \sim (X, Y)\}$ are available for training, but the model is expected to be tested on data sampled from a number of different distributions $\mathrm{D_t} \in \{\mathrm{D_1}, \mathrm{D_2}, \ldots\ldots, \mathrm{D_T}\} \mid D_t = \{(x) \sim (X)\}$. The domain shift is assumed to occur smoothly and progressively through the domains. Due to this domain shift, the model developed for D_0 will experience a progressive performance degradation if used for $\mathrm{D_t}$. Successful Continuous Domain Adaptation provides a framework that can continuously adapt the model developed for D_0 to other domains without forgetting the previous experience, generalization-forgetting trade-off.

Methodology

Given the labeled training dataset from the source domain, in-phase (1), we train a baseline continuous domain adaptation model as proposed by [7], as shown in Figure 1(a). For this baseline model, a domain-specific model $\mathrm{M_t}$ is trained for each target domain $\mathrm{D_1}, \mathrm{D_2}, \ldots\ldots, \mathrm{D_T}$.

Afterward, in phase (2), as shown in Figure 1(b), we use the domain-specific encoders as teachers, and we distill the teacher's models to one student by using pseudo labels. The student is trained to minimize the cross-entropy loss between its predictions and the hard pseudo labels generated by all the teacher models.

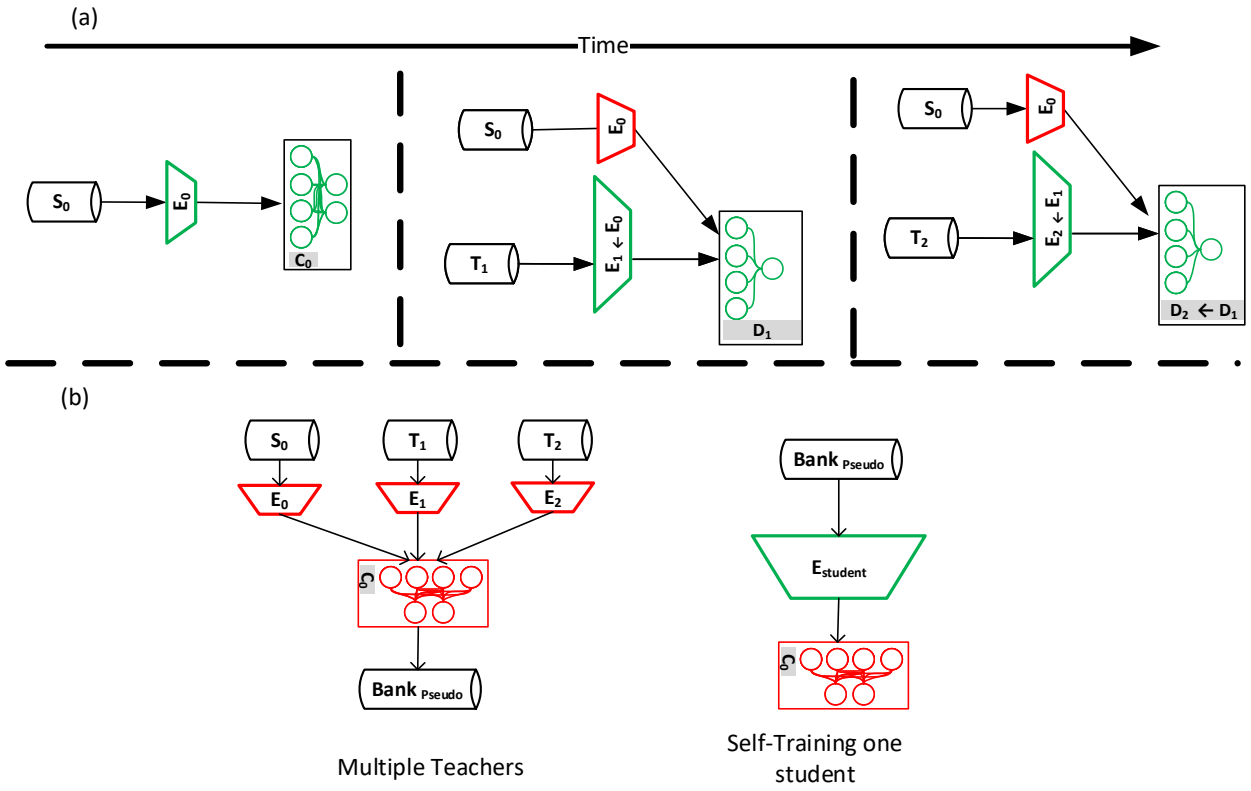

Figure 1: The proposed Methodology

Results

We compare our approach against two states of the art (SOTA) algorithms, Wulfmeier et al. [7] and Bobu et al. [8], on the continuously rotated MNIST. The source domain continuously spans the rotation angle from 0 to 45°. Each subsequent target domain spans additional 45° degrees. Wulfmeier et al. is the baseline model we used in phase 1 in our approach. As shown in Figure 2, Wulfmeier et al. exhibit good generalization capabilities, as evident from relatively high accuracy on the diagonal. However, the model shows very poor performance when it comes to forgetting, as evident in the lower triangular values in the same figure. In an attempt to balance generalization and forgetting, Bobu et al. proposed the usage of replay loss to resist forgetting behavior. As shown in Figure 3, Bobu et al. model show much better forgetting, but this happens at the expense of generalization capabilities, as evident from comparing the diagonals in Figure 2 and Figure 3. Especially in Figure 3, the downward trend inaccuracy is noticeable, making such a method unsuitable for a large number of incremental steps. Finally, in Table 1, we present the results from our proposed method. It is evident that our method shows a much better trade-off between generalization and trade-off, as evident from fairly comparable and high accuracy achieved on both source domain D_0 and D_6. This also shows that our approach is more robust against a larger number of incremental adaptation steps. Finally, compared to Wulfmeier et al., during inference, our approach doesn't require any knowledge about the domain and doesn't perform domain inference. Note that the results are shown in Figure 2, Figure 3, and Table 1 is

done at alpha =10 (alpha is a hyper paramater that controls the generalization-memorization trade-off). For the sake of testing the robustness against these hyperparameters, the same analysis is performed on different values of alpha, and the results are shown are provided in the appendix. The results shows that Bobu approach shows the least robustness against this hyperparamater and that that no alpha value makes Bobu outperform our approach.

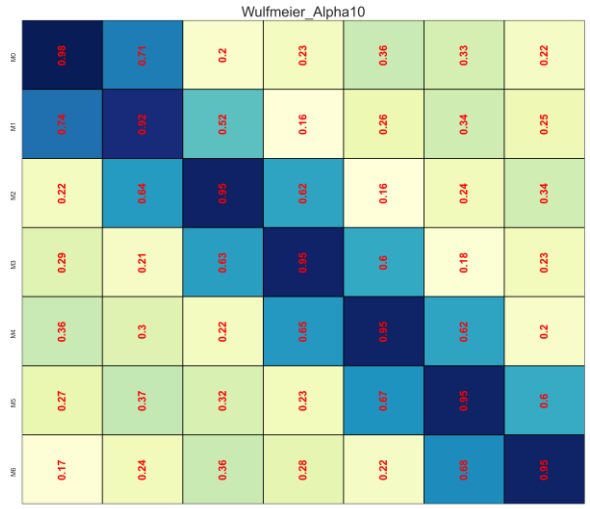

Figure 2: reproduced results from [7] (alpha=10).

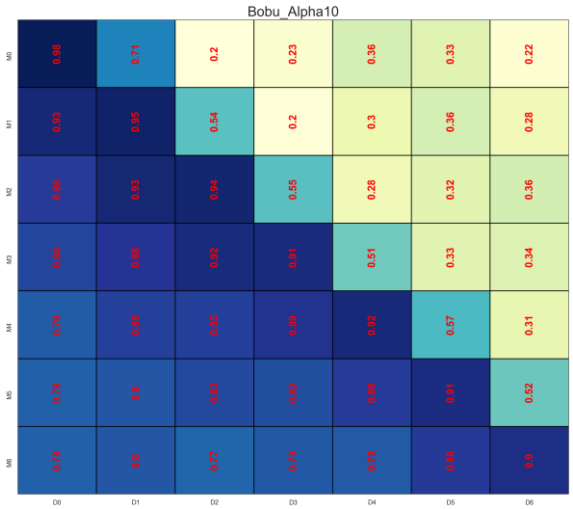

Figure 3: reproduced results from [8] (alpha=10).

Table 1: The result from our proposed method (alpha=10).

Domain	Test Accuracy
D0	0.930088
D1	0.938192
D2	0.94249
D3	0.93829
D4	0.942314
D5	0.940856
D6	0.934396

Appendix

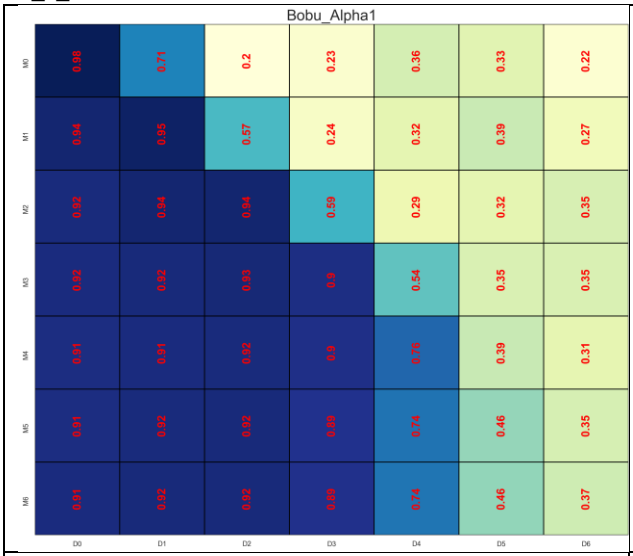

Figure 4: reproduced results from [7] (alpha=1).

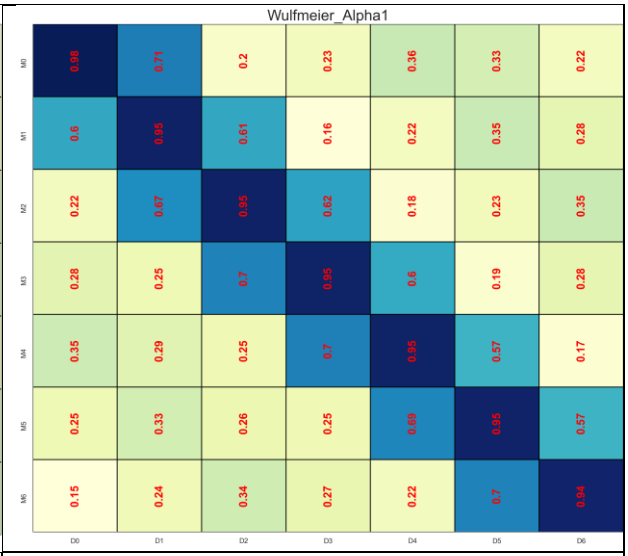

Figure 5: reproduced results from [7] (alpha=1).

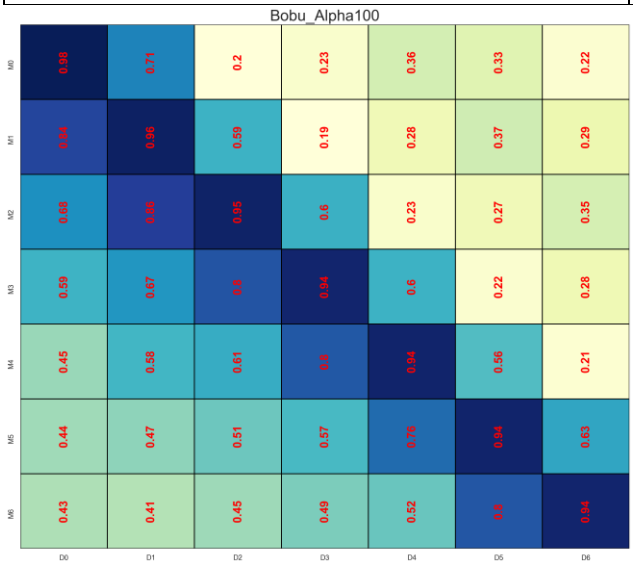

Figure 6: reproduced results from [7] (alpha=100).

Table 2: The result from our proposed method (alpha=1).

Domain	Test Accuracy
D0	0.922856
D1	0.929968
D2	0.941276
D3	0.939198
D4	0.93743
D5	0.935816
D6	0.929562

References

[1] A. Adadi, A survey on data-efficient algorithms in big data era, Springer International Publishing, 2021. https://doi.org/10.1186/s40537-021-00419-9.

[2] J. Wang, C. Lan, C. Liu, Y. Ouyang, T. Qin, Generalizing to Unseen Domains: A Survey on Domain Generalization, (2021) 4627–4635. https://doi.org/10.24963/ijcai.2021/628.

[3] K. Saenko, B. Kulis, M. Fritz, T. Darrell, Adapting visual category models to new domains, Lect. Notes Comput. Sci. (Including Subser. Lect. Notes Artif. Intell. Lect. Notes Bioinformatics). 6314 LNCS (2010) 213–226. https://doi.org/10.1007/978-3-642-15561-1_16.

[4] B. Yang, Y. Lei, S. Xu, C.G. Lee, An Optimal Transport-embedded Similarity Measure for Diagnostic Knowledge Transferability Analytics across Machines, IEEE Trans. Ind. Electron. 0046 (2021). https://doi.org/10.1109/TIE.2021.3095804.

[5] H. Guan, M. Liu, Domain Adaptation for Medical Image Analysis: A Survey, IEEE Trans. Biomed. Eng. (2021) 1–15. https://doi.org/10.1109/TBME.2021.3117407.

[6] A. Elshamli, G.W. Taylor, S. Areibi, Multisource Domain Adaptation for Remote Sensing Using Deep Neural Networks, IEEE Trans. Geosci. Remote Sens. 58 (2020) 3328–3340. https://doi.org/10.1109/TGRS.2019.2953328.

[7] M. Wulfmeier, A. Bewley, I. Posner, Incremental Adversarial Domain Adaptation for Continually Changing Environments, in: 2018 IEEE Int. Conf. Robot. Autom., IEEE, 2018: pp. 4489–4495. https://doi.org/10.1109/ICRA.2018.8460982.

[8] A. Bobu, E. Tzeng, J. Hoffman, T. Darrell, Adapting to continuously shifting domains, in: 6th Int. Conf. Learn. Represent. ICLR 2018 - Work. Track Proc., 2018: pp. 2–5. https://openreview.net/forum?id=BJsBjPJvf.

Predictive Quality Assessment for 3D Printing

Katie Xu

Introduction

3D printing is a class of fabrication methods for making customized 3D objects. Generally, the target geometry is divided into a series of 2D profiles (layers) and objects are built up layer-by-layer. Fused deposition modeling (FDM) is a type of 3D printing where layers are formed by melting a thermoplastic material and depositing it in the desired locations where it solidifies and becomes part of the object. 3D printing has important advantages over traditional manufacturing processes such as the ability to fabricate complex geometries, reduced waste material, and lower tooling costs. However, the need for part-specific parameter tuning and the influence of external disturbances lead can lead to high rejection rates. This limits the usefulness of 3D printing in many practical applications. The goal of this project is to support the development of a closed-loop system to monitor and control the quality of parts made with FDM 3D printing.

The main result of this work is a model which can predict mechanical properties of the manufactured part by considering in-situ observations as well as processing parameters. To accomplish this, we first created a suitable dataset consisting of 3D printed parts and corresponding measurements. We then define a suitable neural network-based model structure and experiment with different feature extraction methods.

Dataset

This work aims to jointly model the impact of in-situ observations and process parameters on the quality of the 3D printed part. To construct a dataset for this modelling task, 359 standard tensile specimens were produced under a wide range of parameter settings. For each specimen, sensor measurements in the form of layer-wise images and stress-strain measurements from tensile tests were recorded. Mechanical property measurements were extracted from the tensile test results, including the ultimate tensile strength (UTS, σ_{UTS}), elastic modulus (E), and fracture strain (ε_x).

For this dataset, two parameters, nozzle speed and material flow rate, were allowed to vary while all others were kept constant. Importantly, the two variable parameters were not constrained to be constant throughout the production of a single part but rather were allowed to change every layer. This choice was made to provide insight into the dynamics of the system, and to make the

data and resulting model more suitable for future work towards closed-loop 3D printing. In closed-loop 3D printing, a natural choice of control action is parameter adjustments. When this type of closed-loop control is applied, process parameters will inherently not remain constant throughout a single run. Thus, it is important to understand the impact of such parameter changes.

Model

The proposed model consists of two main parts: a feature extractor which operates on each image individually, and a temporal model which connects image features as well as parameter information from different time steps. This is shown in Figure 1.

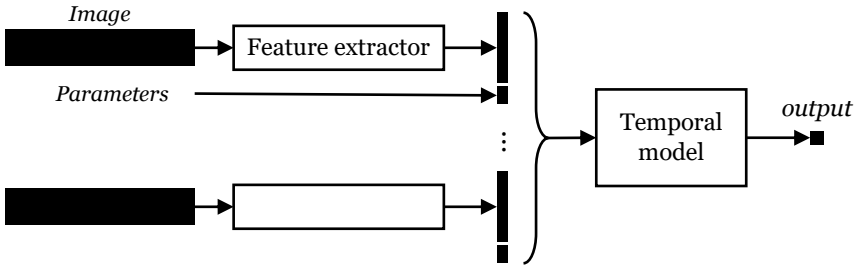

Figure 1: Overall model structure

The model has two main parts: i) A feature extractor which takes an image and outputs a vector of features representing the image. ii) A temporal model which takes in a sequence of inputs and outputs a prediction. The input vector at each layer step is the image feature concatenated with the corresponding process parameters.

Feature extraction with texture analysis

The purpose of feature extraction is to summarize the contents of each image as a vector of features. In this work, we explore two main methods for doing so. The first method is to use hand-picked features computed based on the distribution of pixel intensities of the image. These features comprise variance, entropy, contrast, homogeneity, energy, and correlation which are described below.

Variance (σ^2) and entropy (H) are statistical properties of the histogram of pixel intensities. These are calculated using equations (1) and (2) respectively, where x_i is the intensity of pixel i, μ is the mean intensity across all pixels, N is the number of pixels, and p_x is the frequency of pixels with intensity level x. Only pixels corresponding to the region of interest (ROI) containing the surface of the specimen are use in these calculations.

$$\sigma^2 = \frac{\sum_i (x_i - \mu)^2}{N} \qquad (1)$$

$$H = -\sum_x p_x \cdot \log(p_x) \qquad (2)$$

Contrast, homogeneity, energy, and correlation are features computed from a grey level co-occurrence matrix (GLCM). This matrix encodes information about the relationship between intensity values of neighbouring pixels. A GLCM is constructed for a given displacement vector that specifies which pixels to compare (ie. it defines the meaning of “neighbouring pixel”). From

the GLCM (denoted P, with elements P_{ij}), contrast, homogeneity, energy, and correlation are computed as follows [1] [2].

$$contrast = \sum_{i,j} P_{ij}(i-j)^2 \quad (3)$$

$$homogeneity = \sum_{i,j} \frac{P_{ij}}{1+(i-j)^2} \quad (4)$$

$$energy = \sqrt{\sum_{i,j} P_{ij}^2} \quad (5)$$

$$correlation = \sum_{i,j} P_{ij}\left[\frac{(i-\mu_i)(j-\mu_j)}{\sigma_i \sigma_j}\right] \quad (6)$$

Like variance and entropy, only pixels in the ROI corresponding to the surface of the specimen are used. To accomplish this, the first step is to divide the ROI into patches. For each patch, 3 different distances and 4 different angles were used to compute a total of 12 different GLCM matrices. For each matrix, the 4 GLCM features were computed, resulting in a total of 48 features per patch.

In this work, we experiment with combining features across different distances and angles or not. When not combined, all 48 GLCM features per patch are preserved. When combined, the maximum value for each of contrast, homogeneity, energy, and correlation are taken across the values computed with different GLCM matrices. Thus, patch is summarized by 4 GLCM features.

Finally, the maximum value for each feature is taken across all patches so that each image is summarized by 4 or 48 GLCM features depending on whether features were combined across GLCMs of different displacements. Together with the variance and entropy, each image is therefore represented with either 6 or 50 features. These two configurations are referred to as glcm-6 and glcm-50 respectively in the experiments section.

Feature extraction with convolutional neural networks

The second method of feature extraction is to train a convolutional neural network (CNN). The architecture is shown in Figure 2. It is a basic CNN consisting of 3 convolutional layers. Each layer is followed by a max-pool operation, batch norm, and ReLU activation. The output is then flattened and passed through 2 fully connected layers. The final output is a feature vector with 1000 elements.

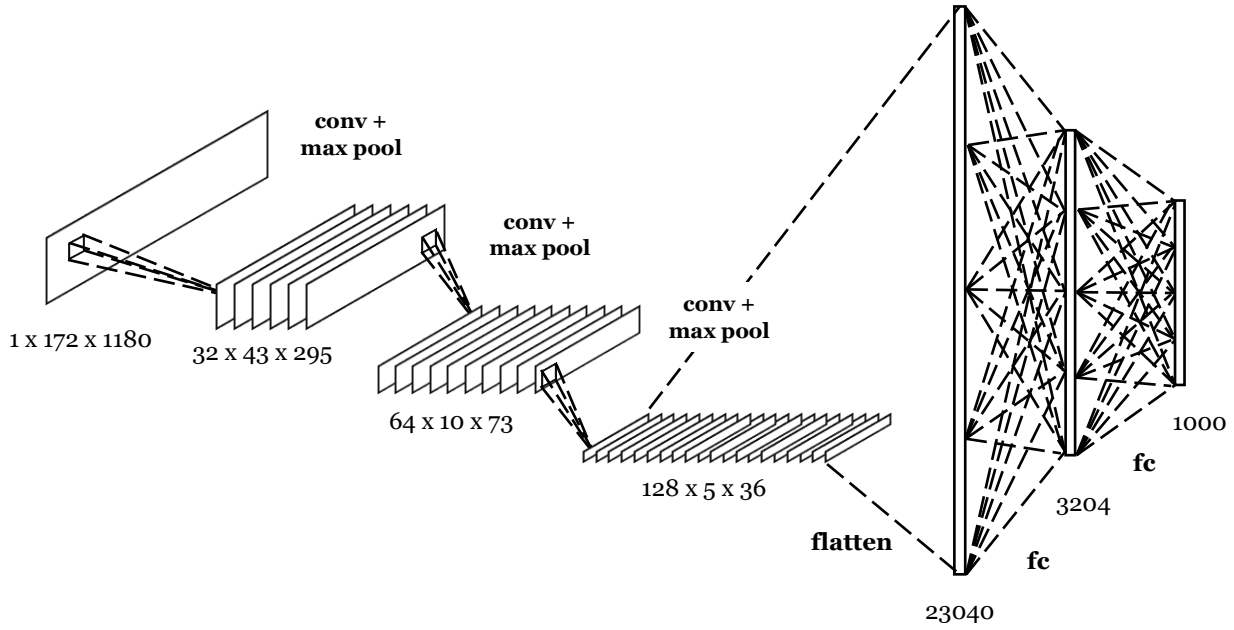

Figure 2: CNN feature extractor
3 convolutional layers (conv + max pool) followed by two fully connected layers (fc). Input is a 172 x 1180 grayscale image and output is a 1000 element feature vector.

Temporal model
To model temporal relationships between inputs at different time steps, a recurrent neural network (RNN) was used. RNNs are similar in structure to dynamic models in that state transitions are computed as a function of past states and new inputs. In RNNs, these transition functions are approximated by neural networks whose weights are learned. RNNs and their variants have been used in fields such as natural language processing and video processing to model sequences with temporal dependencies.

The RNN used in this work has 5 layers, a hidden size of 500, and *tanh* activation. The input to the RNN at each time step is the corresponding image feature and process parameters concatenated together. The output of the RNN at the last time step is passed through two fully connected layers and the final output of the model is a single value representing the UTS. The same RNN is used for all experiments.

Training

Supervised learning
When texture features are used for feature extraction, only the RNN is trained. When a CNN is used for feature extraction, it can be trained together with the RNN. This configuration is referred to as cnn-sup in the experiments and stands in contrast to self-supervised methods described in the next section.

For both texture feature-based models and cnn-sup, all weights in the model are trained to predict the UTS by minimizing the mean square error between the model prediction and the target (measured value). Models are trained by gradient descent with the Adam optimizer. Batch size of 10 and learning rate of 0.001 were used. Weight decay and other regularization methods were not used because overfitting was not observed to be an issue.

Self-supervised representation learning

As experimental results in the following section show, training the CNN feature extractor together with the RNN in a supervised manner yields poor results. This may be because it is difficult to learn good image representations when only a single regression target is available for a sequence of many images. Moreover, the images in this dataset are visually very similar which may also make training more challenging. To address these issues, 2 self-supervised learning methods, SimCLR [3] and SimSiam [4], were applied to guide the representation learning process.

Both SimCLR and SimSiam operate by training a model on pretext tasks involving different views of the dataset's images. A view refers to an augmentation or distortion which preserves the semantic interpretation of the original image. After training, the encoder portion of the model which is responsible for generating image representations can be extracted and used for downstream tasks, such as our regression task. In this work, the CNN illustrated in Figure 2 is used as the encoder.

In SimCLR [3], a contrastive loss is used to train a model to distinguish different views of the same image from views of other images. This algorithm encourages representations originating from the same image to be similar, while encouraging representations from different images to be dissimilar. In SimSiam [4], representations of different views of the same image are trained directly to be similar by minimizing the negative cosine similarity.

In our experiments, cnn-simsiam and cnn-simclr refer to configurations which use CNN feature extractors pretrained with SimSiam and SimCLR respectively.

Experiments and Results

Table 1 summarizes the experiments that were preformed. Details of each experiment group were described in the relevant sections above. For each experiment, the root mean square error (RMSE) are reported for both the training and validation sets. Figure 3 shows the predictions of each model compared to actual values.

Experiment	Description of feature extractor	Train RMSE	Validation RMSE
glcm-6	Variance, entropy, and 4 GLCM features per image	6.015	**5.945**
glcm-50	Variance, entropy and 12x4 GLCM features per image	**5.917**	5.983
cnn-sup	CNN trained jointly with RNN model	7.141	7.182
cnn-simsiam	CNN pretrained with SimSiam	6.103	6.103
cnn-simclr	CNN pretrained with SimCLR	5.983	5.963

Table 1: Summary of experiments and results

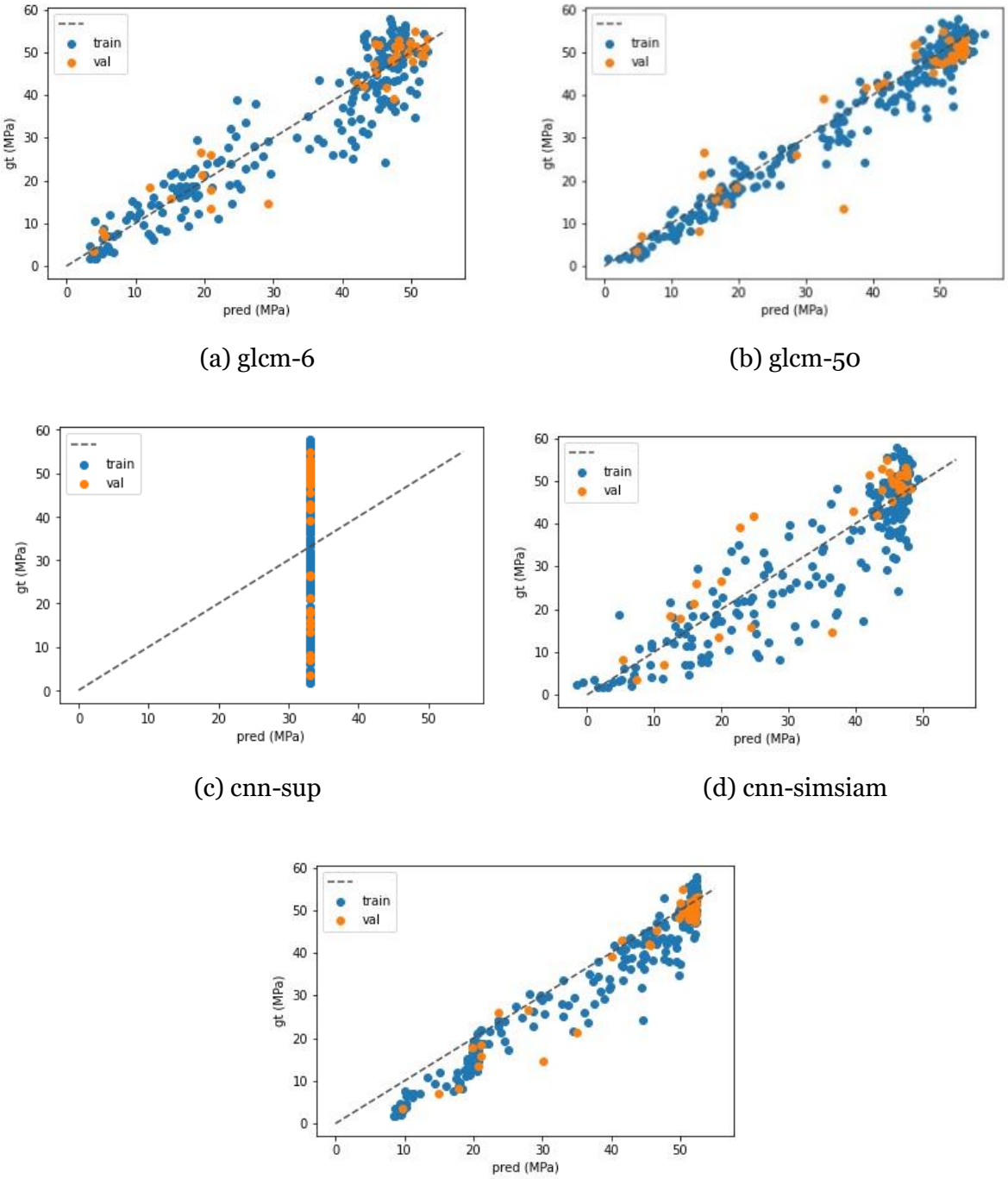

(a) glcm-6

(b) glcm-50

(c) cnn-sup

(d) cnn-simsiam

(e) cnn-simclr

Figure 3: Model predictions (horizontal axis) compared to the true values (vertical axis) Dashed line across the diagonal shows the ideal, when all predictions are perfectly correct.

Discussion

Using texture features yielded the best results, which suggests that the selected features are suitable for this modelling task. However, there are important limitations and considerations which must be acknowledged. First, the texture features used were selected and tested for the specific task and dataset presented here, so it is unclear how these features will generalize to different tasks and datasets in the same application domain. Second, the computation of these texture features is slow compared to a forward pass through a CNN. Depending on latency and bandwidth requirements in future work, this method may or may not be appropriate. It should also be noted that these computations cannot currently be accelerated with specialized hardware such as GPUs. These limitations may motivate the use of a CNN feature extractor in future work despite the superior performance of texture features shown in this study.

When a CNN feature extractor is used, Table 1 and Figure 3 (c) show that end-to-end training was ineffective. The resulting model essentially predicts the mean target value in the dataset, regardless of the input. At a glance, this appears to be an issue of severe underfitting. However, increasing model complexity did not result in improved performance. We can conclude, therefore, that the issue lay not with the model architecture but rather with the training procedure. Indeed, pretraining the feature extractor with self-supervised learning yielded much improved results, as shown in Figure 2 (d) and (e). Between the 2 pretraining methods used, SimCLR outperformed SimSiam and achieved performance that was comparable to models which used texture features. The key difference between SimCLR and SimSiam is that SimCLR considers both negative and positive pairs while SimSiam only looks at positive pairs. This suggests that for this dataset, explicitly training negative pairs to have different representations is particularly useful. Intuitively, this could be because images within this dataset are already visually similar, therefore enforcing similarity of representation between positive pairs may not add much value.

Conclusion

To summarize, a neural network-based model was developed to capture the relationships between parameters, observations, and results of a FDM process.

Experiments showed that informative image features are critical to good performance. Suitable features can either be selected by a practitioner or a feature extraction model can be trained. For the dataset used in this work, hand-picked features based on texture analysis showed promising results. A CNN feature extractor trained in a supervised manner was found to be ineffective, however self-supervised representation learning followed by supervised training yielded results which were comparable to using texture features.

Acknowledgements

The project is in collaboration with Professor Zou and his students from the Department of Material Science and Engineering, who have kindly shared their space, equipment, and expertise to facilitate the creation of the dataset. I would also like to acknowledge and thank Daisy Wang for her contributions in carrying out the tensile test experiments and her assistance with organizing the dataset.

References

[1] R. M. Haralick, K. Shanmugam, and I. Dinstein, "Textural Features for Image Classification," *IEEE Transactions on Systems, Man, and Cybernetics,* vol. SMC-3, no. 6, pp. 610-621, 1973, doi: 10.1109/TSMC.1973.4309314.

[2] M. Hall-Beyer, "GLCM Texture: A Tutorial v. 3.0 March 2017," ed. PRISM: University of Calgary's Digital Repository: University of Calgary, 2017.

[3] T. Chen, S. Kornblith, M. Norouzi, and G. Hinton, "A Simple Framework for Contrastive Learning of Visual Representations," presented at the Proceedings of the 37th International Conference on Machine Learning, 2020, 2020. [Online]. Available: https://proceedings.mlr.press/v119/chen20j.html.

[4] X. Chen and K. He, "Exploring Simple Siamese Representation Learning," in *IEEE/CVF Conference on Computer Vision and Pattern Recognition*, Piscataway, 2021: IEEE, pp. 15745-15753, doi: 10.1109/CVPR46437.2021.01549. [Online]. Available: https://ieeexplore.ieee.org/document/9578004

Prediction of Emergency Response Strategies Based on Combustion Signatures from FTIR Spectroscopy Using Machine Learning Techniques

Sophie Tian, Cathy Feng, Zijian Wang, M. Hamed Mozaffari, Dexen Xi, Yoon Ko, Nour Elsagan, Chi-Guhn Lee, Yoon Ko

1. Introduction

In recent years, machine learning (ML) has been widely applied in fire engineering and science. Machine Learning is a branch of artificial intelligence based on the idea that computers can learn from data, recognize patterns and make decisions automatically with minimum error in compare to human performance. Nazer (2021) introduced a variety of ML and AI techniques such as deep leaning LeCun et al. (2015) and decision Myles et al. (2004) trees in the field, with the remarks that AI and ML may overcome many limitations of conventional (for example, physics-based or mechanistic) approaches that are currently being used in fire science, and invited research efforts to leverage AI and ML to develop and strengthen modern fire assessment tools. In Jain et al. (2020), a review of ML in wildfire science and management has been provided, summarizing popular ML methods and their applications in fuel characterization, fire detection, and fire preparedness and response. Importantly, the authors suggested that a significant challenge exists for the fire research and management community to deploy and enable the ML models to operations within fire management agencies. Recently, a firefighter-wearable device has been created by Garrity & Yusuf (2021), where an artificial neural networks is used to predict temperature in the environment and to warn firefighters of catastrophic temperature increases. This device was successful in protecting firefighters by triggering an alarm before a flashover in controlled fire behavior training environments. ML algorithms, when integrated into a tangible device or software such as in Garrity & Yusuf (2021), will bring tangible improvements in the first responders' safety and aid the adoption of such technologies when deployed on a large scale.

In responding to freight transportation fire incidents, identifying the scope of the emergency from the early stage of the fire is critical to protect people, property, and the environment from the effects of the fire. In the emergency response to such incidents, the first responders are trained to use the materials and hazards labeled on the burning freights to refer to the Emergency Response Guidebook (ERG, 2020) for appropriate emergency response strategies. Generally, the ERG lists different hazardous freight materials and classifies them according to their hazard (e.g toxicity, flammability, explosiveness), then provides guidance to first responders based on that classification. The ERG provides guidance in case of incidents

involving hazardous materials. However, the emissions from the fire of non-hazardous materials can impose potential risk to first responders. For example, polyvinyl chloride (PVC) is not considered as hazardous material by ERG, but toxic and corrosive hydrochloric gas (HCL) is produced during PVC fire. As a result, when first responders confront non-hazardous or unknown materials, they will be referred to a blanket guide: "Guide 111 – Mixed Load / Unidentified Cargo" in the ERG, which may be too general for selecting the appropriate protective clothing, equipment, fire and spill control, and BLEVE (boiling liquid expanding vapor explosion) safety precautions.

Spectroscopic data such as the Fourier Transform Infrared (FTIR) data have been used in literature to train ML models. Generally, The FTIR analyzer is used for simultaneous detection and quantification of different chemical compounds by scanning the infrared spectrum. Kim et al. (2017) used a convolutional neural network (CNN) were used to classify hazardous gases. In the field of combustion studies Jiang et al. (2021), ML has also been increasingly applied such as in predicting combustion and flammability properties, and both theoretical and industrial studies on tasks such as aiding chemical reactions, combustion modeling, and combustion measurement as summarized in Zhou et al. (2022), Zheng et al. (2020). However, our literature survey suggested that the only work that applied ML on combustion data measured by a FTIR gas analyzer was an early work by Chen et al. (2000) where an artificial neural network (ANN) was trained to classify fires into flaming, smoldering, or nuisance categories.

In order to provide specific response guides to the first responders, in this work, we propose an artificial intelligence (AI) enabled tool to aid first responders in determining the best fire mitigation strategy and the required protective gears when they encounter unknown materials and unlabeled freights in a transportation fire accident. The tool is built based on time series classification models, with samples of combustion signatures as the input and a binary output indicating the presence of a specific fire hazard (i.e. flammability, toxicity, explosivity, corrosiveness and oxidizing). To train the model, we collected 38 samples of combustion signatures using the FTIR gas analyzer and the cone calorimeter at the National Research Council (NRC) to estimate model parameters (Figure 1). When applying the tool in a real freight fire scenario (Figure 2), the tool asks the first responder to survey the scene of the fire incident and analyze a smoke sample using a gas analyzer like the FTIR spectroscopy gas analyzer. Using the smoke composition, the AI tool will identify the presence of each fire hazard found within the emissions through its ML model. The tool has been developed into a software package with a user interface (UI) to display the chemicals found in the fire, the fire hazards found by the ML model, as well as the appropriate emergency response guide number to the first responders, guiding the first responders in selecting the most effective and the safest fire mitigation measures. Following the call from Nazer (2021) for using ML in modern fire assessment tools and from Jain et al. (2020) to make ML models more accessible for fire management agencies, we propose the first AI-enabled tool applicable in freight transportation fires that provides not only predictions of the fire hazards but also actionable intelligence for safe and effective mitigation strategies, and therefore paves the way for further research in accessible, easily-deployable AI-enabled tools in fire science and management.

Following this line of work, recently, we (Tian et al.) proposed to use time series classification methods, a type of ML algorithms, to make classification decisions using FTIR spectroscopy on combustion processes. FTIR data from the burning of thirty eight samples in a cone calorimeter were collected for training the ML models to predict five fire hazards, namely flammability, toxicity, explosivity, corrosiveness and oxidizing. We demonstrated that ML can be applied to characterize hazards in the burning goods. In addition, a review of applications of machine learning in combustion processes and the classification of gases was presented. In the current paper, an improved machine learning model with a larger dataset and a software to display the fire hazards found in a given sample and actionable intelligence are presented.

(a) (b)

Figure 1: (a) Test setup within the cone calorimeter. (b) Experiment on burning the Lithium-ion battery

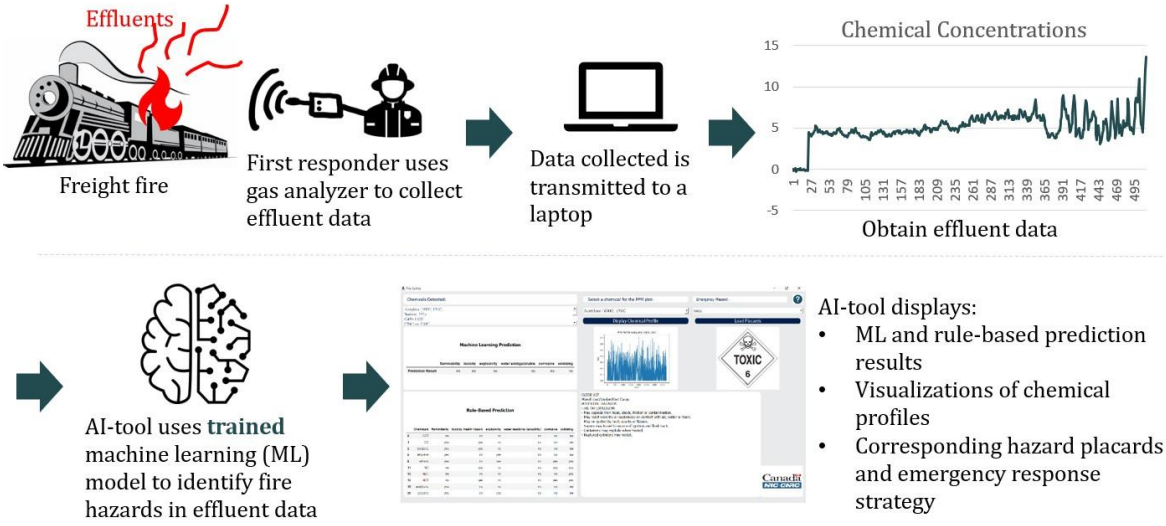

Figure 2: Overview of the proposed AI Tool

We present the data collection procedures in sections 2 and the formulations of the models in section 3. Section 4 discusses the results obtained from training the models with the NRC data along with the user interface of the tool. The paper closes with conclusions in section 5.

2. Data Collection

To collect emission data from sample materials, experiments were conducted with a cone calorimeter and a FTIR gas analyzer.

Figure 1 shows the experimental setup, where a sample is placed inside the cone calorimeter and ignited. The cone calorimeter measures the fire performance of a solid material by subjecting it to a pre-specified heat flux and measuring its heat release rate and mass loss. In this work we set the heat flux to 50kW/m2 for all tests conducted.

The FTIR gas analyzer was connected to the cone calorimeter to detect the chemical composition of the gaseous effluents over time. In this work, we used a MKS Multi-gas 2030 continuous FTIR gas analyzer, which was equipped with a 200 mL gas cell heated to 191°C as well as a 5.110 m optical path with a liquid nitrogen cooled detector.

In the next phase of experiment, the MKS software (MG2000, Analysis Validation Utility and Gas Search Utility) was used to determine the concentrations of the chemicals present in the effluents. The MG2000 software automatically performs quantitative calibrations and further verification was performed using the analysis validation utility (AVU) on specific spectra with elevated concentration of targeted chemical compounds. This step enabled estimations on the detection limits, confidence limits, maximum bias and values specified in ASTM D6348 and EPA 320. The AVU was used strictly as a check to confirm the analysis made by the MG2000 software and to check the remaining spectral residuals, therefore we did not report the values recorded by AVU.

Following the procedures outlined above, we conducted experiments on 38 samples from 24 distinct materials. Table 1 shows all materials tested and the number of experiments conducted on each. Then, the data were analyzed and hazard labels were assigned to each sample. For example, the data obtained from burning the Lithium-ion battery was assigned the labels of flammable, toxic, explosive, corrosive, and not oxidizing. These labels were provided to train the ML model.

Table 1: Materials tested and the number of experiments conducted on each material.

Material	Number of Experiments Conducted
Lithium-ion battery	5
ABS	3
Polyisocyanurate	3
PVC	3
Crude oil	2
Diesel	2
Phenolic panel	2
Polystyrene	2
Carpet flooring	1
CAT-6 wiring	1
Clorox wipes	1
Consumer electronics shell	1
Dettol	1
Electrical wiring	1
Epoxy	1
Hand sanitizer	1
Heptane	1
Intumescent caulking	1
Melamine board	1
PMMA	1
Polyethylene	1
Polyurethanes foam	1
Tar shingle	1
Wall	1

3. Methods

In this section, we describe the ML model used to classify fire hazards, the model training and the design requirements for creating the fire safety software.

3.1. Machine Learning Model Used: MultiRocket

The data collected in each experiment included the concentration profiles of all chemicals detected in the effluents throughout the entire burning process of each material, therefore it followed the form of a multivariate time series. To detect the presence of five independent hazards within each sample of burning materials, namely flammability, toxicity, explosivity, corrosiveness and oxidizing, a ML model for each hazard category was trained separately. This detection or binary classification problem on multivariate time series data required a multivariate time series classification (MTSC) model. A MTSC model named MultiRocket (Tan et al. 2021) was applied, which is a fast and scalable MTSC method that achieves state-of-the-art accuracy. The training procedures for MultiRocket are as follows:

- Let $X = \{x_t : \forall t \in \{1,...,l\}\}$ and $X' = \{x_t - x_{t-1} : \forall t \in \{2,...,l\}\}$ be a sequence of time series observations and its first order difference. For each observation in X, the observation of the convoluted output, $Z = \{z_t : \forall t \in \{1,...,l\}\}$, is given by

$$z_t = x_t * \Omega = \sum_{j=0}^{l-1} x_{t+(j\times d)} \times w_j \quad (1)$$

  where $\Omega = \omega_0,...,\omega_{l-1}$ is a kernel with dilation, d. The term Z is also referred to as feature maps. The procedure is also performed to X' to yield Z' analogously.

- Using the convoluted feature maps, we compute four key statistics to summarize their characteristics. These key statistics are: Proportion of Positive Values (PPV), Mean of Positive Values (MPV), Mean of Indices of Positive Values (MIPV) and Longest Stretch of Positive Values (LSPV).

- Finally, these key statistics and the binary label of the fire hazard associated with the tests are used as inputs and outputs to train a linear classification model (ridge regression or logistic regression classifier).

In this work, we trained one MultiRocket model for each of the five hazard category, using the default hyperparameter values used in the original paper. The implementation of MultiRocket was used from Sktime (L¨oning et al.,2019), a Python library for time series analysis using machine learning.

3.2. Data Pre-processing for Machine Learning Model

Since the burning characteristics of different materials vary, the experiments in the dataset had different durations. To standardize the data, zero-padding was applied on the dataset, which means zeros were added to shorter experiments so that each experiment took the duration of the longest experiment in the dataset. Using the combustion signature dataset comprising of 38 data samples, 70% (or 26 data samples) of the data was used to train the machine learning model, and 30% (or 12 data samples) of the data was used to test the performance of the model on new, unseen data.

Another consideration for the combustion signature datasets was the imbalance for some hazard categories. For example, 31 out of 38 data samples were labeled as nonexplosive, and only 7 were labeled as explosive. This means that a trained ML model may assign all given data as nonexplosive, and achieve a high training classification accuracy without actually learning the underlying patterns of the data. To overcome this issue, one approach is to resample the dataset such that each class has the same number of examples. This can be achieved through either oversampling or undersampling, such as performed by Mohammed et al. (2020). Oversampling randomly duplicates the data samples in the minority class to match the size of the majority class, and undersampling randomly samples data from the majority class until it matches the size of the minority class. In the example of the explosivity of our dataset, the oversampling technique would sample the 7 explosive data samples with replacement to create 31 data

samples, and the undersampling technique would sample the 31 nonexplosive data samples with replacement to obtain only 7 samples. Either technique will allow the ML model to see a balanced class distribution between nonexplosive and explosive data samples. By doing so, the ML model will be forced to learn the characteristics required to differentiate between the explosive and nonexplosive classes. This resampling technique was only applied to the training dataset to influence the learning process of the ML algorithm. In this work, we experimented with MultiRocket models trained with the original dataset as well as datasets enhanced with resampling techniques, and compared their performance in Section 4.1.

3.3. AI-Enabled Software

3.3.1. Design Requirements

The AI-enabled software is a multi-functional interface powered by a decision-making model. The designed interface can used as an aid for first responders in freight fire incidents with unknown burning goods.

Given a data sample of combustion signatures collected with a FTIR, the designed user interface called the embedded ML algorithm, MultiRocket, to detect the presence of five fire hazards of the burning materials and showed the appropriate response guide number from the ERG handbook. Additionally, the AI-enabled software showed the chemicals detected in the effluents, displayed their profiles for inspection, as well as displayed the appropriate emergency response guides and associated hazard placards based on the ML model predictions.

For nonfunctional requirements, the designed platform should be user friendly and easy to understand for first responders. The final product should fulfill aspects of satisfaction, usability, and efficiency.

3.3.2 Qt Framework and Qt Creator

In this work, Qt was selected as the development framework for the AI-enabled software. Qt is a crossplatform software development framework, compatible with a variety of operating systems and hardware (Company n.d.). With approximate 1 million developers worldwide, Qt is the leading software behind millions of devices and applications (*QT Group Oyj Managers' transactions* n.d.). It provides support for a range of devices such as cell phones and desktops platforms including Windows and Mac OS X, which allowed our software to be easily adapted to any platform that the first responder may use when responding to freight fire incidents.

Qt libraries are implemented using QT Creator, a Graphical User Interface (GUI) tool that integrates several user interface technologies. It includes a project management file with a cross-platform format (.pro). This project file include all program files, configuration options to use, and paths for the building process (*QMAKE project files: QT 4.8* n.d.). Qt Creator also integrates a C++ code editor along with Qt Designer, a software specialized for designing GUIs from Qt Widgets. These UI components are then connected to the program code with the help of Qt signals and slots (VANDANA & VISHWANATH 2016), in which a method is called in response to a certain signal sent from the interface.

4. Results and Discussion

In this section, we present the results obtained by applying the machine learning model on the combustion signature dataset and the software of the AI-enabled tool.

4.1. Machine Learning Prediction Results

The training and testing accuracies in percentage for each hazard category and the average performance across all hazard categories are shown in Table 2. The table compares the classification results from the model trained with the original (unbalanced) dataset and the

undersampled and oversampled (balanced) datasets. For each row, the higher test accuracy is shown in bold.

From Table 2, we observe that the models trained with the undersampled dataset achieved higher overall training accuracy than models trained with the original dataset (100% vs. 91%, respectively). However, the overall testing accuracy worsened with the undersampling technique (82% vs. 69%, respectively). This occurred because even though undersampling allows the ML model to be exposed to a balanced distribution of data, the overall size of the training data was reduced. Since we used a small-scale dataset for training, the size of a minority class could be less than 10 training examples. Undersampling the data in this case resulted in many examples to be randomly deleted from the majority class to match the size of a minority class, causing a significant amount of information loss. As a result, during the training process, the ML model may have learned to differentiate between the two classes well, however, it failed to generalize well to new, unseen data due to the significant information loss. In general, the undersampling technique may be more suitable with a larger imbalanced dataset where there are sufficient samples in the minority class.

Comparing the models trained with the original dataset and with the oversampled dataset, we observe that both the average training and average testing accuracies improved (from 91% to 100% for training accuracy, and from 82% to 90% for testing accuracy). With the training accuracy, the models trained with the oversampled dataset were exposed to a balanced data distribution and were thus able to learn the underlying patterns of the data well. Also, since there was no or little information loss with oversampling, the models were able to retain the generalization ability on unseen data, resulting in an improved testing accuracy. Overall, using the oversampled dataset was the optimal choice for augmenting the combustion signature dataset when training ML models to identify fire hazards.

Table 2: Classification results using the MultiRocket model

	Original Dataset		Undersampled Dataset		Oversampled Dataset	
Hazard Category	Training Accuracy (%)	Testing Accuracy (%)	Training Accuracy (%)	Testing Accuracy (%)	Training Accuracy (%)	Testing Accuracy (%)
Flammability	85	67	100	67	100	**92**
Toxicity	100	83	100	83	100	**92**
Explosivity	100	**100**	100	83	100	92
Corrosiveness	100	**75**	100	**75**	100	**75**
Oxidizing	100	**92**	100	33	100	**92**
Average Performance	97	83	100	68	100	**88**

It is also important to evaluate the time required to train and deploy the ML model. For deploying the ML model to the field and allow the first responders to receive actionable intelligence as soon as possible, the time required to train and test the model must be short.

Since the ML model can be trained prior to arriving at the scene of a freight transportation fire, the on-site training time is effectively zero. In terms of the evaluation time, the MultiRocket model only required 0.003s to classify the testing set for each hazard category, which comprises 12 data samples. In terms of detecting the presence of five hazards from one data sample, only 0.0015s will be required for this algorithm, therefore the evaluation time of MultiRocket is satisfactory as well.

Overall, the MultiRocket model performed well in both classification accuracy as well as the time required to make predictions on new data, despite a relatively small training dataset with 38 data samples. As a result, it can be concluded that MultiRocket is suitable for identifying fire hazards from the FTIR gas analyzer under tight time constraints.

4.2.AI-Enabled Fire Safety Software

The AI-enabled tool, implemented using Qt (Company n.d.), can be initiated by clicking on an executable (.exe) file named *FireSafety.exe*. The Fire Safety software consists of two windows, the DataLoad window and the Result Display window. The DataLoad window initiates the process of data analysis and hazard identification given a data sample collected at the scene of a fire, and is described in detail in Appendix A. The Result Display window, shown in Figure 3, displays results from both the chemicals found within the data sample as well as fire hazard prediction results from the ML model. Based on the ML model prediction results, we display the associated emergency placards and response strategies from the ERG (*2020 Emergency Response Guidebook* 2020).

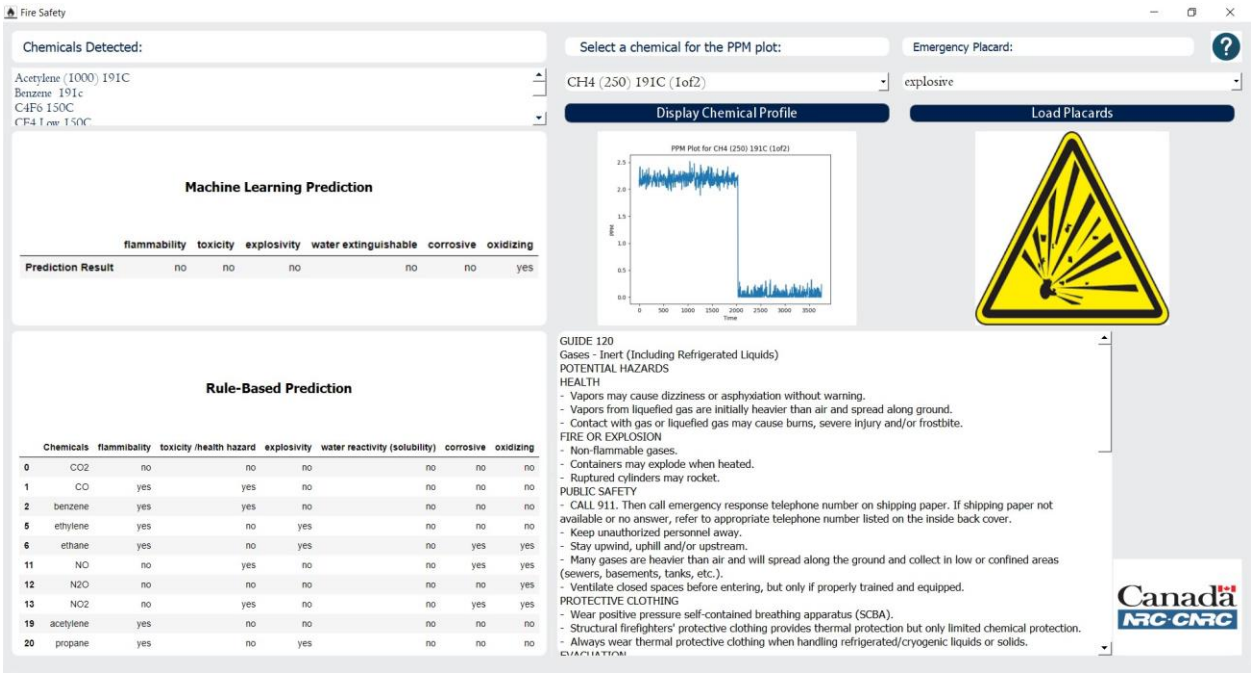

Figure 3: Result Display window

On the leftmost column of the Result Display window, we display rule-based and machine-learning-based results. The section at the top displays all chemicals detected within the data sample. The section in the middle displays the hazard predicted from the data sample by running the final selected ML model (4.1), which is a trained MultiRocket model with oversampling technique. As shown in Figure 3, the current data sample was predicted to be not flammable, not toxic, not explosive, not corrosive, and not oxidizing. This prediction is made to

consider the overall effect of a burning material considering the time series profiles of all chemicals detected in a burning situation.

The section on the bottom of the leftmost column shows the properties of each individual chemical that was found in the data sample. This data is referenced from a chemical property table stored in the software. However, note that even though chemicals with a specific fire hazard may be found, the entire data sample may not be considered to possess that fire hazard. For example, even though toxic gases such as CO, benzene and NO were detected in the Rule-Based Prediction section in Figure 3, the overall data sample was predicted to be not toxic in the Machine Learning Prediction section. This may be caused by the low concentrations of the toxic gases.

Next, on the top of the middle column, we prompt the user to select a chemical in the drop-down menu to display its concentration plot in PPM. These concentration plots were the raw measurements from the FTIR analyzer and as a result, there may be some noise present in the plots. On the top of the rightmost column, there is another drop-down menu that allows the user to view all relevant emergency placards based on the hazard predictions from the machine-learning model. Finally, the section on the bottom of the rightmost column displays the relevant emergency strategy guide using the Machine Learning prediction results and the ERG.

Overall, the Result Display window summarizes all relevant information from a given data sample collected at the scene of a fire and allows the first responder to not only analyze the chemicals found in a fire and their visualizations, but also to obtain actionable intelligence with the relevant response guides from the ERG and the associated hazard placards.

5. Conclusion

This work presented an AI-enabled tool to help first responders select the most appropriate emergency response guide from the ERG guidebook based on effluent data collected using FTIR. The proposed tool leveraged a MTSC model named MultiRocket to detect five fire hazards, namely the flammability, toxicity, explosivity, corrosiveness and oxidizing properties of the fire effluents. The MultiRocket model was trained with data samples collected by FTIR from burning tests in cone calorimeter. Using the predictions made by the model, the software can display the hazard imposed by the fire effluents and the corresponding guides from the ERG. By using data-driven algorithms to provide actionable intelligence to the first responders, this AI-enabled tool will better protect the first responders and the environment when the scientific expertise is absent in an emergency response scenario.

The proposed AI-enabled tool requires further enhancements and testing before it can be deployed. In this study, we were limited by a small dataset with only 38 data samples and all samples were obtained from small-scale testing. As a result, further data collection from both small and large scale testing in addition to real-world incidents is required. Moreover, the developing and deploying of a ML model to support decision-making requires creating a tolerance level for risks. For example, at what classification accuracy do we accept the ML model as accurate and safe to deploy to a real-world scenario? As future work, we will continue to improve the dataset used to train the ML models, and explore the idea of risk tolerance in the performance of ML models. These tasks will allows us to eventually deploy the AI-enabled tool to the field and support first responders when they encounter unlabeled, burning goods.

6. Acknowledgement

This project was supported by collaborative research funding from the National Research Council of Canada's Artificial Intelligence for Logistics Program.

References

2020 Emergency Response Guidebook (2020), Transport Canada.

Chen, Y., Serio, M. & Sathyamoorthy, S. (2000), 'Development of a fire detection system using ft-ir spectroscopy and artificial neural networks', *Fire Safety Science* **6**, 791–802.

Company, T. Q. (n.d.), 'The qt company'.

URL: *https://www.qt.io/company*

Garrity, D. J. & Yusuf, S. A. (2021), 'A predictive decision-aid device to warn firefighters of catastrophic temperature increases using an ai-based time-series algorithm', *Safety Science* **138**, 105237. **URL:** *https://www.sciencedirect.com/science/article/pii/S0925753521000825*

Jain, P., Coogan, C., Subramanian, S. G., Crowley, M., Taylor, S. & Flannigan, M. D. (2020), 'A review of machine learning applications in wildfire science and management', *Environmental Reviews* .

Jiang, L., Mensah, R. A., Asante-Okyere, S., F¨orsth, M., Xu, Q., Ziggah, Y. Y., Restas, A., Berto, F. & Das, O. (2021), 'Developing an artificial intelligent model for predicting combustion and flammability properties', *Fire and Materials* .

URL: *https://onlinelibrary.wiley.com/doi/10.1002/fam.3030?af=R*

Kim, Y. C., Yu, H.-G., Lee, J.-H., Park, D.-J. & Nam, H.-W. (2017), Hazardous gas detection for FTIRbased hyperspectral imaging system using DNN and CNN, *in* D. A. Huckridge, R. Ebert & H. Bu¨rsing, eds, 'Electro-Optical and Infrared Systems: Technology and Applications XIV', Vol. 10433, International Society for Optics and Photonics, SPIE, pp. 341 – 349. **URL:** *https://doi.org/10.1117/12.2279077*

LeCun, Y., Bengio, Y. & Hinton, G. (2015), 'Deep learning', *nature* **521**(7553), 436–444.

L¨oning, M., Bagnall, A., Ganesh, S., Kazakov, V., Lines, J. & Kir´aly, F. (2019), 'sktime: A unified interface for machine learning with time series'.

Mohammed, R., Rawashdeh, J. & Abdullah, M. (2020), Machine learning with oversampling and undersampling techniques: Overview study and experimental results, *in* '2020 11th International Conference on Information and Communication Systems (ICICS)', pp. 243–248.

Myles, A. J., Feudale, R. N., Liu, Y., Woody, N. A. & Brown, S. D. (2004), 'An introduction to decision tree modeling', *Journal of Chemometrics: A Journal of the Chemometrics Society* **18**(6), 275–285.

Nazer, M. Z. (2021), 'Mechanistically informed machine learning and artificial intelligence in fire engineering and sciences', *Fire Technology* **57**, 2741–2784.

QMAKE project files: QT 4.8 (n.d.).

URL: *https://doc.qt.io/archives/qt-4.8/qmake-project-files.html*

QT Group Oyj Managers' transactions (n.d.).

URL: *https://www.qt.io/stock/qt-group-oyj-managers-transactions-1491998400000*

Tan, C. W., Dempster, A., Bergmeir, C. & Webb, G. I. (2021), 'MultiRocket: Multiple pooling operators and transformations for fast and effective time series classification', *arxiv:2102.00457* .

Tian, S., Lee, C.-G., Xi, D. D., Ko, Y. & Elsagan, N. (2021), 'Prediction of emergency response strategies based on combustion signatures from ftir spectroscopy using machine learning techniques', *Canadian & Cold Regions Rail Research Conference* .

VANDANA, T. S. & VISHWANATH, M. (2016), 'Wireless network control system for environment monitoring using linux os', *International Journal of Advanced Technology and Innovative Research* **08**(06), 1066–1069.

Zheng, Z., Lin, X., Yang, M., He, Z., Bao, E., Zhang, H. & Tian, Z. (2020), 'Progress in the application of machine learning in combustion studies', *ES Energy & Environment* **9**, 1–14. **URL:** *http://dx.doi.org/10.30919/esee8c795*

Zhou, L., Song, Y., Ji, W. & Wei, H. (2022), 'Machine learning for combustion', *Energy and AI* **7**, 100128.

URL: *https://www.sciencedirect.com/science/article/pii/S2666546821000756*

Appendix A AI-Enabled Software: DataLoad Window

The DataLoad window is the first window displayed to the first responder when the Fire Safety software is initiated. As shown in Figure 4, the DataLoad window requests the first responder to place the new data sample (which will be a *.prn* file produced by the FTIR software) measured at the scene of a fire into a specific folder. Then, the first responder will click on the "Run Model" button. This button prompts the software to read the data from the folder, run the machine-learning model to predict the fire hazards identified, and generate visualizations of the chemicals found in the data sample (which we call parts per million or PPM plots). The process took around one minute to run. While running the program in the backend, the progress will be printed on the text box below the buttons. Once the message "ML prediction model is done" is displayed, the user may click on the "Show Result" button, which will direct the user to the main window of the proposed AI tool, the Result Display window.

Figure 4: DataLoad window

Unsupervised few-shot learning

Kuilin Chen

Introduction

Few-shot learning (Fei-Fei et al., 2006) aims to learn a new classification or regression model on a novel task that is not seen during training, given only a few examples in the novel task. Existing few-shot learning methods either rely on episodic meta-learning (Finn et al., 2017; Snell et al., 2017) or standard pretraining (Chen et al., 2019; Tian et al., 2020b) in a supervised manner to extract transferrable knowledge to a new few-shot task. Unfortunately, these methods require many labeled meta-training samples. Acquiring a lot of labeled data is costly or even impossible in practice. Recently, several unsupervised meta-learning approaches have attempted to address this problem by constructing synthetic tasks on unlabeled meta-training data (Hsu et al., 2019; Khodadadeh et al., 2019; 2021) or meta-training on self-supervised pretrained features (Lee et al., 2021a). However, the performance of unsupervised meta-learning approaches is still far from their supervised counterparts. Empirical studies in supervised pretraining show that representation learning via grouping similar samples together (Chen et al., 2019; Tian et al., 2020b; Dhillon et al., 2020; Laenen & Bertinetto, 2021) outperforms a wide range of episodic meta-learning methods, where the definition of similar samples is given by class labels. The motivation of this study is to develop an unsupervised representation learning method by grouping unlabeled meta-training data without episodic training and close the performance gap between supervised and unsupervised few-shot learning.

Contrastive self-supervised learning has shown remarkable success in learning representation from unlabeled data, which is competitive with supervised learning on multiple visual tasks (Tian et al., 2020a; H ´enaff et al., 2020). The common underlying theme behind contrastive learning is to pull together representation of augmented views of the same training sample (positive sample) and disperse representation of augmented views from different training samples (negative sample) (Wu et al., 2018; Wang & Isola, 2020). Typically, contrastive learning methods require a large size of negative samples to learn high-quality representation from unlabeled data (Chen et al., 2020; He et al., 2020). This inevitably requires a large batch size of samples, demanding significant computing resources. Non-contrastive methods try to overcome the issue by accomplishing self-supervised learning with only positive pairs. However, non-contrastive methods suffer from trivial solutions where the model maps all inputs to the same constant vector, known as the collapsed representation. Various methods have been proposed to avoid collapsed representation on an ad hoc basis, such as asymmetric network architecture

(Grill et al., 2020), stop gradient (Chen & He, 2021), and feature decorrelation (Ermolov et al., 2021; Zbontar et al., 2021; Hua et al., 2021). However, theoretical understanding about how non-contrastive methods avoid collapsed representation is limited, though some preliminary attempts are made to analyze the training dynamics of non-contrastive methods (Tian et al., 2021). Besides, most self-supervised learning methods focus on the linear evaluation task where the training and test data come from the same classes. They do not account for the domain gap between training and test classes, which is the case in few-shot learning and cross-domain few-shot learning.

We develop a novel unsupervised representation learning method for few-shot learning. The proposed method significantly closes the performance gap between unsupervised and supervised few-shot learning methods.

Methodology

Given an unlabeled training dataset, we augment each training sample using the augmentations defined in SimCLR. We Euclidean distance between the representation of positive pairs within a mini-batch

$$L_{trace} = E_{z,z+}||z - z_{+}||\text{^}2$$

where z and z+ are representation of augmented views from the same image. In addition, we also minimize the mean squared error on off-diagonal entries of the covariance matrix

$$L_{const} = \sum_{k=1}^{K} \sum_{l=1, l \neq k}^{K} c_{kl}$$

where c_{kl} is an entry of the covariance matrix. The total loss function is

$$L = L_{trace} + \gamma L_{const}$$

where γ is the weight to balance two loss terms.

Results

We conduct few-shot classification experiments on three widely used few-shot image recognition benchmarks.

miniImageNet is a 100-class subset of the original ImageNet dataset (Deng et al., 2009) for few-shot learning (Vinyals et al., 2016). miniImageNet is split into 64 training classes, 16 validation classes, and 20 testing classes, following the widely used data splitting protocol (Ravi and Larochelle, 2017).

FC100 is a derivative of CIFAR-100 with minimized overlapped information between train classes and test classes by grouping the 100 classes into 20 superclasses (Oreshkin et al., 2018). They are further split into 60 training classes (12 superclasses), 20 validation classes (4 superclasses), and 20 test classes (4 superclasses).

miniImageNet to CUB is a cross-domain few-shot classification task, where the models are trained on miniImageNet and tested on CUB (Welinder et al., 2010). Cross-domain few-shot classification is more challenging due to the big domain gap between two datasets. We can better evaluate the generalization capability in different algorithms. We follow the experiment setup in (Yue et al., 2020).

The feature extractor contains two components: a backbone network and a projection network. The backbone network can be a variant of ResNet architecture (He et al., 2016). The projection network is a 3-layer MLP with batch normalization and ReLU activation. The dimension of each layer in the projection MLP is 2048. We use the same augmentations defined in SimCLR (Chen et al., 2020), including horizontal flip, Gaussian blur, color jittering, and random cropping.

We use ResNet12 (Lee et al., 2019, Ravichandran et al., 2019) and WRN-28-10 (Yue et al., 2020) as the backbone networks for few-shot learning and cross-domain few-shot learning, respectively. Those two backbone networks are selected because they are widely used in SOTA few-shot learning methods. The feature extractor is trained on unlabeled meta-training data by the SGD optimizer (momentum of 0.9 and weight decay of 5e-4) with a mini-batch size of 128. The learning rate starts at 0.05 and decreases to 0 with a cosine schedule. The projection network in the feature extractor is discarded after training on unlabeled data.

During meta-testing, we train a regularized logistic regression model using 5 or 25 support samples on frozen representations after the global average pooling layer in the backbone network. Each few-shot task contains 5 classes and 75 query samples. The classification accuracy is evaluated on the query samples.

Table 1: Few-shot classification results on miniImageNet and FC100.

Method	Backbone	miniImageNet 5-way		FC100 5-way	
		1-shot	5-shot	1-shot	5-shot
Supervised					
Proto Net (Snell et al., 2017)	ResNet-12	60.37 ± 0.83	78.02 ± 0.57	41.5 ± 0.7	57.0 ± 0.7
MAML (Finn et al., 2017)	ResNet-12	56.58 ± 1.84	70.85 ± 0.91	36.9 ± 0.6	51.2 ± 0.7
TADAM (Oreshkin et al., 2018)	ResNet-12	58.50 ± 0.30	76.70 ± 0.30	40.1 ± 0.4	56.1 ± 0.4
Baseline++ (Chen et al., 2019)	ResNet-12	60.83 ± 0.81	77.81 ± 0.76	41.3 ± 0.7	58.7 ± 0.7
MetaOptNet (Lee et al., 2019)	ResNet-12	62.64 ± 0.61	78.63 ± 0.46	41.1 ± 0.6	55.5 ± 0.6
Unsupervised					
CACTUs-MAML (Hsu et al., 2019)	ResNet-12	49.41 ± 0.92	63.72 ± 0.83	31.3 ± 0.8	45.7 ± 0.8
UMTAR (Khodadadeh et al., 2019)	ResNet-12	49.62 ± 0.91	62.43 ± 0.84	31.5 ± 0.8	45.3 ± 0.8
Meta-GMVAE (Lee et al., 2021)	ResNet-12	55.93 ± 0.85	74.28 ± 0.72	36.3 ± 0.7	49.7 ± 0.7
SimCLR (Chen et al., 2020)	ResNet-12	55.76 ± 0.88	75.59 ± 0.69	36.2 ± 0.7	49.9 ± 0.7
MoCo v2 (He et al., 2020)	ResNet-12	57.73 ± 0.84	77.51 ± 0.63	37.7 ± 0.7	53.2 ± 0.7
BYOL (Grill et al., 2020)	ResNet-12	56.17 ± 0.89	76.17 ± 0.66	37.2 ± 0.7	52.8 ± 0.6
Barlow Twins (Zbontar et al., 2021)	ResNet-12	57.79 ± 0.89	77.42 ± 0.66	37.9 ± 0.7	54.1 ± 0.6
Ours	ResNet-12	59.47 ± 0.87	78.79 ± 0.58	39.7 ± 0.7	57.9 ± 0.7

Table 2: Cross-domain few-shot classification results on miniImageNet to CUB.

Method	Backbone	miniImageNet to CUB 5-way	
		1-shot	5-shot
Supervised			
MAML (Finn et al., 2017)	WRN-28-10	39.06 ± 0.47	55.04 ± 0.42
LEO (Rusu et al., 2019)	WRN-28-10	41.45 ± 0.54	56.66 ± 0.48
MTL (Sun et al., 2019)	WRN-28-10	43.15 ± 0.44	56.89 ± 0.41
Matching Net (Vinyals et al., 2016)	WRN-28-10	42.04 ± 0.57	53.08 ± 0.45
SIB (Hu et al., 2020)	WRN-28-10	43.27 ± 0.44	59.94 ± 0.42
Baseline (Chen et al., 2019)	WRN-28-10	42.89 ± 0.41	62.12 ± 0.40
Unsupervised			
CACTUs-MAML (Hsu et al., 2019)	WRN-28-10	33.48 ± 0.49	49.97 ± 0.41
UMTAR (Khodadadeh et al., 2019)	WRN-28-10	33.59 ± 0.48	50.21 ± 0.45
Meta-GMVAE (Lee et al., 2021)	WRN-28-10	38.09 ± 0.47	55.65 ± 0.42
SimCLR (Chen et al., 2020)	WRN-28-10	38.25 ± 0.49	55.89 ± 0.46
MoCo v2 (He et al., 2020)	WRN-28-10	39.29 ± 0.47	56.49 ± 0.44
BYOL (Grill et al., 2020)	WRN-28-10	40.63 ± 0.46	56.92 ± 0.43
Barlow Twins (Zbontar et al., 2021)	WRN-28-10	40.46 ± 0.47	57.16 ± 0.42
Ours	WRN-28-10	41.08 ± 0.48	58.86 ± 0.45

The results of the proposed method and previous few-shot learning methods using similar backbones are reported in Table 1. The proposed method outperforms existing unsupervised few-shot learning methods such as CACTUS (Hsu et al., 2019) and UMTAR (Khodadadeh et al., 2019) by a large margin. It demonstrates that high-quality representation for downstream few-shot tasks can be learned from unlabeled meta-training data without episodic training. Our method is in the category of self-supervised representation learning like SimCLR (Chen et al., 2020), MoCo v2 (He et al., 2020), BYOL (Grill et al., 2020), and Barlow Twins (Zbontar et al., 2021) as it does not perform episodic learning. SimCLR achieves weaker performance than other self-supervised learning methods because it typically requires very large batch sizes to perform well. Although Meta-GMVAE (Lee et al., 2021) performs unsupervised meta-learning on top of the pretrained features from SimCLR, the performance gain versus vanilla representation from SimCLR is at most marginal when deep backbones are used in our reproduction. This observation aligns with the empirical results in supervised few-shot learning where the advantage of episodic meta-learning diminishes as the backbone becomes deep (Chen et al., 2019, Tian et al., 2020b). Our method is also compared with some strong baselines in supervised few-shot learning. The performance gap between supervised and unsupervised few-shot learning is significantly reduced by our method, compared with previous results in unsupervised few-shot learning (Hsu et al., 2019, Khodadadeh et al., 2019, Lee et al., 2021).

Our method is also applied to the cross-domain few-shot classification task as summarized in Table 2. The proposed method outperforms other unsupervised methods in this challenging task, indicating that the learned representation has strong generalization capability. We use the same hyperparameters (training epochs, learning rate, etc.) from in-domain few-shot learning to train the model. The strong results indicate that our method is robust to hyperparameter choice. Although meta-learning methods with adaptive embeddings are expected to perform better than a fixed embedding when the domain gap between base classes and novel classes is large, empirical results show that a fixed embedding from supervised or unsupervised pretraining achieves better performance in both cases. (Tian et al., 2020b) also reports similar results that a fixed embedding from supervised pretraining shows superior performance on a large-scale cross-domain few-shot classification dataset. We still believe that adaptive embeddings should be helpful when the domain gap between base and novel classes is large. Nevertheless, how to

properly train a model on unlabeled meta-training training to obtain useful adaptive embeddings in novel tasks is an open question.

References

Francis R Bach and Michael I Jordan. Learning spectral clustering, with application to speech separation. The Journal of Machine Learning Research, 7:1963–2001, 2006.

Mikhail Belkin and Partha Niyogi. Laplacian eigenmaps for dimensionality reduction and data representation. Neural computation, 15(6):1373–1396, 2003.

Ting Chen, Simon Kornblith, Mohammad Norouzi, and Geoffrey Hinton. A simple framework for contrastive learning of visual representations. In International conference on machine learning, pages 1597–1607. PMLR, 2020.

Wei-Yu Chen, Yen-Cheng Liu, Zsolt Kira, Yu-Chiang Frank Wang, and Jia-Bin Huang. A closer look at few-shot classification. In International Conference on Learning Representations, 2019.

Xinlei Chen and Kaiming He. Exploring simple siamese representation learning. In Proceedings of the IEEE/CVF Conference on Computer Vision and Pattern Recognition, 2021.

Adam Coates, Andrew Ng, and Honglak Lee. An Analysis of Single Layer Networks in Unsupervised Feature Learning. In AISTATS, 2011.

Jia Deng, Wei Dong, Richard Socher, Li-Jia Li, Kai Li, and Li Fei-Fei. Imagenet: A large-scale hierarchical image database. In 2009 IEEE conference on computer vision and pattern recognition, pages 248–255. Ieee, 2009.

Guneet Singh Dhillon, Pratik Chaudhari, Avinash Ravichandran, and Stefano Soatto. A baseline for few-shot image classification. In International Conference on Learning Representations, 2020.

Aleksandr Ermolov, Aliaksandr Siarohin, Enver Sangineto, and Nicu Sebe. Whitening for self-supervised representation learning. In International Conference on Machine Learning, pages 3015–3024. PMLR, 2021.

Li Fei-Fei, Rob Fergus, and Pietro Perona. One-shot learning of object categories. IEEE transactions on pattern analysis and machine intelligence, 28(4):594–611, 2006.

Chelsea Finn, Pieter Abbeel, and Sergey Levine. Model-agnostic meta-learning for fast adaptation of deep networks. In Proceedings of the 34th International Conference on Machine Learning-Volume 70, pages 1126–1135. JMLR. org, 2017.

Jean-Bastien Grill, Florian Strub, Florent Altché, Corentin Tallec, Pierre H Richemond, Elena Buchatskaya, Carl Doersch, Bernardo Avila Pires, Zhaohan Daniel Guo, Mohammad Gheshlaghi Azar, et al. Bootstrap your own latent: A new approach to self-supervised learning. In Proceedings of the 33nd International Conference on Neural Information Processing Systems, 2020.

Kaiming He, Xiangyu Zhang, Shaoqing Ren, and Jian Sun. Deep residual learning for image recognition. In Proceedings of the IEEE conference on computer vision and pattern recognition, pages 770–778, 2016.

Kaiming He, Haoqi Fan, Yuxin Wu, Saining Xie, and Ross Girshick. Momentum contrast for unsupervised visual representation learning. In Proceedings of the IEEE/CVF Conference on Computer Vision and Pattern Recognition, pages 9729–9738, 2020.

Olivier J Hénaff, Aravind Srinivas, Jeffrey De Fauw, Ali Razavi, Carl Doersch, SM Eslami, and Aaron van den Oord. Data-efficient image recognition with contrastive predictive coding. In International Conference on Machine Learning, pages 4182–4192. PMLR, 2020.

Kyle Hsu, Sergey Levine, and Chelsea Finn. Unsupervised learning via meta-learning. In International Conference on Learning Representations, 2019.

Shell Xu Hu, Pablo Garcia Moreno, Yang Xiao, Xi Shen, Guillaume Obozinski, Neil Lawrence, and Andreas Damianou. Empirical bayes transductive meta-learning with synthetic gradients. In International Conference on Learning Representations, 2020.

Tianyu Hua, Wenxiao Wang, Zihui Xue, Sucheng Ren, Yue Wang, and Hang Zhao. On feature decorrelation in self-supervised learning. In Proceedings of the IEEE/CVF International Conference on Computer Vision, pages 9598–9608, 2021.

Tero Karras, Samuli Laine, and Timo Aila. A style-based generator architecture for generative adversarial networks. In Proceedings of the IEEE/CVF Conference on Computer Vision and Pattern Recognition, pages 4401–4410, 2019.

Siavash Khodadadeh, Ladislau Boloni, and Mubarak Shah. Unsupervised meta-learning for few-shot image classification. In Advances in neural information processing systems, 2019.

Siavash Khodadadeh, Sharare Zehtabian, Saeed Vahidian, WeijiaWang, Bill Lin, and Ladislau Boloni. Unsupervised meta-learning through latent-space interpolation in generative models. In International Conference on Learning Representations, 2021.

A Krizhevsky. Learning Multiple Layers of Features from Tiny Images. PhD thesis, University of Toronto, 2009.

Steinar Laenen and Luca Bertinetto. On episodes, prototypical networks, and few-shot learning. In Advances in Neural Information Processing Systems, 2021.

Dong Bok Lee, Dongchan Min, Seanie Lee, and Sung Ju Hwang. Meta-gmvae: Mixture of gaussian vae for unsupervised meta-learning. In International Conference on Learning Representations, 2021.

Kwonjoon Lee, Subhransu Maji, Avinash Ravichandran, and Stefano Soatto. Meta-learning with differentiable convex optimization. In Proceedings of the IEEE Conference on Computer Vision and Pattern Recognition, pages 10657–10665, 2019.

Marina Meila. Spectral clustering: a tutorial for the 2010's. Handbook of cluster analysis, pages 1–23, 2016.

Marina Meila and Jianbo Shi. Learning segmentation by random walks. In Advances in neural information processing systems, volume 13, pages 873–879, 2000.

Tomás Mikolov, Kai Chen, Greg Corrado, and Jeffrey Dean. Efficient estimation of word representations in vector space. In Yoshua Bengio and Yann LeCun, editors, 1st International Conference on Learning Representations, ICLR 2013, 2013.

Boris Oreshkin, Pau Rodríguez López, and Alexandre Lacoste. Tadam: Task dependent adaptive metric for improved few-shot learning. In Advances in Neural Information Processing Systems, pages 721–731, 2018.

Sachin Ravi and Hugo Larochelle. Optimization as a model for few-shot learning. In 5th International Conference on Learning Representations, ICLR 2017, Toulon, France, April 24-26, 2017, Conference Track Proceedings. OpenReview.net, 2017.

Avinash Ravichandran, Rahul Bhotika, and Stefano Soatto. Few-shot learning with embedded class models and shot-free meta training. In Proceedings of the IEEE International Conference on Computer Vision, pages 331–339, 2019.

Andrei A Rusu, Dushyant Rao, Jakub Sygnowski, Oriol Vinyals, Razvan Pascanu, Simon Osindero, and Raia Hadsell. Meta-learning with latent embedding optimization. In International Conference on Learning Representations, 2019.

Jianbo Shi and Jitendra Malik. Normalized cuts and image segmentation. IEEE Transactions on pattern analysis and machine intelligence, 22(8):888–905, 2000.

Jake Snell, Kevin Swersky, and Richard Zemel. Prototypical networks for few-shot learning. In Advances in Neural Information Processing Systems, pages 4077–4087, 2017.

Qianru Sun, Yaoyao Liu, Tat-Seng Chua, and Bernt Schiele. Meta-transfer learning for few-shot learning. In Proceedings of the IEEE conference on computer vision and pattern recognition, pages 403–412, 2019.

Yonglong Tian, Dilip Krishnan, and Phillip Isola. Contrastive multiview coding. In ECCV 2020, pages 776–794. Springer International Publishing, 2020a.

Yonglong Tian, Yue Wang, Dilip Krishnan, Joshua B Tenenbaum, and Phillip Isola. Rethinking fewshot image classification: a good embedding is all you need? In European conference on computer vision. Springer, 2020b.

Yuandong Tian, Xinlei Chen, and Surya Ganguli. Understanding self-supervised learning dynamics without contrastive pairs. In Marina Meila and Tong Zhang, editors, Proceedings of the 38th International Conference on Machine Learning, ICML 2021, 18-24 July 2021, Virtual Event, volume 139 of Proceedings of Machine Learning Research, pages 10268–10278. PMLR, 2021.

Vikas Verma, Alex Lamb, Christopher Beckham, Amir Najafi, Ioannis Mitliagkas, David Lopez-Paz, and Yoshua Bengio. Manifold mixup: Better representations by interpolating hidden states. In International Conference on Machine Learning, pages 6438–6447. PMLR, 2019.

Oriol Vinyals, Charles Blundell, Timothy Lillicrap, Daan Wierstra, et al. Matching networks for one shot learning. In Advances in neural information processing systems, pages 3630–3638, 2016.

Tongzhou Wang and Phillip Isola. Understanding contrastive representation learning through alignment and uniformity on the hypersphere. In International Conference on Machine Learning, pages 9929–9939. PMLR, 2020.

P. Welinder, S. Branson, T. Mita, C. Wah, F. Schroff, S. Belongie, and P. Perona. Caltech-UCSD Birds 200. Technical Report CNS-TR-2010-001, California Institute of Technology, 2010.

Zhirong Wu, Yuanjun Xiong, Stella X Yu, and Dahua Lin. Unsupervised feature learning via nonparametric instance discrimination. In Proceedings of the IEEE conference on computer vision and pattern recognition, pages 3733–3742, 2018.

Shuo Yang, Lu Liu, and Min Xu. Free lunch for few-shot learning: Distribution calibration. In International Conference on Learning Representations, 2021.

Zhongqi Yue, Hanwang Zhang, Qianru Sun, and Xian-Sheng Hua. Interventional few-shot learning. Advances in Neural Information Processing Systems, 33, 2020.

Jure Zbontar, Li Jing, Ishan Misra, Yann LeCun, and Stéphane Deny. Barlow twins: Self-supervised learning via redundancy reduction. In Proceedings of the 38th International Conference on Machine Learning, ICML 2021, 18-24 July 2021, Virtual Event, volume 139 of Proceedings of Machine Learning Research, pages 12310–12320. PMLR, 2021.

KPI Study for Mining Industry:
Eliminate the Communication Gaps Within Organizations
Final Report

Gabriel Marisanu, Danmeng Cui
University of Toronto
April 20, 2022

Table of Contents

Introduction

Within the mining industry, the library of KPIs has not kept up with data that has become increasingly available through digitization, therefore leading to an overuse of lagging performance indicators. Additionally, due to the fact that strategic corporate goals are oftentimes built on the basis of soft or perceptual measures from stakeholders, which are subjective in nature, organizations struggle with the process of linking strategic level goals to KPIs on the shop floor. Therefore, creating a communication gap between technical teams and senior management. As a consequence, maintenance leaders have a difficult time demonstrating the added value that maintenance activities create with an organization, leading to challenges in securing the resources required for things such as continuous improvement projects.

In order to address these challenges, this report will be investigating a holistic approach that can be leveraged to develop maintenance KPIs that are integrated into corporate strategic goals, as well as identify time series models that achieve high accuracy on small datasets in order to improve organizational forecasting. Through achieving these goals the intended outcome is to create a more contemporary data driven methodology for selecting organizational KPIs, as well as directly demonstrating the added value that the various business units create within the organization.

An Approach to Developing Maintenance KPIs

Maintenance is the combination of all technical and administrative actions required to maintain or restore equipment to a state where it can perform its intended function [1]. Therefore, an effective maintenance performance measurement (MPM) system must evaluate the total maintenance effectiveness, which consists of two components: internal effectiveness and external effectiveness [1]. The term internal effectiveness refers to performance measures that are typically measured in terms of cost effectiveness and productivity. A traditional measurement of internal effectiveness is OEE, which is a reflection of availability, performance speed, and quality [1]. As the name suggests, external effectiveness refers to performance measures that evaluate the organization's ability to deliver the type of maintenance that is required to meet client needs (i.e the long term impact on profitability) [1].

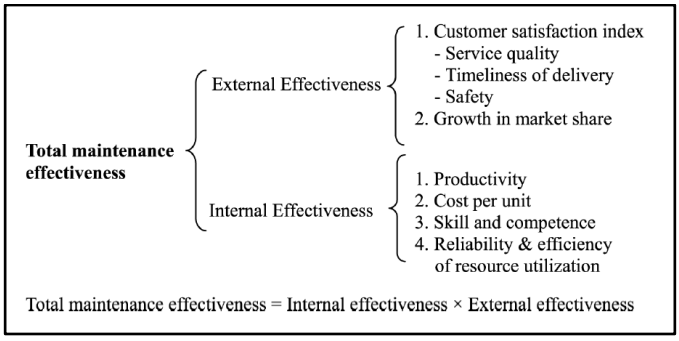

Fig 1. Total Maintenance Effectiveness [1]

As a consequence, in order to drive high level corporate goals, the maintenance strategy must be derived and integrated with the overall corporate strategy of the organization [2].

The first step to achieving this is known as maintenance process mapping, which is critical in understanding the existing workflow of current maintenance and operations tasks [3]. This is then followed by an interview stage that provides the opportunity to identify pain points and understand how the various departments such as production, maintenance, automation, and finance impact a maintenance task [3]. Once a clear scope has been established in the two previous stages, existing KPIs can be identified that link back to the higher-level corporate objectives of the organization. It is important to highlight that during this stage KPIs providing insights into both the internal and external maintenance performance of the organization must be leveraged to ensure a holistic approach to performance measurement [3]. Additionally, management must ensure that the selected metrics are SMART: specific, measurable, attainable, realistic, timely [1]. A few of the various categories of performance indicators that must be considered have been provided below:

- Equipment-Related Indicators
- Cost/Finance-Related Indicators
- Maintenance Task-Related Indicators
- Customer Satisfaction-Related Indicators
- Learning and Growth-Related Indicators
- Health and Safety Indicators
- Employee Satisfaction-Related Indicators

Lastly, it is important to highlight that strategic corporate goals are oftentimes built on the basis of soft or perceptual measures from stakeholders and are therefore subjective. In comparison, subjectivity decreases as moving down the hierarchical levels, with the greatest level of objectivity being found on the shop floor [2].

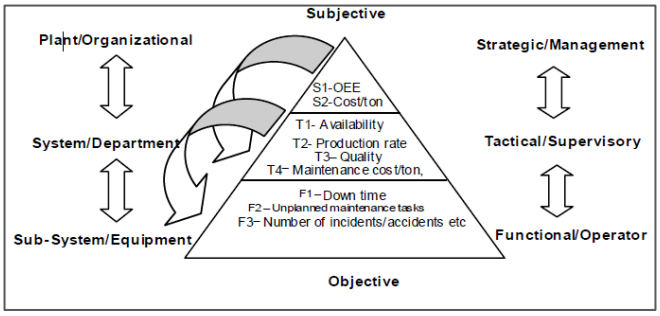

Fig 2. KPIs at the Various Levels of an Organization [2]

As a consequence, a strong value proposition must be established for new KPIs to ensure commitment from all levels of the organization. Additionally, to further strengthen the relationship between KPIs at the various hierarchical levels and strategic goals, efforts must be made to find a common language within the organization that streamlines the process of quantifying subjective goals. A potential solution to this is framing maintenance performance from the perspective of cost and organizational risk, as these are common areas of focus for senior management.

Findings from South African Mining Industry Case Study

To provide a better overview of current industry practices, the *South African Journal of Industrial Engineering* article published in 2012: "An Analysis of Maintenance Performance Systems in the South African Mining Industry", which was written by R.L.M Kotze & J.K Visser, was used.

The South African Mining Industry is primarily composed of diamonds, gold, platinum-group metals, ferrous & non-ferrous metals, coal, and various miscellaneous commodities [4]. In 2008, the output of the South African mining industry contributed 9.5% of GDP, therefore making it an integral part of the South African economy [4]. Considering that maintenance accounts for 20-50 % of the production costs within the mining industry, reducing maintenance expenditure by $1 million contributes as much to profits as increasing sales by $3 million and therefore also renders maintenance an equally integral part of the South African Economy.

Through conducting an email based survey, this article analyses the responses received from 72 engineering managers working within the South African mining industry [4]. Additionally, it is important to highlight that the survey respondents all worked at various mines within the country, meaning that the survey was able to capture the current state of maintenance practices at 72 out of 186 mines in South Africa [4].

Considering that the primary objective of this study was to determine if maintenance departments of mining organizations in South Africa leverage performance measurement effectively, several pain points were identified and highlighted as a focus for the purpose of this project.

The first critical finding from this article is that there is a reactive management approach to maintenance within the mining industry, with 6 out of the 10 most frequently used KPIs for maintenance performance measurement being lagging indicators [4].

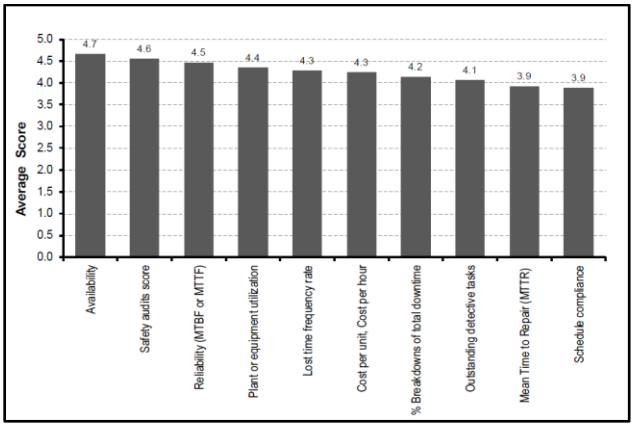

Fig 3. Indicators Used Most Often for Maintenance Performance Measurement [4]

Additionally, it must also be mentioned that there is a disconnect between the overall strategic goals of the organizations and the actions of the employees on the shop floor. This can be seen in the lack of motivation in performance management, employee ownership, and sense of contribution [4]. Considering that many of the survey respondents stated that they do not place a great importance on identifying KPIs for the different hierarchical levels within the organization,

this once again highlights the importance of leveraging the previously discussed holistic approach to *developing maintenance KPIs* [4].

Although academic literature indicates that the overall attitude towards maintenance has changed and it is generally accepted that an effective maintenance strategy adds value to an organization, based on this article it is clear that many organizations still operate on the 1950s to 2000s concept of maintenance and are relying on lagging performance indicators.

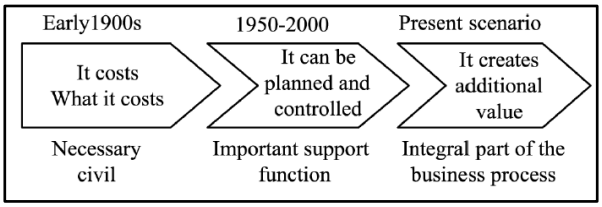

Fig 4. Paradigm Shift in Maintenance [1]

As a consequence, it can be concluded that organizations are struggling with linking strategic level goals to KPIs on the shop floor and there is an overwhelming use of lagging performance indicators. Considering that there is an abundance of data that is being generated by assets within the mining industry, there is an opportunity to resolve the previously mentioned communication gaps through developing more robust performance reporting solutions.

Challenges Associated with Implementing Predictive KPIs

Although the need for predictive performance tools is generally agreed upon, many organizations still struggle with the process of developing a strategic plan to implement data-driven solutions. The below table contains a brief summary of the questions that were encountered upon presenting the mid-term project findings to the consortium members during the bi-annual meeting held in December 2021.

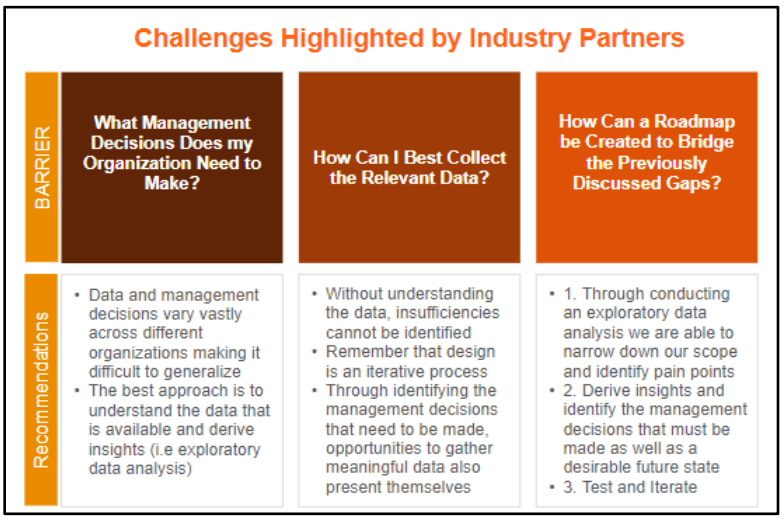

Fig 5. Challenges Associated with Implementing Predictive KPIs within an Organization

As a consequence, it is important to highlight that the implementation of a predictive KPI framework is an alignment of three key areas: people, process, and technology. Through

acknowledging the presence of this relationship, organizational leaders must also work towards standardizing data gathering procedures in order to create a trustworthy system that can be leveraged for decision making, as well as hiring and training qualified individuals to maintain the system.

Model Development

Currently a major challenge associated with developing predictive tools for evaluating performance within organizations is limited access to data. Considering that most KPIs are collected on a monthly or quarterly basis, the training sets for forecasting models are extremely limited. In order to address this challenge, the following time series models will be applied to a KPI dataset in order to identify which model performs best with limited training data: LSTM, Univariate Facebook Prophet, and Multivariate Facebook Prophet.

1. Data Preparation

Kinross Gold Corporation has provided a collection of Maintenance KPIs data for the CAT 793D mining truck, the data entries were updated on a monthly basis. The original dataset contained 161 entries, with 4 KPI entries (one entry for each individual truck) each month. To improve readability and simplify analysis, the average KPI score between the 4 trucks was calculated to reduce the dataset to 1 KPI value for each month. The final dataset contains 47 entries and 9 columns, which contains the following KPIs: MTTR (hrs), MTBF(hrs), % Effective Utilization, % of Late PMs, % of Weekly Schedule Compliance, % Cost from PMs, Practive Hours, Cost, % Proxy for Planned. ***Fig 1.1*** displays the header of the final Kinross maintenance dataset.

Date	Average of MTTR (hrs)	Average of MTBF (hrs)	Average of % effective utilization	Average of % OF Late PM'S	Average of % of weekly schedule compliance	Average of %cost from PM's (Y)	Average of practive hours	Average of Cost	Average of % proxy for planned
2013-06-01	2.342026	50.638074	0.614548	0.332143	0.666667	0.248940	66.000000	11982.085000	0.741071
2013-07-01	2.447439	44.741011	0.651945	0.290000	0.638333	0.562535	68.200000	5447.408000	0.717879
2013-08-01	4.733469	40.465127	0.430029	0.196429	0.535714	0.895239	90.500000	5748.085000	0.750000
2013-09-01	3.438239	31.977520	0.498614	0.091270	0.800000	0.587957	74.750000	4809.995000	0.761905
2013-10-01	5.739721	60.640284	0.636958	0.180556	0.622222	0.628922	71.666667	17492.263333	0.793447
2013-11-01	2.827191	63.182008	0.688126	0.263393	0.745042	0.726746	65.750000	4409.370000	0.782143

Fig 6. Header of Final Kinross Maintenance Dataset

In this study, the objective is to see how different factors impact the target variable Mean Time Between Failures (MTBF). ***Fig 1.2*** demonstrates how the MTBF changes over time. A strong decreasing trend can be observed after the month of January 2015. From ***Fig 1.3*** Kinross MTBF Decomposition Plot, there is a strong decreasing trend and seasonality component in the data, which will be further discussed when evaluating the Facebook Prophet model.

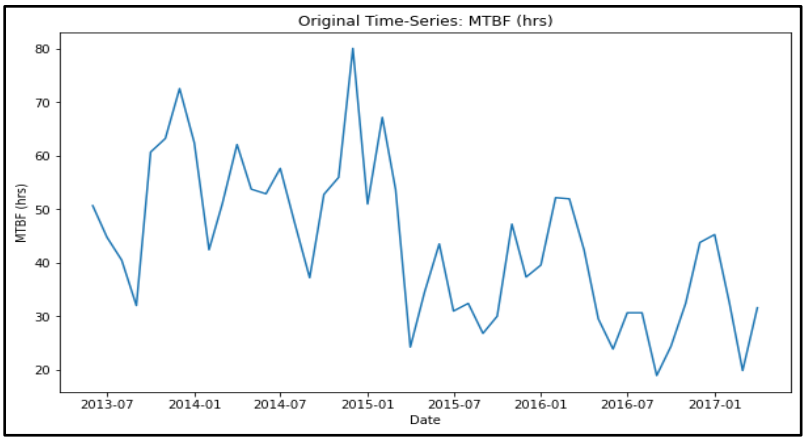

Fig 7. MTBF Change Over Time

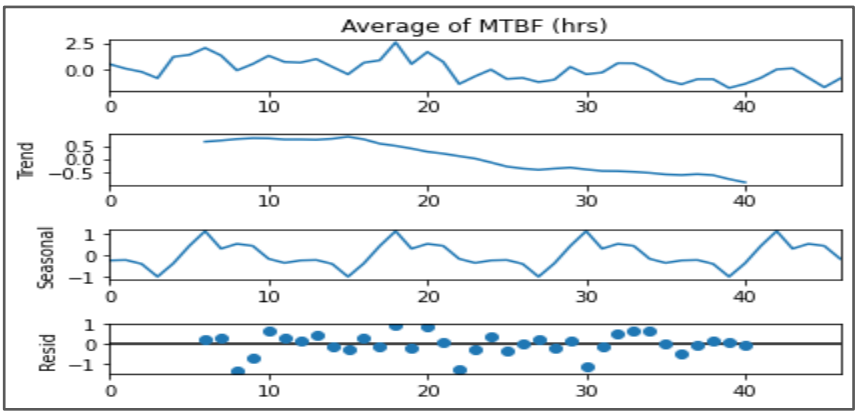

Fig 8. Kinross MTBF Decomposition Plot

To determine which feature has the greatest impact on the target variable MTBF, ***Fig 1.4*** displays the correlation matrix between each KPI. As a result, there are strong correlations between MTBF, % of Late PMs, % Cost from PM's, & Cost.

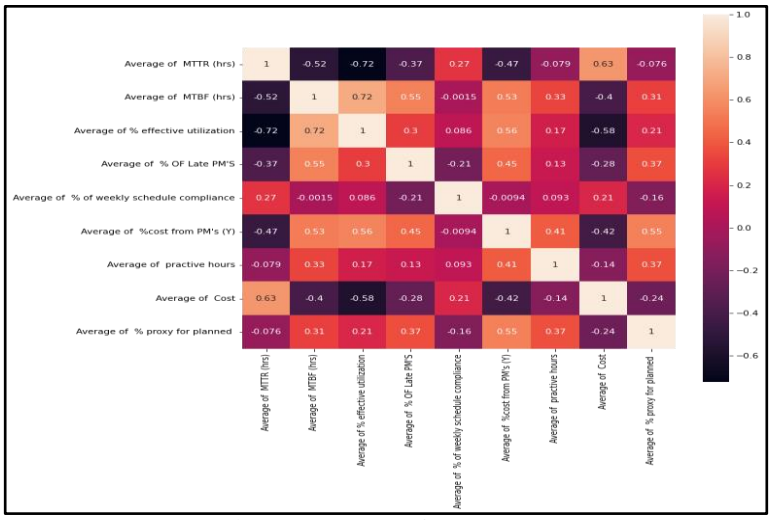

Fig 9. Correlation Matrix for Kinross Data KPIs

It is important to test stationarity before developing time-series models. The autocorrelation and partial-autocorrelation functions analyze a data set for statistical significance between the first data point and prior data points. Based on ***Fig 1.5***, it is unclear if the data is stationary or non-stationary, since non-stationary data typically shows significance between itself and its lagged values, and that significance decays to zero slowly.

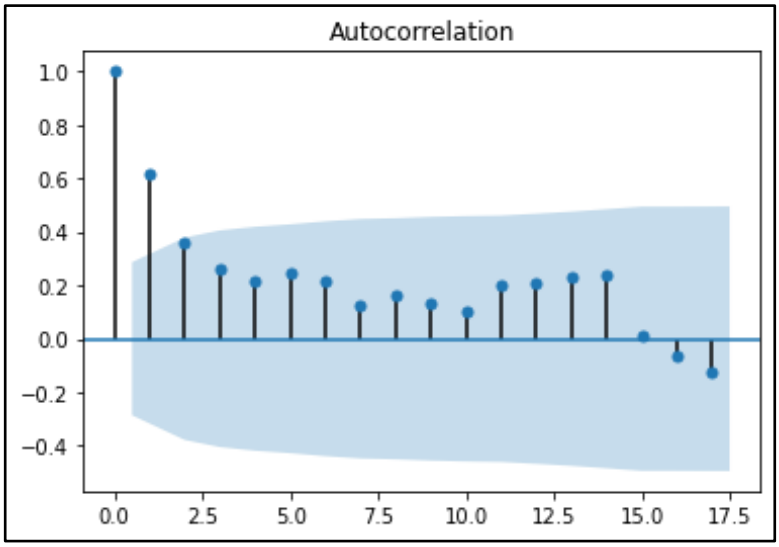

Fig 10. Autocorrelation Plot

LSTM and RNN models typically handle non-stationary data quite well when compared to a simple regression model such as ARIMA [7]. However, LSTM and RNN have been proven to perform better on stationary data [7], which is why a stationarity test, and performing the required transformations if it is not stationary is necessary. To further prove stationarity, Augmented dickey-fuller test and Kwiakowski-Phillips-Schmidt-Shin (KPSS) test were performed to verify if the time series is stationary. ***Fig 1.6*** shows the results of the ADF test and KPSS test, which all indicates the series is stationary.

	KPSS Statistic: 0.45
	num lags: 10
	Critial Values:
ADF Statistic: -3.17	10%, 0.35
Critial Values:	Critial Values:
1%, -3.58	5%, 0.46
Critial Values:	Critial Values:
5%, -2.93	2.5%, 0.57
Critial Values:	Critial Values:
10%, -2.60	1%, 0.74
p-value: 0.02	p-value: 0.06
Result: The series is stationary	Result: The series is stationary

Fig 11. ADF Test & KPSS Test

2. Univariate Long-Short-Term-Memory (LSTM) Model

LSTM models are based on recurrent neural networks, which are commonly used in the field of deep learning [8]. LSTM cells contain three primary components: an input gate, an output gate, and a forget gate, which regulate the flow of information through the cell [8]. Based on this architecture, LSTM models can keep, forget, or ignore data points based on a probabilistic model, therefore meaning that they are well-suited to generate predictions based on time series data. However, it must also be noted that due to limited literature available on this emerging methodology, implementation may prove to be more challenging when compared to a conventional ARIMA model [8].

The Tensorflow, Keras library was used to implement this LSTM model and the following parameters were used to generate time series predictions for the dataset:

Model Parameters	Parameter
Library	Tensorflow, Keras
Number of Neurons	200
Activation Function	ReLU
Optimizer	Adam
Loss Function	MSE

Fig 11. LSTM: Model Parameters

Additionally, a total of 250 epochs were used to train the model as indicated in the below figure:

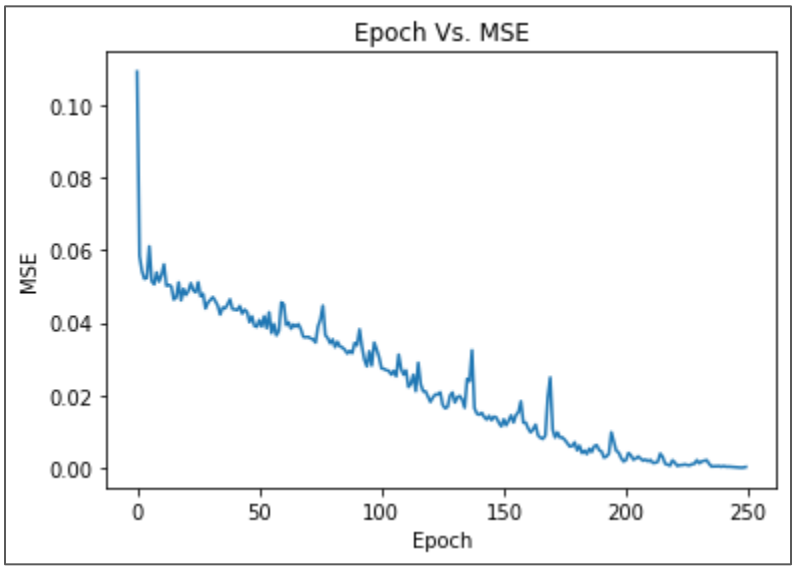

Fig 12. LSTM: Epoch Vs. MSE

Based on these parameters, the LSTM model was able to achieve a training RMSE of 16.27 and a testing RMSE of 24.61. As seen in the below chart, the model performs quite well up until January 2015, however; after this point it is clear that the model cannot capture the decreasing trend in the data.

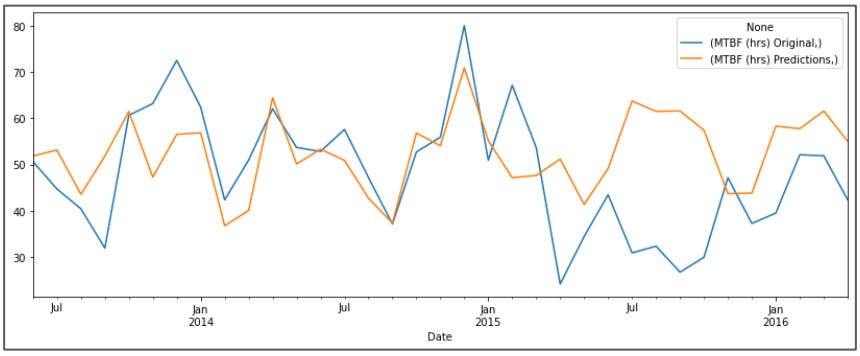

Fig 13. LSTM: Training Data Predict values vs. True values

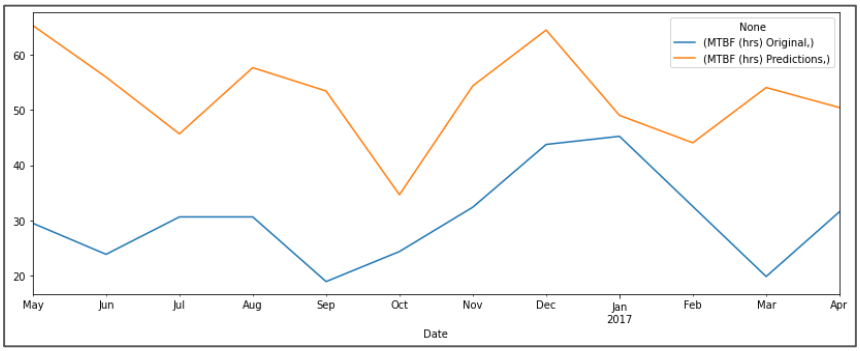

Fig 14. LSTM: Testing Data Predict Values vs. True Values

As seen in the above figure, the model was once again unable to capture the decreasing trend in the testing data. However, it must be noted that the model was able to capture the general variations in the data. For example, the model was able to predict that some sort of peak will occur in December 2016, however; it was not able to predict the exact value occurring at the peak.

3. Facebook Prophet Model

Facebook Prophet is a forecasting method based on an additive model that fits non-linear trends with yearly, monthly, and daily seasonality, as well as holiday effects [5]. It usually works best with time series that have strong seasonal effects and several seasons of historical data [5]. Prophet struggles with non-stationary data since it's difficult to determine the data's true seasonality and trend when the patterns are inconsistent. The Average of MTBF from June 2013 to April 2017 was plotted in ***Fig 3.1***, the Average of MTBF usually reaches the peak around the new year or the end of the year. It appears to be seasonal with a period of one year. Thus, the Facebook Prophet Model seems appropriate for our data.

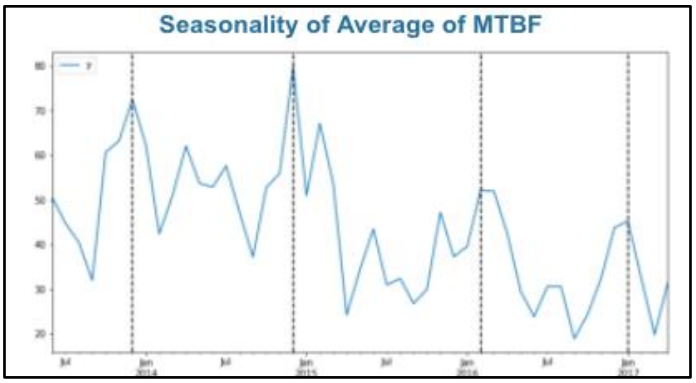

Fig 15. Seasonality of Average of MTBF

3.1 Univariate Facebook Prophet Model

The univariate Facebook Prophet Model consists of only one variable that changes over time [6]. The first step to perform prediction of Average of MTBF using univariate Facebook Prophet Model, is to split the dataset to train and test sets, which contains the first 35 data points (June 2013 - April 2016), and the rest 12 data points (May 2016 - April 2017), respectively. By fitting the train set into the single variate Facebook prophet model, and predict the whole data set. As shown in ***Table 3.1.1***, the orange line represents the true MTBFs from the original dataframe, and the forecast is the blue line with upper and lower bounds in a light blue shaded area.

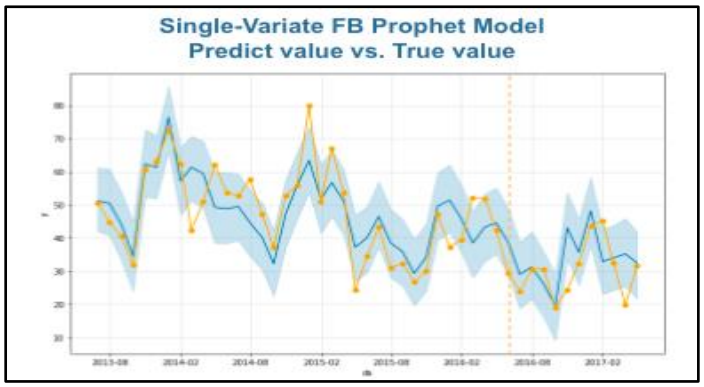

Fig 16. Single-Variate FB Prophet Model Predict value vs. True value

The Univariate Facebook Prophet Model yields a precise estimation for this dataset, the majority of the true MTBF data points can be captured in the predictive area. To further prove its accuracy, the RMSE is around 8.14. The RMSE for the train set is 7.94 and the test set is 8.70. Therefore, the univariate model is not overfitting or underfitting.

The component plots for the Univariate Facebook Prophet Model is shown in ***Table 3.1.2***, the overall trend for the average MTBF in this model has a decreasing trend over time. The yearly component shows that the average MTBF fluctuates every month, it usually increases dramatically at the end of each year.

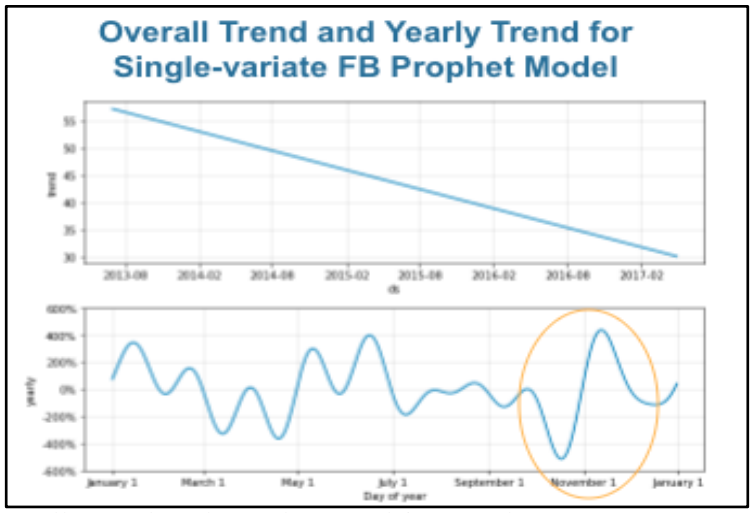

Fig 17. Overall Trend and Yearly Trend for Single-Variate FB Prophet Model

In this dataset, the Univariate Facebook Prophet Model appears to perform effectively. In the following section, the multivariate Facebook Prophet Model aims to determine whether there's any other parameter that has a substantial impact on predictions.

3.2 Multivariate Facebook Prophet Model

The multivariate Facebook Prophet Model allows to forecast the labelled output based on multiple features [9]. The first procedure is to incorporate all of the factors as regressors to evaluate the feature importance and follow the same steps as the univariate Facebook Prophet Model. ***Fig 3.2.1*** displays the prediction outcome.

The RMSE for the whole dataset is 6.95, RMSE for the train and test sets are 4.69 and 11.17, respectively. As a result, this model is overfitting since it predicted well in the train set interval after fitting it with the train set, but it has relatively poor accuracy in the test set.

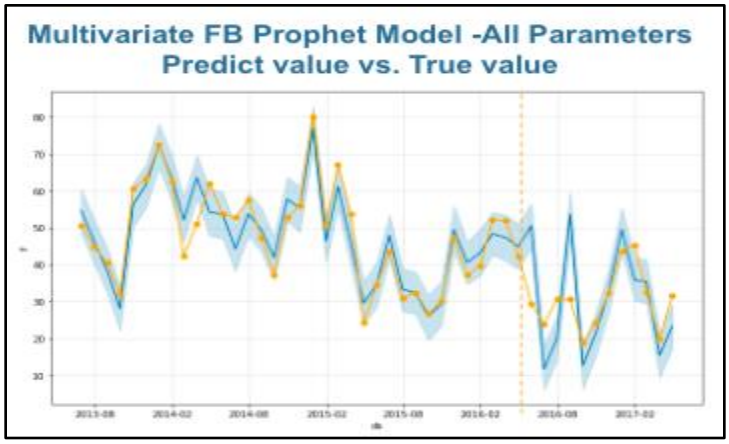

Fig 18. Multivariate FB Prophet Model - All Parameters

Then, by calculating the coefficient of each parameter, ***Fig 3.2.2*** shows Average of % effective utilization and Average of % Late PMs have the highest coefficient. Thus, the next model will only preserve these two parameters.

Feature Coefficients

	regressor	regressor_mode	coef
1	Average of % effective utilization	additive	108.140488
2	Average of % OF Late PM'S	additive	61.229940
0	Average of MTTR (hrs)	additive	0.213513
5	Average of practive hours	additive	0.211302
6	Average of Cost	additive	-0.000060
7	Average of % proxy for planned	additive	-5.492093
4	Average of %cost from PM's (Y)	additive	-7.580887
3	Average of % of weekly schedule compliance	additive	-9.020345

Fig 19. Feature Coefficients

In the following model with only two parameters with the highest coefficients, which are Average of % effective utilization and Average of % Late PMs. As expected, this model would give the best prediction since it has two parameters with the highest coefficients, but the result seems still extremely overfitted, as shown in ***Fig 3.2.3***. The model still worked flawlessly for the training set. However, in the test set, there are large disparities between forecasted and true MTBFs.

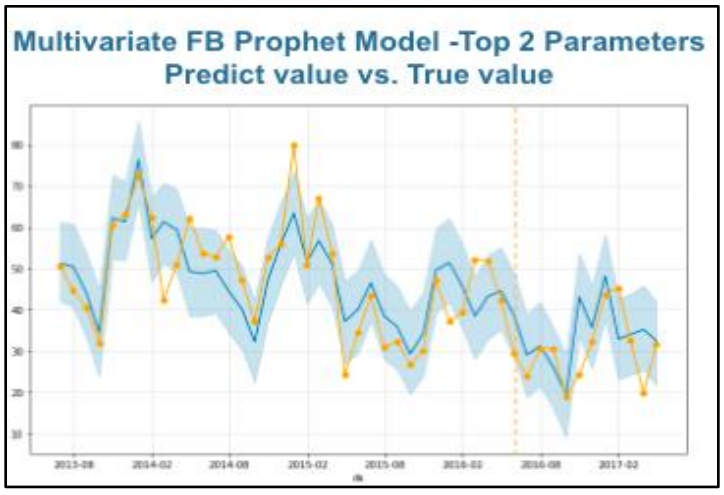

Fig 20. Multivariate FB Prophet Model - Top 2 Parameters

4. Model Recommendation

In conclusion, the LSTM and Facebook Prophet models provide a straightforward way to forecast MTBF data, with the Facebook Prophet model's prediction being more accurate than the LSTMs. The RMSEs for each of the three models are shown in ***Fig 4.1***.

RMSE \ Model	LSTM	Single variate FB Prophet	Multivariate FB Prophet
Overall	18.76	8.14	7.02
Train	16.27	7.94	4.92
Test	24.61	8.70	11.06

Fig 21. RMSEs for Three Models

In conclusion, the Univariate Facebook Prophet Model is more appropriate at properly predicting MTBF based on our comparisons. It is considered understandable when contemplating the fundamental mechanics of the models. The data for MTBF has a strong seasonal tendency, as illustrated. The LSTM forecast is based on a collection of last values that does not take seasonality into account. The prophet model, on the other hand, does a good job at modelling as an additive system and detecting and presenting seasonalities. Since the historical data is quite sparse, the multivariate FB prophet model did not perform as well on the test set as anticipated. As a result, the parameters' importance in this scenario isn't very significant.

Conclusion

Within organizations, the concepts of cost and organizational risk are the most universally understood when communicating with senior management. As a consequence, maintenance leaders must strive to frame maintenance performance from the perspective of cost and organizational risk to bridge communication gaps and streamline the process of quantifying subjective goals. Additionally, considering that strategic corporate goals are oftentimes built on the basis of soft or perceptual measures from stakeholders and are therefore subjective, a framework of KPIs must be developed to ensure that the actions of employees on the shop floor are guided by the overall strategic goals of the organization.

In order to address the reliance on lagging performance indicators within maintenance departments, organizational leaders must accept that the implementation of a predictive KPI framework is an alignment of three key areas: people, process, and technology. Therefore, organizational leaders must also work towards standardizing data gathering procedures in order to create a trustworthy system that can be leveraged for decision making, as well as hiring and training qualified individuals to maintain the system.

Aside from the previously discussed administrative challenges associated with data gathering within organizations, it must also be highlighted that KPIs are collected on a monthly or quarterly basis, meaning that training sets for forecasting models are extremely limited. In order to address these forecasting challenges, the multivariate Facebook Prophet Model yielded the best results when modelling time series data with a limited training set. Therefore, providing an opportunity to forecast a target KPI based on a variety of other input variables.

Next Steps

The topic of key performance indicators within the mining industry is extremely broad, making it very easy to experience scope creep while working on a project. As a consequence, when carrying this project forward it is important to stick to the following guideline that has been established by Professor Lam and Professor Lee during the final team meeting in April 2022.

Principles to Guide Future KPI Research:

1) KPIs should be focused on three core functional groups: maintenance operators, maintenance leaders, and senior management.
2) Given CMORE's research mandate, KPIs must integrate concepts of reliability and cost. Although organizational risk is also an important metric, it can be considered out of scope for the team due to its broad nature.
3) The next deliverable must focus on providing a proof of concept (i.e a mock-up dashboard). The concepts of KPI frameworks and time series modelling that have been discussed in this report can be used to provide a starting foundation for developing this dashboard.
4) Incorporate the concept of data mining into the dashboard to identify opportunities for extracting additional business insights through leveraging machine learning models.

Summary of KPI Data Obtained from Consortium Members

Organization	Point of Contact	Data Received	Included in Zip Folder (Y/N)
Cameco	Jean-Pierre Pascoli jean-pierre_pascoli@cameco.com	- Maintenance Program Measures and Indicators - Unscheduled Work Ratio - Maintenance Proactive Work - Maintenance Schedule Compliance	Y
Kinross Gold	Vatsal Agarwal vatsal.agarwal@kinross.com	- Screenshots of annual maintenance survey conducted by Emilio - Blair and I have forwarded Kinross a list of desirable KPIs, however; we have not yet received any data - The chain of emails has been included as a PDF for Reference - Maintenance KPI data for CAT793D	Y

Fig 22. Summary of KPI Data Obtained from Consortium Members

References

[1] A. Parida and U. Kumar, “Maintenance performance measurement (MPM): Issues and challenges,” Journal of Quality in Maintenance Engineering, vol. 12, no. 3, pp. 239–251, 2006.

[2] A. Parida and U. Kumar, “Maintenance productivity and performance measurement,” Handbook of Maintenance Management and Engineering, pp. 17–41, 2009.

[3] A. Parida, “Study and analysis of Maintenance Performance Indicators (mpis) for LKAB,” Journal of Quality in Maintenance Engineering, vol. 13, no. 4, pp. 325–337, 2007.

[4] R. L. M. Kotze and J. K. Visser, “An analysis of maintenance performance systems in the South African mining industry,” The South African Journal of Industrial Engineering, vol. 23, no. 3, p. 13, 2012.

[5] Aarthi, Ramalingam. Nov 10, 2021. Time Series Forecasting using Facebook Prophet. https://medium.com/@aarthiram96/time-series-forecasting-using-facebook-prophet-716843670a75

[6] Francis, Ndiritu. Mar 18, 2022. Univariate Time Series using Facebook Prophet. https://www.section.io/engineering-education/univariate-time-series-using-facebook-prophet/

[7] Joseph, Mushailov. Mar 29, 2021. LSTM Framework For Univariate Time-Series Prediction. https://towardsdatascience.com/lstm-framework-for-univariate-time-series-prediction-d9e7252699e

[8] “Long short-term memory,” *Wikipedia*, 14-Apr-2022. [Online]. Available: https://en.wikipedia.org/wiki/Long_short-term_memory. [Accessed: 21-Apr-2022].

[9] Soubhik, Khankary. Jan 30, 2022. Multivariate Time Series Forecasting using FBProphet. https://medium.com/mlearning-ai/multivariate-time-series-forecasting-using-fbprophet-66147f049e66

MENG Project Report

Physical Asset Management (PAM): An Economical Asset Replacement Model for Large Mining Equipments

In cooperation with Kinross Gold Corporation
May, 2022
Prepared by: Sean (Xiaonian) He

Table of Contents

<u>Section Abbreviation</u>

Background - BG
Asset Replacement Problem - ARP
Problem Definition - PD
Literature Review - LR
Current Method - CM
Objective - OJ
Dataset Preprocessing and Exploration - DPE
Improvement Methods and Results - IM
Limitations and future directions - LF

Executive Summary

This is a report that studies the economical asset replacement model for large mining equipment. Asset management is an important area for consideration in the mining industry. The client, Kinross Gold Corporation - a senior gold mining company with a diverse portfolio of mines and projects across the globe, wants to find a model for defining the optimal life of an asset, deciding when is a good time to replace it at the beginning of the equipment lifecycle. They also want the model to be general enough so it can be applied to other large equipment as well.

Literature review was conducted at first to study the related problem of asset management. It helps to understand the physical asset replacement problem in breadth and depth. The three resources give the mathematical calculation of when is the optimal time to replace an asset, provide a framework approach to the asset replacement problem and also discuss from a business perspective, and provide mathematical models on how to calculate the optimal time to replace an asset under different scenarios respectively.

Next, the current model is studied. The current model is an excel template that evaluates the replacement and repair decision at a certain point in time. An example was recreated based on the excel template provided and the limitations were listed at the end of the section. The limitation found after studying the current model aligns with the requirements proposed in the problem definition.

As mentioned earlier, the goal is to find the optimal economic life of an asset and make the model general enough so it can be applied to other equipment. The solution to the problem is tackled in a 2-step process. The first step is to calculate the optimal economic life of an asset. The second step is from the adjustable parameter perspective to make the model more general (i.e. Unscheduled MTBF in this case). The ultimate goal is to combine both improvements, making a connection between the formula from the first improvement and using the parameter obtained from the second improvement to have a general model for different types of equipment.

In the solution section, various models for the first step were proposed and a case study was performed to determine the optimal economic life of the haul truck. The second step is to determine the trend of the unscheduled MTBF and make this parameter more accurate for the model. Trend analysis, survival analysis, and machine learning methods were deployed.

In the end, the limitations and future directions were discussed.

Background

Asset management is an important area for consideration in the mining industry. The management and maintenance cost of mining equipment ranges from 30 to 50 percent of total operating costs on average, 60 percent of the mining workforce could be distributed to servicing or repairing the asset in the field [1]. Due to the high allocation of costs to asset management and maintenance, mining companies are implementing new asset management strategies yearly. A mining company can have thousands of initiatives in different areas to reduce the cost and preserve the margin [2]. Cutting down the cost of asset management can bring a lot of extra benefits to the mining companies, leading to better productivity, improved safety, security, and compliance.

The client, Kinross Gold Corporation - a senior gold mining company with a diverse portfolio of mines and projects across the globe, has a similar demand and is consistently looking for strategies to reduce the cost of asset management and maintenance [3]. Kinross recognized that the decision whether to continue to repair equipment or to replace it with a new one can have significant economical consequences. A suboptimal decision can increase maintenance and operating costs and result in below target equipment availability, capacity, and/or reliability.

Asset Replacement Problem

These types of problems are known as the “Asset Management Problem”. There are many branches of Asset Management, this report focuses on the problem of asset replacement decisions. All organizations have certain physical assets such as vehicles, equipment, and machinery, these assets typically consume a considerable amount of money to operate and maintain, and they depreciate as the service ages go up. Based on previous research, failure to replace an asset usually leads to higher energy consumption, maintenance costs, and increased risk [4].

Maintenance is one way to extend the life cycle of an asset, but when the physical asset is under reduced performance through degradation or the equipment becomes not repairable at all or the cost of keeping the asset exceeds the cost of replacing an asset even if the asset is under stable condition or there is safety and environment concerns of the physical asset, the organization needs to decide to replace it. However, replacing an asset may lead to other negative impacts and it is often described as being complex, unstructured, and inherently risky. Therefore, this presents a big challenge for asset owners [5]. The organizations need a systematic approach to the development of replacement plans, and

the proper physical asset management strategies can make the organization have better control over the expenditure and lead to higher productivity.

Problem Definition

Kinross has proposed a project to enhance the current model for **defining the optimal life of an asset and deciding when is a time to replace an asset**. They want the decision of replacement made based on economical conditions with various technical considerations as input. The model should also be **general enough and can be applied to different mining equipment** (i.e. different haul trucks or extraction shovels). The ultimate objective is to reduce the cost through asset management.

The client is particularly interested in studying the replacement time for the haul trucks and extraction shovels. Haul trucks and extraction shovels are physical assets that are significant investments in nature. Haul trucks are mainly used for transporting mined materials from the mining site to the dumping or processing site, shovels are used for digging and loading the earth or fragmented rock and for mineral extraction. They are essential for the mining site to operate. If they break down, many activities will cease, so it is always in the mining company's interest to have them available and operational all the time. Good repair and replacement decisions can reduce the costly and time-consuming vehicle breakdown and increase the mining productivity.

Literature Review

The following literature reviews help to understand the physical asset replacement problem in breadth and depth. A high-level summary of the resources is included in this section. The three resources are:

1. Physical asset replacement problem: an analytical approach
   Gives the mathematical calculation of when is the optimal time to replace an asset
2. An integrated framework for the management of strategic physical asset repair/replace decisions
   Provides a framework approach to the asset replacement problem and also discusses from a business perspective
3. Maintenance, Replacement, and Reliability: Theory and Applications - Chapter 4: Capital Equipment Replacement Decision
   Provides mathematical models on how to calculate the optimal time to replace an asset under different scenarios

1. ***Physical asset replacement problem: an analytical approach [6]***

In the classical papers, many authors have used principles of engineering economics, as net present value and annuity equivalents in the asset replacement problem. However, the main attributes for those literature were proved with intuitive ideas with no mathematical accuracy. In the literature physical assets replacement: An analytical approach, the author studies these principles of engineering economics with mathematical analysis.

The author first discussed the concept of economic life. An asset's economic life is the length of its usefulness and it is the optimum moment to replace the asset. The concept of economic life can be modeled by the equivalent capital cost (ECC), equivalent maintenance cost (EMC), and equivalent property cost (EPC).

The formulas of the cost mentioned above can be represented as below, all the costs mentioned here are represented by converting from the future value to the present value.

A: $acquisition\ cost$, $R(t)$: $salvage\ value$, $M(t)$: $maintenance\ cost$
t: $time\ interval$, r: $nominal\ interest\ rate$

$$Equivalent\ Capital\ Cost: ECC = g(t) = \frac{e^{r}-1}{e^{rt}-1}(Ae^{rt} - R(t))$$

$$Equivalent\ Maintenance\ Cost: EMC = f(t) = \frac{e^{r}-1}{e^{rt}-1}e^{rt}\int_{0}^{t} M(s)e^{-rs}ds$$

$$Equivalent\ Property\ Cost: EPC = h(t) = f(t) + g(t)$$

From the figure below, the equivalent maintenance costs (EMC) increase while the equivalent capital cost (ECC) decreases. The optimal point reaches at year 5. The paper then used nonsmooth analysis to classify all the possibilities for the minimum of a class of equivalent property cost (EPC) functions of assets. The minimums of these functions gives the optimum moment for an asset to be replaced.

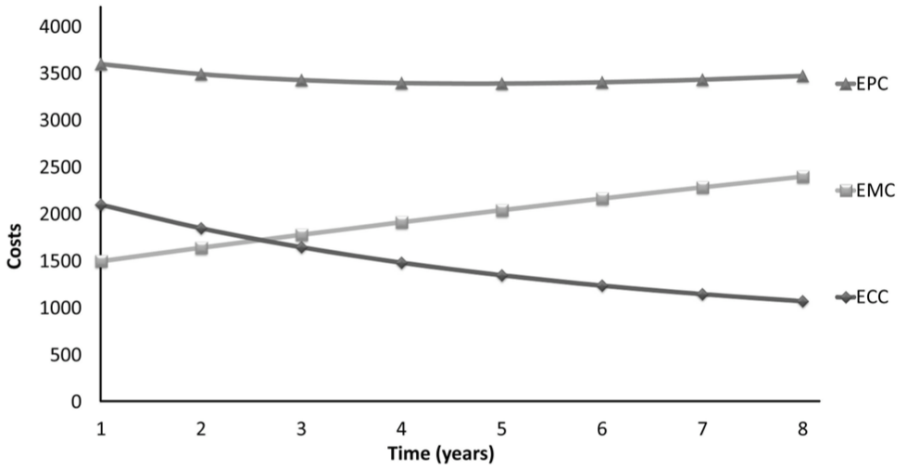

Figure LR-1: Different trends of the cost and the time

2. ***An integrated framework for the management of strategic physical asset repair/replace decisions [7]***

In this literature, an integrated framework for the management of strategic physical asset repair and replace decisions, the author talks about the fact that a lot of times the decision-makers are determining the optimal period when replacing a physical asset based on intuition or purely based on financial aspects. However, it is a multidisciplinary field and the decisions should incorporate the impact of multiple financial and non-financial criteria. So this is an addition to the previous literature which focuses on the financial aspect.

The author raises a hypothesis that it is possible to improve the outcome of current physical asset decisions by developing a multi-criteria decision-making framework to assist the management of physical assets in physical asset-intensive industries.

The study proposed a strategic, multiple criteria-based, decision-making framework for the management of physical asset replacement decisions by providing decision-makers with a practical structured decision-making process. There are six steps involved in the overall development of the framework to make the physical asset replacement decision, which are problem research, problem conceptualization, problem contextualization, problem synthesis, analysis, and framework validation (Figure LR-2). Among the 6 steps, the problem contextualization is the most important one and contains many different analyses like the identification of the multi-criteria decision-making process, so basically, the MCDM technique serve as the basis of the framework development.

Step	Work Cluster	Description
1	Problem Research	Examine the literature in the relevant fields of study
2	Problem Conceptualization	Determine the main focus areas within the relevant fields of study
3	Problem Contextualization	Identify the strategic physical asset repair/replace decision-making governing process/model
4	Problem Synthesis	Develop the strategic physical asset repair/replace decision-making framework
5	Problem Analysis	Assess criteria influencing the strategic physical asset repair/replace decision-making process
6	Framework Validation	Evaluate strategic physical asset repair/replace decision-making framework

Figure LR-2: Framework of the physical asset replacement decision

The next step is to identify the influencing criteria (Figure LR-3). The first criterion is the rate of return of the potential investment. The evaluation includes the calculation of the

internal rate of return. The second criterion is the value created by the potential investment The third criterion is the analysis of the effect of the physical asset repair and replacement decision on the five competitive forces. The last two are the effect of the physical asset replacement decision on social and environmental sustainability to be incorporated into the framework

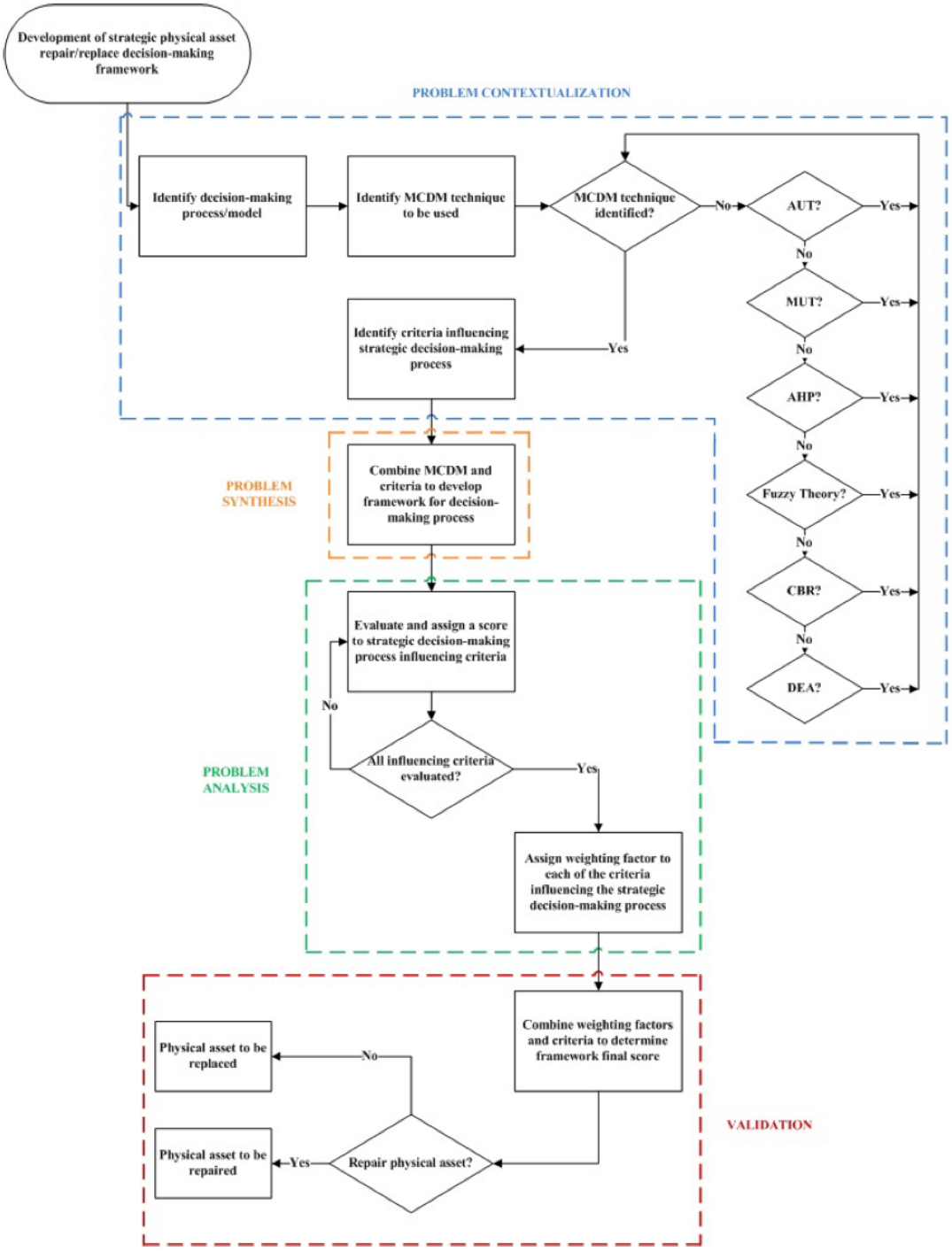

Figure LR-3: Determine the influencing criteria

After evaluating all the criteria here, the author reaches a final score based on the influencing criteria with their assigned scores and respective weight factor. It can be then used to determine the replacement decision and compare it with the repair option.

3. ***Maintenance, Replacement, and Reliability: Theory and Applications [8]***

The book provides several mathematical tools that can be used to optimize a variety of key maintenance/replacement/reliability decisions over a product's life cycle. Chapter 4 of the book goes in-depth to discuss the mathematical models that can be used to determine the replacement interval by addressing life cycle costing decisions (LCC). The application of these models applies to a variety of settings such as the military, mining, and transportation sectors.

On a high level, as the replacement age of an item increases, the operations and maintenance (O&M) costs per unit time increases as shown in the figure below, whereas the ownership cost decreases (Figure LR-4). The ownership cost is the purchase price minus the resale value at the time of replacement divided by the replacement age. The optimal replacement age is the point where the total cost is minimum (Similar to bias-variance tradeoff concept).

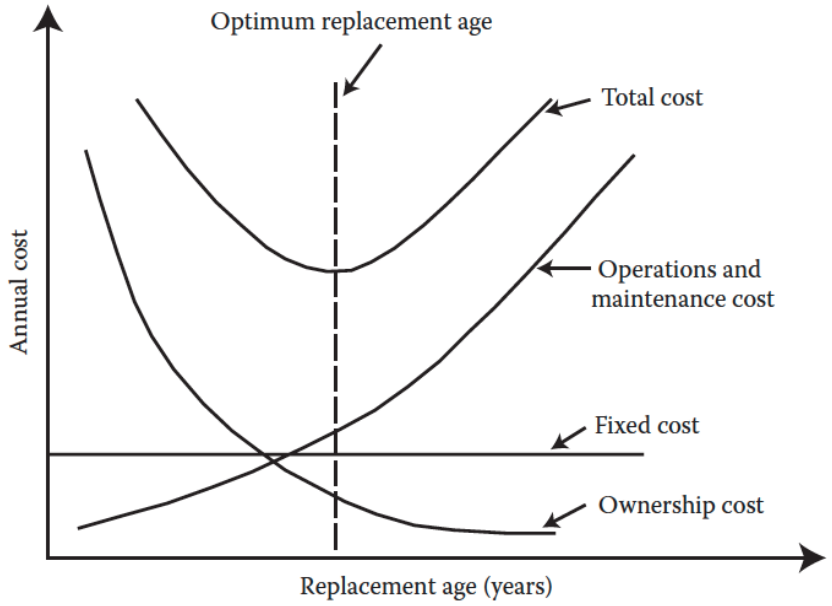

Figure LR-4: Typical cost diagram as the machine ages

The book presents a number of scenarios to determine the optimal replacement interval. These scenarios and models are discussed in the following sections.

(1) Optimal replacement interval for capital equipment (CE): minimization of total cost for an infinite horizon

All equipment essentially deteriorates over the time and the increasing operations and maintenance cost is a good measure of deterioration. Under the assumption that the equipment is replaced by an identical item, and the trends in O&M costs after the replacement remain identical. The author proposed a way to determine the optimal replacement interval based on the following model. The model takes in the acquisition, resale and O&M cost to calculate the total discounted cost of operating with replacements occurring at the interval of n periods.

The objective is to determine the optimal interval between replacements to minimize total discounted costs, $C(n)$.

- A is the acquisition cost of the capital equipment.
- C_i is the operation and maintenance cost in the i th period from new, assumed to be paid at the end of the period, i = 1, 2,…, n.
- S_i is the resale value of the equipment at the end of the i th period of operation, i = 1, 2,…, n.
- r is the discount factor
- n is the age in periods (such as years) of the equipment when replaced.
- $C(n)$ is the total discounted cost of operating, maintaining, and replacing the equipment (with identical equipment) over a long period, with replacements occurring at intervals of n periods.

In the first cycle of operation, the total discount cost at the end of the operation is:

$$C_1(n) = C_1 r^1 + C_2 r^2 + C_3 r^3 + \ldots + C_n r^n + A r^n - S_n r^n = \sum_{i=1}^{n} C_i r^i + r^n (A - S_n)$$

Similarly, the future cost of each cycle is the same as the first one

$$C_2(n) = \sum_{i=1}^{n} C_i r^i + r^n (A - S_n)$$

In an infinite horizon: $C(n) = C_1(n) + C_2(n) r^n + C_3(n) r^{2n} + \ldots + C_n(n) r^{(n-1)n} + \ldots$

$$C(n) = \frac{C_1(n)}{1 - r^n} = \frac{\sum_{i=1}^{n} C_i r^i + r^n (A - S_n)}{1 - r^n}$$

Rather than presenting the cost associated with an infinite chain of replacement, to calculate the equivalent annual cost of the equipment from present value use the following equation (annuity value to smooth out the peaks and troughs).

$EAC = PV * CRF\ (Capital\ recovery\ factor)$ where $CRF = \frac{i(i+1)^n}{(i+1)^n-1}$

$CRF = i$ in an infinite horizon

Overall, to find the optimal economic life under this scenario

$$Optimal\ Economic\ Life = Min[\frac{\sum_{i=1}^{n} C_i r^i + r^n(A-S_n)}{1-r^n}] * CRF$$

(2) Optimal replacement interval for CE: maximization the discounted benefits

There are two differences compared to 3-1, this model is used to determine the replacement interval that maximizes the total discounted net benefits instead of the total discounted cost. The trend in cost is taken to be continuous, rather than discrete.

The objective is to determine the optimum interval between replacements to maximize the total discounted net benefits derived from operating and maintaining the equipment over a long period.

- $b(t)$ is the net benefit obtained from equipment at time t (Revenue derived from operating the equipment minus the operating costs). The $b(t)$ is usually higher in the beginning but trend downwards as the operating cost goes up
- $c(t)$ is the net cost of replacing equipment at age t (The acquisition cost offset the salvage value). The $c(t)$ is usually lower in the beginning but trend upwards as the salvage value goes down
- T_r is the time required to replace the equipment
- t_r is the age of equipment when replacement commences
- $T_r + t_r$ is the replacement cycle, the time from end of one replacement to the end of the next replacement action
- $B(t_r)$ is the total discounted net benefits derived from operating the equipment for periods of length t_r over a long time

In the first cycle of operation, the total discounted benefits over the first cycle minus the discounted replacement cost at the end of first cycle.

$$B_1(t_r + T_r) = \int_0^{t_r} b(t)exp[-it]dt - c(t_r)exp[-it_r]$$

Similarly, the future cost of each cycle is the same as the first one.

$$B_n(t_r + T_r) = \int_0^{t_r} b(t)exp[-it]dt - c(t_r)exp[-it_r]$$

Discounted back to the start of first cycle gives: $B_n(t_r + T_r)exp[-i(n-1)(t_r + T_r)]$

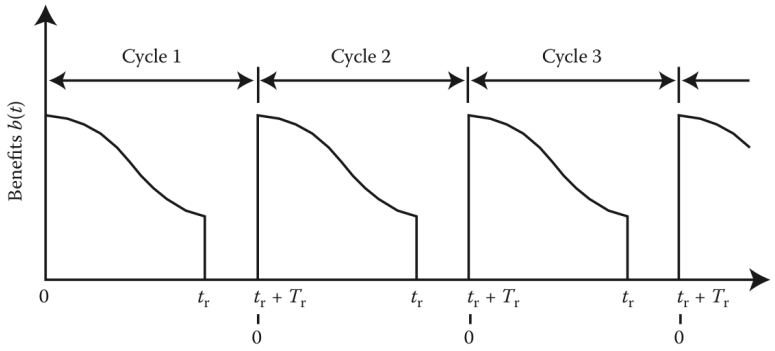

Figure LR-5: Discounted benefits over time

The total discounted cost with replacement at age t can give:

$$B(t_r) = B_1(t_r + T_r) + ... + B_n(t_r + T_r)exp[-i(n-1)(t_r + T_r)] + ...$$

Where $B_1(t_r + T_r) = ... = B_n(t_r + T_r)$

Overall, to find the optimal economic life under this scenario in a geometric progression to infinity.

$$Optimal\ Economic\ Life = Max[B(t_r)] = Max[\frac{B_1(t_r+T_r)}{1-exp[-i(t_r+T_r)]}]$$

(3) Optimal replacement interval for CE whose planned utilization pattern is variable: minimization of total cost

This class of problem will be applicable to a fleet of equipment, the utilization usually decreases as the age increases. The model establishes the economic life of equipment operated in a varying utilization scenario such that the total costs to satisfy the demands of a fleet are minimized.

The objective is to determine the optimal interval between replacements to minimize total discounted costs, C(n), or equivalently, EAC(n).

- A is the acquisition cost of the capital equipment.

- $c(t)$ is the trend in operation and maintenance cost per unit time of equipment of age t; working age t can be measured in terms of utilization such as, in case of vehicles, cumulative kilometers since new
- y(x) is the utilization trend of the xth equipment to meet the annual demand
- S_i is the resale value of the equipment at the end of the i th period of operation, $i = 1, 2, \ldots, n$.
- r is the discount factor
- n is the age in periods (such as years) of the equipment when replaced.
- N is the fleet size
- $C(n)$ is the total discounted cost of operating, maintaining, and replacing the equipment (with identical equipment) over a long period, with replacements occurring at intervals of n periods.
- EAC(n) is the equivalent annual cost associated with replacing the equipment at age n periods

Consider a replacement cycle of n years:
In a steady state, the number or replacements per year will be N/n. (e.g., 10 trucks in a mining site and they are replaced on a 10 year cycle, then 10/10=1 will be replaced each year)

The work undertaken by the newest N/n: $\int_0^{N/n} y(x)dx = D_1$

Cos of this by considering the average distance: $\int_0^{D_1/(N/n)} c(t)dt = C_1$

The cost for other equipment in subsequent years can be obtained as $C_1, C_2, \ldots, C_n$.

The EAC associated with a replacement cycle of n years:

$$Min[EAC(n)] = [A + C_1 + C_2 r^1 + C_3 r^2 + \ldots + C_n r^{n-1} - S_n r^n] * CRF = [A + \sum_{i=1}^{n} C_i r^{i-1} - S_n r^n] * CRF$$

Overall, to find the optimal economic life under this scenario

$$Optimal\ Economic\ Life = Min[EAC(n)] = [A + \sum_{i=1}^{n} C_i r^{i-1} - S_n r^n] * CRF$$

(4) Optimal replacement policy for CE taking into account technological improvement (TI): finite planning horizon (PH)

As the technology improves over the year, it is normal to have a technological improvement over the equipment currently being used. As a result, the maintenance and operating costs may be lower, and the quality of output may be better.

The objective is to determine the value of T at which replacement should take place with the new equipment, T=0, 1, 2, …, n.

- n is the number of operating periods during which equipment will be required
- $C_{p,i}$ is the operating and maintenance costs of the present equipment in the i th period from now, payable at time i, i =1,2,...,n
- $S_{p,i}$ is the resale value of the present equipment at the end of i th period from now, i =1,2,...,n
- A is the acquisition cost of the technologically superior equipment
- $C_{t,j}$ is the operating and maintenance costs of the technologically superior equipment in the jth period after its installation and payable at time j, j =1, 2, …, n
- $S_{t,j}$ is the resale value of the present equipment at the end of j th period from now, j =1,2,...,n
- r is the discount factor

The total discounted cost over n periods, with replacement occurring at the end of T th period: $C(T)$ = discounted maintenance costs for present equipment over period (0,T) + discounted maintenance costs for technologically superior equipment over period (T,n) + discounted acquisition cost of new equipment - discounted resale value of present equipment at the end of Tth period - discounted resale value of technologically superior equipment at the end of nth period =

$$(C_{p,1}r^1 + C_{p,2}r^2 + ... + C_{p,T}r^T) + (C_{t,1}r^{T+1} + C_{t,2}r^{T+2} + ... C_{t,n-T}r^n) + Ar^t - (S_{p,T}r^T + S_{t,n-T}r^n)$$

Overall, to find the optimal economic life under this scenario

$$Optimal\ Economic\ Life = Min[C(T)] = \sum_{i=1}^{T} C_{p,i}r^i + \sum_{j=1}^{n-T} C_{t,j}r^{T+1} + Ar^t - (S_{p,T}r^T + S_{t,n-T}r^n)$$

(5) Optimal replacement policy for CE taking into account TI: infinite PH

Similar to the previous example, but consider it for an infinite horizon of time. Variables are the same as defined in the previous section.

Objective is to minimize: $C(T,\ n)\ =\ Cost\ over\ interval\ (0,T)\ +\ future\ costs$

$$Cost\ over\ interval\ (0,T)\ =\ \sum_{i=1}^{T} C_{p,i} r^{i} + Ar^{t} - S_{p,T} r^{T}$$

Future costs = discounted to time T is similar to the equation in 3-1

$C(n)\ = \frac{\sum_{j=1}^{n} C_{t,j} r^{j} + r^{n}(A - S_{n})}{1 - r^{n}}$, C(n) discounted to time 0 is $C(n) r^{T}$

Overall, to find the optimal economic life under this scenario

$$Optimal\ Economic\ Life\ =\ Min[\mathrm{C(T, n)}] = \sum_{i=1}^{T} C_{p,i} r^{i} + Ar^{t} - S_{p,T} r^{T} + \left(\frac{\sum_{j=1}^{n} C_{t,j} r^{j} + r^{n}(A - S_{n})}{1 - r^{n}}\right) r^{T}$$

Current Method

Kinross has the current mobile equipment repair or replacement model in Excel. The evaluation model utilizes this file and calculates the net present value to determine the Total Cost of Ownership (TCO) based on the information entered for the repair or replace option.

There are several inputs required for the model, such as the known maintenance schedules for the major component changes and regular maintenance servicing costs. Availability, utilization, MTBF (Mean Time Between Failure) and MTTR (Mean time to recovery), capital cost, disposal cost, operation cost, etc. are also required for the model calculation.

The current model makes decisions based on the differences in the net present value (NPV) between the repair and replacement cost, when the NPV is positive then there is an economic benefit in replacing the equipment. The company will then consider making a replacement decision. The model also allows the replacement of a unit with a different capacity under the assumption that the production of the new unit will remain the same and so the model reduces the utilization accordingly.

Mathematical Representation

Using the replacement template provided by Kinross, the user is able to enter the necessary information and make the decision to continue repairing or replacing the existing equipment at the beginning of a year.

The excel model has three sheets, 'repair case TCO', 'replace case TCO', 'Evaluation'.

The repair sheet is used to calculate the total cost of ownership for continuing owning the current equipment. The following information are required for the repair sheet:

- Major components replacement costs for a given year (CC_t)
- Availability ($A_t = \frac{MTBF}{MTBF+MTTR}$) and utilization ($U_t$) percentage for a given year (Used to calculate number of operated hours each year)
- Labor Cost per hour (LC)
- Mean time between failure ($MTBF_{Unplanned}$), part costs ($PC_{Unplanned}$), number of repair hours ($T_{Unplanned}$) for unplanned maintenance (this is used to calculate the unplanned maintenance cost)
- Mean time between planned maintenance ($MTBF_{Planned}$), part costs ($PC_{Planned}$), number of repair hours ($T_{Planned}$) for planned maintenance (this is used to calculate the scheduled maintenance cost)
- Mean time between oil change ($MTBF_{oil\ change}$), part costs ($PC_{oil\ change}$), number of repair hours ($T_{oil\ change}$) for oil change (this is used to calculate the oil change maintenance cost)
- Percentage of the increase in unplanned maintenance or decrease in $MTBF_{Unplanned}$ for unplanned maintenance over the year (α)
- Operation Cost per hour (OC), Fuel cost per hour (FC)

The total costs are then calculated based on the total maintenance costs (which includes the component costs and the planned/unplanned maintenance costs) and the total operating costs.

$$Total\ Operated\ Hours\ (TOH_t) = A_t * U_t * 24 * 365$$

$$Total\ Maintenance\ Cost\ (TMC_t) = (CC_t + \frac{TOH_t}{MTBF_{Unplanned} * (1-\alpha)^t} * LC * T_{Unplanned} + \frac{TOH_t}{MTBF_{Planned}} * LC * T_{Planned} + \frac{TOH_t}{MTBF_{oil\ change}} * LC * T_{oil\ change})$$

$$Total\ Operating\ Cost\ (TOC_t) = (OC + FC) * TOH_t$$

$$Total\ Cost\ of\ Ownership\ to\ repair\ (TCO_t(Repair)) = TMC_t + TOC_t$$

The replace sheet is used to calculate the total cost of ownership after replacing with a new equipment (either a new model of equipment or the same model in a newer version). The information required for the replacement sheet is similar to the repair sheet with an additional parameter called production benefits (PB_t). As mentioned above, the model also allows replacement of a unit with different capacity under the assumption that the production of the new unit will remain the same and so the model reduces the utilization accordingly). Production benefit is tricky to determine and can directly impact the decision of replacement. The acquisition cost and salvage value is considered in the last part - evaluation.

$$Total\ Cost\ of\ Ownership\ to\ Replace\ (TCO_t(Replace)) = TMC_t + TOC_t - PB_t$$

In the evaluation sheet, the model uses the following parameters to determine the net present value (NPV) and the cumulative NPV over the year. :

- New equipment capital cost (A)
- Current equipment book value or the resale value of the previous equipment (S)
- Cash discount rate (r)
- Depreciation (D_t)
- Tax credit percentage (γ)

The NPV of replace and not repair uses the total NPV of replace minus the total NPV of repair. If the value is positive, then the model makes a recommendation to replace.

The total NPV for repair:

$$Before\ Tax\ Cash\ Flow\ (CFBT_t) = -\ TCO_t(Repair) + D_t$$

$$Tax\ Credit\ for\ a\ given\ year\ (TC_t) = \gamma\ *\ CFBT_t$$

$$After\ Tax\ Cash\ Flow\ (CFAT_t) = CFBT_t + TC_t + D_t$$

$$NPV\ of\ cash\ flow\ for\ a\ given\ year\ (NPV_t(Repair)) = CFAT_t\ *\ \frac{1}{(1+\gamma)^t_t}$$

$$Cumulative\ cash\ flow\ over\ the\ analysis\ period\ (CNPV_t(Repair)) = \sum_{t=1} (NPV_t(Repair))$$

The total NPV for replace:

$$Before\ Tax\ Cash\ Flow\ (CFBT_t) = -\ TCO_t(Replace) + D_t$$

$$Tax\ Credit\ for\ a\ given\ year\ (TC_t) = \gamma\ *\ CFBT_t$$

$$After\ Tax\ Cash\ Flow\ (CFAT_t) = CFBT_t + TC_t + D_t$$

$$NPV\ of\ cash\ flow\ for\ year\ 1\ (NPV_1(Replace)) = A + CFAT_t\ *\ \frac{1}{(1+\gamma)^t}$$

$$NPV\ of\ cash\ flow\ for\ a\ given\ year\ (NPV_{t|t>1}(Replace)) = CFAT_t\ *\ \frac{1}{(1+\gamma)^t_t}$$

$$Cumulative\ cash\ flow\ over\ the\ analysis\ period\ (CNPV_t(Replace)) = \sum_{t=1} (NPV_t(Replace))$$

Example

Please see attached spreadsheet for details (**Mobile Equipment Repair - Example Demonstration.xlsx**).

- Assumptions made on:
  - Salvage Value (exponentially decreasing)
  - % increase in terms of the unscheduled maintenance (equivalent % decrease in terms of MTBF) for repair and replace
  - Labor, part, fuel, component cost remain constant
  - Discount rate (5% provided by the client)

Evaluation

Assume the current model was purchased in the beginning of 2019 and it has been in service for 3 years, the repair unscheduled MTBF decrease by 7.5% annually, the replacement unscheduled MTBF decreases by 3.5% annually since a newer model should perform better.

Repair Equipment

		Y1 2021	Y2 2022	Y3 2023	Y4 2024	Y5 2025	Y6 2026	Y7 2027	Y8 2028	Y9 2029	Y10 2030
Current Book Value		2,842,439									
Cash Flow		(1,904,723)	(1,747,253)	(1,392,300)	(1,997,085)	(1,756,264)	(1,819,586)	(1,734,142)	(1,699,364)	(2,114,903)	(1,760,217)
Depreciation		(284,244)	(284,244)	(284,244)	(284,244)	(284,244)	(284,244)	(284,244)	(284,244)	(284,244)	(284,244)
Before Tax Cash Flow		(2,188,967)	(2,031,497)	(1,676,544)	(2,281,329)	(2,040,508)	(2,103,830)	(2,018,386)	(1,983,607)	(2,399,146)	(2,044,461)
Federal Tax Credit @	15%	328,345	304,725	251,482	342,199	306,076	315,574	302,758	297,541	359,872	306,669
Add Back Depreciation		284,244	284,244	284,244	284,244	284,244	284,244	284,244	284,244	284,244	284,244
After Tax Cash Flow		(1,576,378)	(1,442,528)	(1,140,818)	(1,654,886)	(1,450,188)	(1,504,011)	(1,431,384)	(1,401,822)	(1,755,031)	(1,453,548)
Present Value Factor		100%	95%	91%	86%	82%	78%	75%	71%	68%	64%
NPV of cash flow		(1,576,378)	(1,373,836)	(1,034,756)	(1,429,552)	(1,193,073)	(1,178,432)	(1,068,121)	(996,249)	(1,187,874)	(936,970)
Cumulative NPV		(1,576,378)	(2,950,215)	(3,984,970)	(5,414,523)	(6,607,596)	(7,786,028)	(8,854,149)	(9,850,398)	(11,038,272)	(11,975,242)
Total Net Present Value		(11,975,242)									

Replace Equipment

		Y1 2021	Y2 2022	Y3 2023	Y4 2024	Y5 2025	Y6 2026	Y7 2027	Y8 2028	Y9 2029	Y10 2030
Capital Cost		(3,824,299)									
Salvage Value-Repair Unit Book Value		(594,735)									
Cash Flow		(963,678)	(1,144,204)	(1,745,390)	(1,579,317)	(1,214,569)	(1,808,260)	(1,554,928)	(1,604,190)	(1,503,001)	(1,450,640)
Depreciation		(327,287)	(327,287)	(327,287)	(327,287)	(327,287)	(327,287)	(327,287)	(327,287)	(327,287)	(327,287)
Before Tax Cash Flow		(1,290,965)	(1,471,491)	(2,072,677)	(1,906,603)	(1,541,856)	(2,135,547)	(1,882,214)	(1,931,477)	(1,830,288)	(1,777,926)
Federal Tax Credit @	15%	193,645	220,724	310,902	285,990	231,278	320,332	282,332	289,722	274,543	266,689
Add Back Depreciation		327,287	327,287	327,287	327,287	327,287	327,287	327,287	327,287	327,287	327,287
After Tax Cash Flow		(770,033)	(923,480)	(1,434,489)	(1,293,326)	(983,291)	(1,487,928)	(1,272,595)	(1,314,469)	(1,228,458)	(1,183,951)
Present Value Factor		100%	95%	91%	86%	82%	78%	75%	71%	68%	64%
NPV of cash flow		(770,033)	(879,505)	(1,301,124)	(1,117,224)	(808,956)	(1,165,831)	(949,630)	(934,168)	(831,469)	(763,185)
Cumulative NPV		(4,594,333)	(5,473,838)	(6,774,962)	(7,892,185)	(8,701,141)	(9,866,972)	(10,816,602)	(11,750,771)	(12,582,239)	(13,345,425)
Total Net Present Value		(13,940,159)									

Figure CM-1. Screenshot of repair versus replace an equipment

	2021	2022	2023	2024	2025	2026	2027	2028	2029	2030
	Y1	Y2	Y3	Y4	Y5	Y6	Y7	Y8	Y9	Y10
Repair	(1,576,378)	(2,950,215)	(3,984,970)	(5,414,523)	(6,607,596)	(7,786,028)	(8,854,149)	(9,850,398)	(11,038,272)	(11,975,242)
Replace	(4,594,333)	(5,473,838)	(6,774,962)	(7,892,185)	(8,701,141)	(9,866,972)	(10,816,602)	(11,750,771)	(12,582,239)	(13,345,425)
Difference	(3,017,955)	(2,523,623)	(2,789,991)	(2,477,663)	(2,093,545)	(2,080,944)	(1,962,453)	(1,900,373)	(1,543,968)	(1,370,183)

Table CM-1. Yearly TCO cost for the repair and replace options

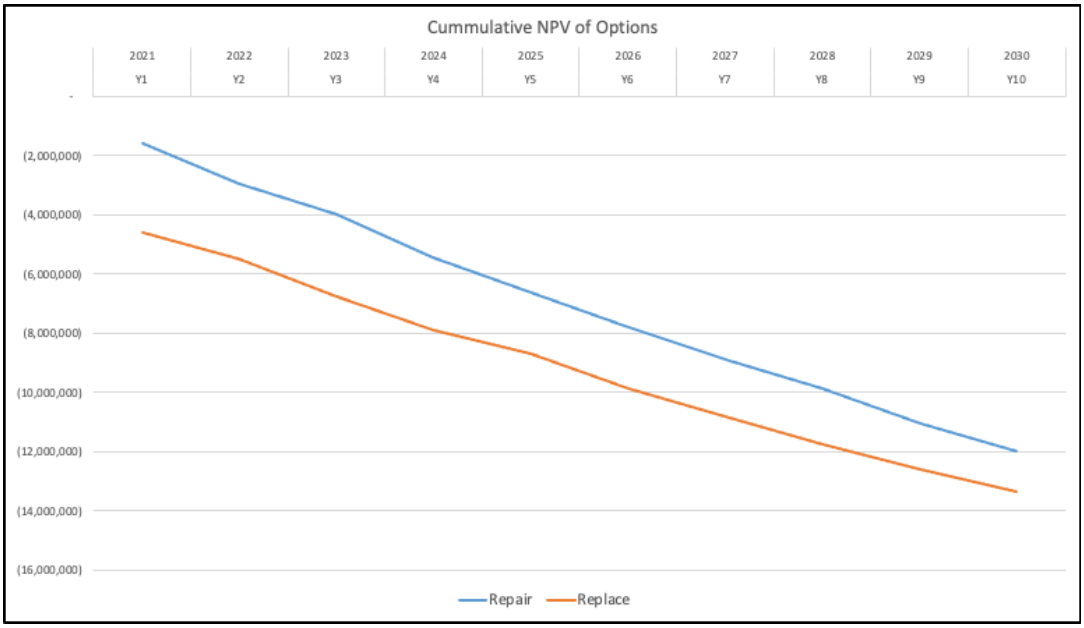

Figure CM-2. NPV Graph

We can see the difference is getting smaller, but continue to repair is a better option since the replacement capital cost is too high and it will take more time to offset this cost

However, it looks like the current worksheet is missing one important factor which is the salvage value. By including the salvage value into the consideration (also assume the equipment gets sold right away upon replacement decision made), replacement can be a better option compare to repair.

Repair Equipment

		Y1 2021	Y2 2022	Y3 2023	Y4 2024	Y5 2025	Y6 2026	Y7 2027	Y8 2028	Y9 2029	Y10 2030
Current Book Value		2,842,439									
Cash Flow		(1,904,723)	(1,754,069)	(1,407,243)	(2,021,655)	(1,792,177)	(1,868,800)	(1,798,890)	(1,782,188)	(2,218,695)	(1,888,260)
Depreciation		(284,244)	(284,244)	(284,244)	(284,244)	(284,244)	(284,244)	(284,244)	(284,244)	(284,244)	(284,244)
Before Tax Cash Flow		(2,188,967)	(2,038,313)	(1,691,487)	(2,305,899)	(2,076,421)	(2,153,044)	(2,083,134)	(2,066,432)	(2,502,939)	(2,172,504)
Federal Tax Credit @	15%	328,345	305,747	253,723	345,885	311,463	322,957	312,470	309,965	375,441	325,876
Add Back Depreciation		284,244	284,244	284,244	284,244	284,244	284,244	284,244	284,244	284,244	284,244
After Tax Cash Flow		(1,576,378)	(1,448,322)	(1,153,520)	(1,675,770)	(1,480,714)	(1,545,843)	(1,486,420)	(1,472,224)	(1,843,254)	(1,562,384)
Present Value Factor		100%	95%	91%	86%	82%	78%	75%	71%	68%	64%
NPV of cash flow		(1,576,378)	(1,379,355)	(1,046,277)	(1,447,593)	(1,218,187)	(1,211,209)	(1,109,190)	(1,046,282)	(1,247,587)	(1,007,127)
Cumulative NPV		(1,576,378)	(2,955,733)	(4,002,009)	(5,449,603)	(6,667,790)	(7,878,998)	(8,988,188)	(10,034,470)	(11,282,057)	(12,289,183)
Total Net Present Value		(12,289,183)									

Replace Equipment

		Y1 2021	Y2 2022	Y3 2023	Y4 2024	Y5 2025	Y6 2026	Y7 2027	Y8 2028	Y9 2029	Y10 2030
Capital Cost		(3,824,299)									
Salvage Value-Repair Unit Book Value		(794,735)									
Cash Flow		(963,678)	(1,140,604)	(1,737,986)	(1,567,894)	(1,198,908)	(1,788,127)	(1,530,081)	(1,574,378)	(1,467,961)	(1,410,096)
Depreciation		(327,287)	(327,287)	(327,287)	(327,287)	(327,287)	(327,287)	(327,287)	(327,287)	(327,287)	(327,287)
Before Tax Cash Flow		(1,290,965)	(1,467,890)	(2,065,272)	(1,895,181)	(1,526,194)	(2,115,414)	(1,857,368)	(1,901,665)	(1,795,247)	(1,737,383)
Federal Tax Credit @	15%	193,645	220,184	309,791	284,277	228,929	317,312	278,605	285,250	269,287	260,607
Add Back Depreciation		327,287	327,287	327,287	327,287	327,287	327,287	327,287	327,287	327,287	327,287
After Tax Cash Flow		(770,033)	(920,420)	(1,428,195)	(1,283,617)	(969,978)	(1,470,815)	(1,251,476)	(1,289,129)	(1,198,674)	(1,149,489)
Present Value Factor		100%	95%	91%	86%	82%	78%	75%	71%	68%	64%
NPV of cash flow		(770,033)	(876,591)	(1,295,415)	(1,108,837)	(798,004)	(1,152,422)	(933,871)	(916,160)	(811,309)	(740,971)
Cumulative NPV		(2,846,628)	(3,723,219)	(5,018,633)	(6,127,470)	(6,925,474)	(8,077,896)	(9,011,767)	(9,927,926)	(10,739,236)	(11,480,207)
Total Net Present Value		(12,274,941)									

Figure CM-3. Screenshot of repair versus replace an equipment after salvage value added

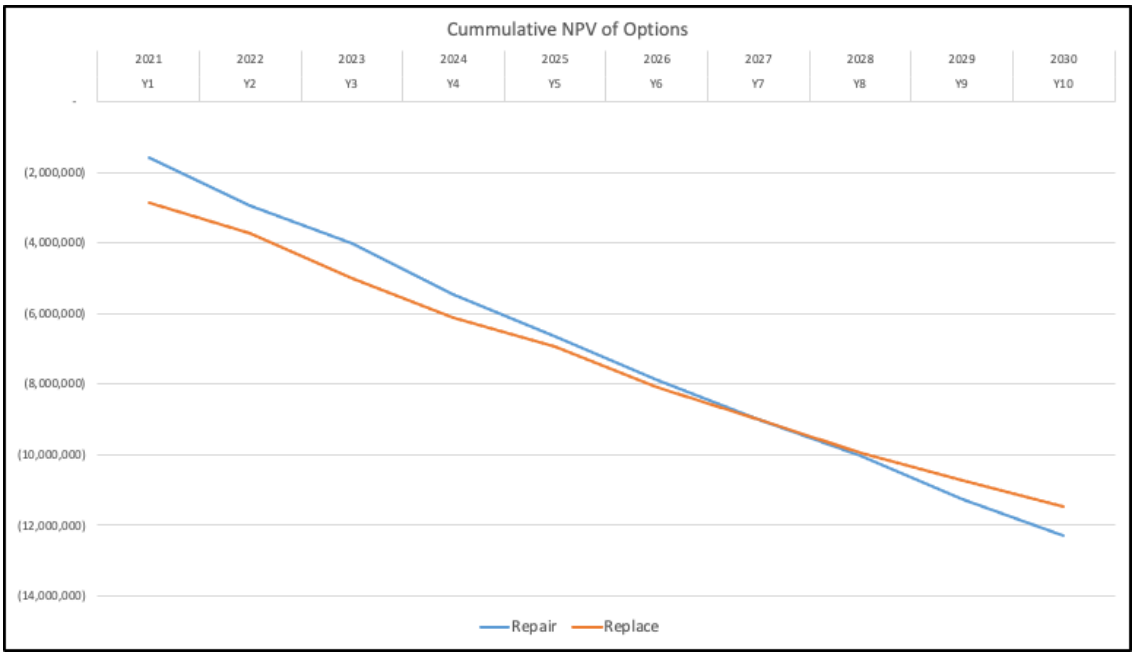

Figure CM-4. NPV Graph after salvage value added

Limitations with the current method

- The evaluation requires the values for both repair and replace scenarios, it is more of a model to determine a more cost-effective way rather than deciding the number of years to replace equipment is optimal.
- The current analysis assumes the equipment will be used for n years. (N is predetermined and is not a variable. This will impact the calculation of depreciation)
- It does not provide the optimal economic life for an equipment
- Some variables or parameters are constants or change linearly into the future
- The current model does not show generality, to apply it to different equipment is a key requirement.

Objectives

As mentioned in the problem definition, the goal is to find the optimal economic life of an asset and make the model general enough so it can be applied to other equipment, the requirements align with the limitation found with the current method. The solution to the problem is tackled in a 2-step process.

The first step is to calculate the optimal economic life of an asset. To calculate the optimal life of an asset, this first improvement method takes a reference from the literature review 3, 'Maintenance, Replacement, and Reliability', to calculate the discounted cost for each

period and determine an optimal life. The details of this solution is included in the first part of the 'Improvement Methods and Results' section below.

The second step is from the adjustable parameter perspective to make the model more general. After calculating the optimal life of equipment, the next focus is on how to make the model more general and applicable to different equipment. Some things will remain the same. For example, the evaluation method. It is an economic replacement problem, so whenever the cost exceeds the benefit, the replacement option should be considered. Most of the inputs also remain the same, there is still acquisition cost, maintenance cost, operation cost, labor cost, etc. Although the exact cost will change, the input parameters remain the same.

Considering the things that are different from equipment to equipment will make the model more general. For example, fuel efficiency, the exact cost of the equipment, component, parts, salvage value, etc, component Interval and unscheduled MTBF (Utilization, availability of equipment). Based on the available data and the level of difficulty to estimate the above variables that are going to change from equipment to equipment, the second improvement focuses on the last variable - unschedule MTBF.

The goal is to predict a trend of how the unscheduled maintenance increases over time or even predict when the unscheduled maintenance will happen, to make the unscheduled cost more accurate. Therefore, correctly predicting the trend of unscheduled MTBF can improve the unscheduled maintenance cost inputs in the mathematical models. This is discussed further in the second part of the 'Improvement Methods and Results' section below.

In the end, the ideal solution combines both improvements, making a connection between the formula from the first improvement and using the parameter obtained from the second improvement to have a general model for different equipment.

Dataset Preprocessing and Exploration

To study the asset replacement problem, it is necessary to obtain the basic component and vehicle information. The solution starts with the dataset preprocessing and exploration.

- The first dataset gives an overview of the life and cost of major equipment in a truck.
- The second dataset is generated from combining the sensor and unscheduled down data.

1. Total cost of ownership (TCO) for 793D

This dataset presents the high-level vehicle, component cost, and interval (component life) information. In the sample data provided by Kinross, the Caterpillar 793D haul truck has a total capital cost of close to $4M (USD). Caterpillar 793D is one of the largest and heaviest machines on the mining site [9]. The production capacity is around 218 tons. The haul truck consists of many major components including an engine, tires, and transmission.

After plotting out the bar charts for the component cost and interval (Figure DPE-1), we can see air conditioner service and tires are the two components that have the shortest life, with 7500 hours and 6800 hours respectively, both under 10,000 hours which means they need to be replaced each year through scheduled maintenance. Engines and tires are the two most expensive components, with a cost of $325,500 and $166,043 respectively. By checking the cost per hour, the Engine and Tires are two components that require the most attention, they have a cost of $21.7/hour and $24.42/hour respectively. This aligns with expectations since the Engine is the most expensive component in a vehicle and tires wear a lot faster under the mining site condition.

Other than the information mentioned above, they provided the best, base, and worst cases of the unplanned maintenance intervals (MTBF) and the best, base, and worst scenarios of the cost of the labor. They also provided the operating cost which includes the fuel consumption and driver cost. Those data points do not require further manipulation.

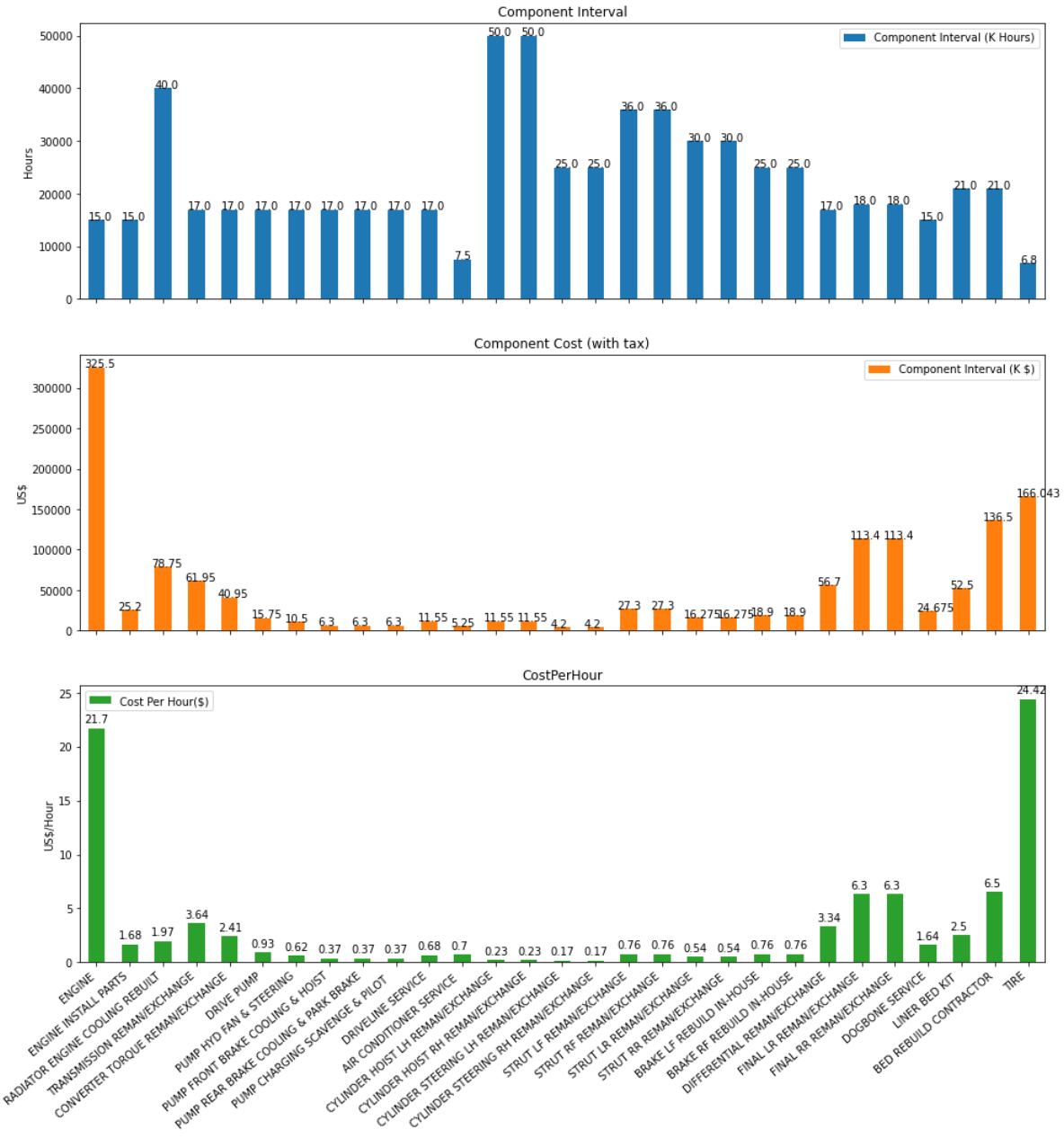

Figure DPE-1: major components cost and interval of 793D

2. ***System Sensor Data and Unscheduled Down Dataset***

System Sensor Data

The Kinross sensor dataset recorded data for 5 different assets (DT82, DT83, DT84, DT85, DT86) from the end of September 2019 to the end of March 2020 (6 months span). The data are recorded at an interval of 5 minutes during service hours. Each timestamp recorded 4 sensor data, the sensors are 'atmospheric pressure', 'engine power derate

percentage', 'peak air filter restriction', 'right minus left exhaust temperature'. Other than the sensor data, the position of the equipment, loaded state, speed, moving status, and service hours are also recorded along with the sensor data. The raw data form is included in Figure DPE-2.

	Asset	Timestamp	Sensor	Data	PositionX	PositionY	LoadedState	Speed	MovingState	ServiceHours
0	DT82	2019-09-30 00:22:53	Atmospheric Pressure	100.5	47359	75139	0	0.0	0	5534.095
1	DT82	2019-09-30 00:22:53	Engine Power Derate Percentage	0.0	47359	75139	0	0.0	0	5534.095
2	DT82	2019-09-30 00:22:53	Peak Air Filter Restriction	0.0	47359	75139	0	0.0	0	5534.095
3	DT82	2019-09-30 00:22:53	Right Minus Left Exhaust Temperature	1.0	47359	75139	0	0.0	0	5534.095

Figure DPE-2: raw sensor dataset

For the sensor data, there are null values appearing in the worksheet. Null values mainly appeared in the 'Speed' and the 'ServiceHours' column. We can populate some of the null values based on the timestamp and service hours and asset (i.e., if the line with null value has a timestamp that is 10 seconds within the previous or next timestamp, the value copies from the previous or next line). Otherwise, the null values get dropped. Duplicate and incorrect data are also being dropped.

After the data manipulation, the next step is to pivot the data so that the sensor data will be on the same row if the asset and timestamp match. The data looks like what figure DPE-3 is showing.

Sensor	Asset	Timestamp	PositionX	PositionY	LoadedState	Speed	MovingState	ServiceHours	Atmospheric Pressure	Engine Power Derate Percentage	Peak Air Filter Restriction	Right Minus Left Exhaust Temperature
0	DT82	2019-09-30 00:22:53	47359	75139	0	0.0	0	5534.095	100.5	0.0	0.0	1.0
1	DT82	2019-09-30 00:27:54	47379	75139	0	3.0	1	5534.179	100.5	0.0	0.0	-7.0
2	DT82	2019-09-30 06:57:41	47133	75201	0	4.0	1	5534.417	100.5	0.0	0.5	-2.0
3	DT82	2019-09-30 07:45:18	46986	74331	0	49.5	1	5534.514	100.0	0.0	0.5	4.0
4	DT82	2019-09-30 07:50:18	47909	71442	0	3.0	1	5534.598	100.5	0.0	0.0	-2.0

Figure DPE-3: sensor dataset after data processing

After removing some outliers, the distribution of the data looks like what is showing in the figures below. The Figure DPE-4 shows the distribution of some general features including position of the machine, speed and service hour in a time series plot. The Figure DPE-5 shows the distribution of the sensor data.

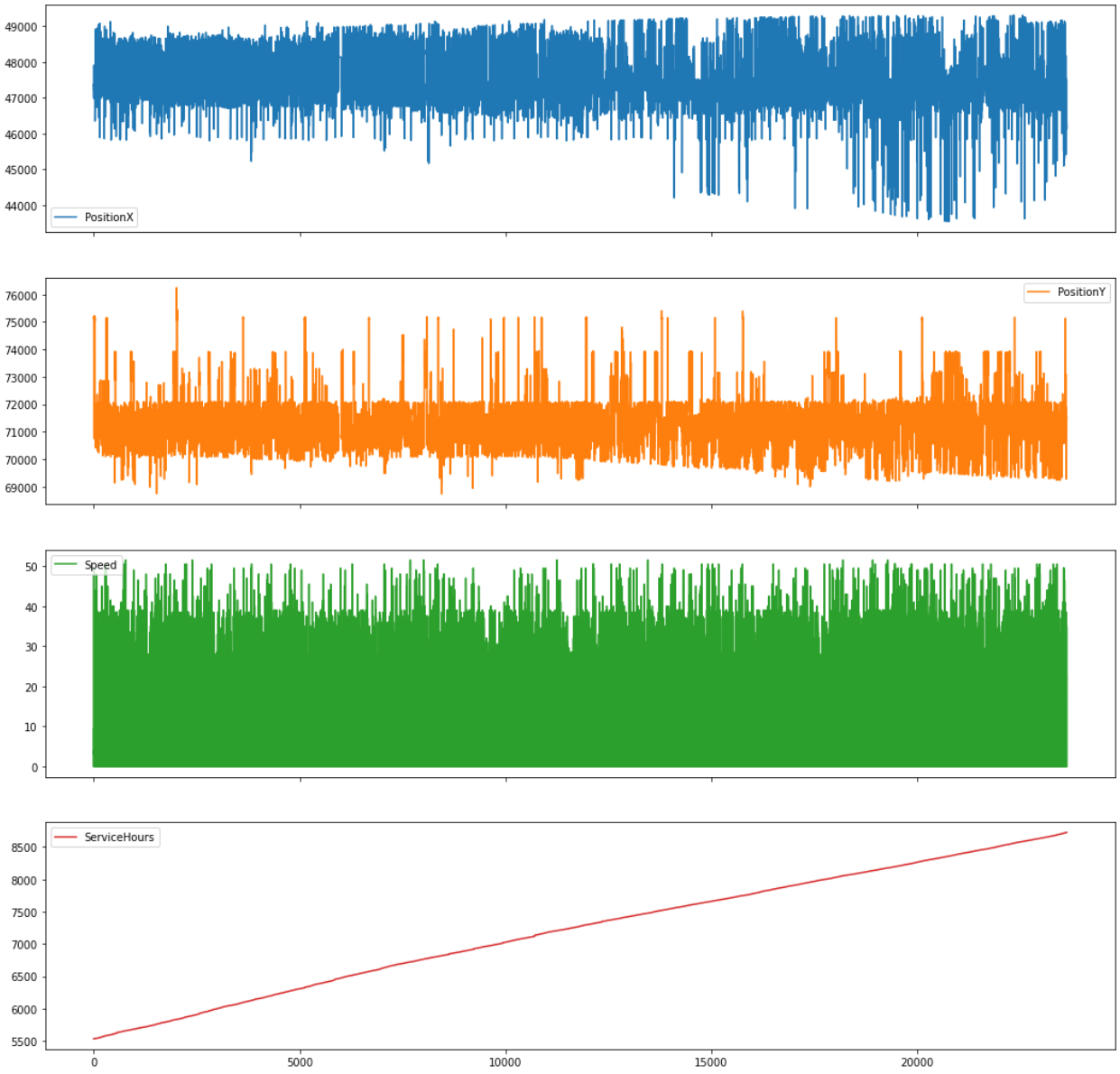

Figure DPE-4: Distribution of the general features

Figure DPE-5: Distribution of the sensor features

Unscheduled Down Data

The unscheduled down data covers the same time period as the sensor data. It includes the equipment unscheduled down data for 4 assets (DT82, DT84, DT85, DT86). Each unscheduled down category has a description and a comment related to the equipment down reason. The start time, end time and duration of the equipment down are also recorded. Looking at the dataset, we are able to see the number of unscheduled down events for each machine (Figure DPE-6) and the category of the unscheduled down events for each machine (Figure DPE-7).

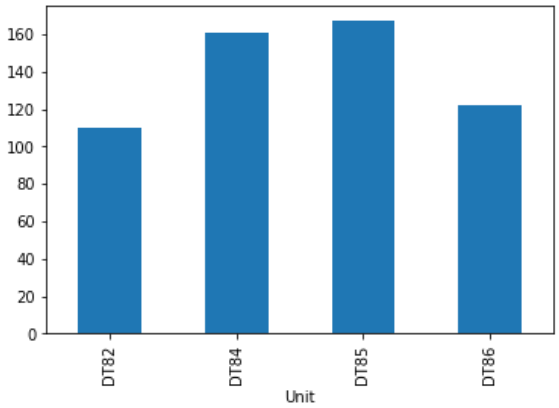

Figure DPE-6: unscheduled down events for each machine

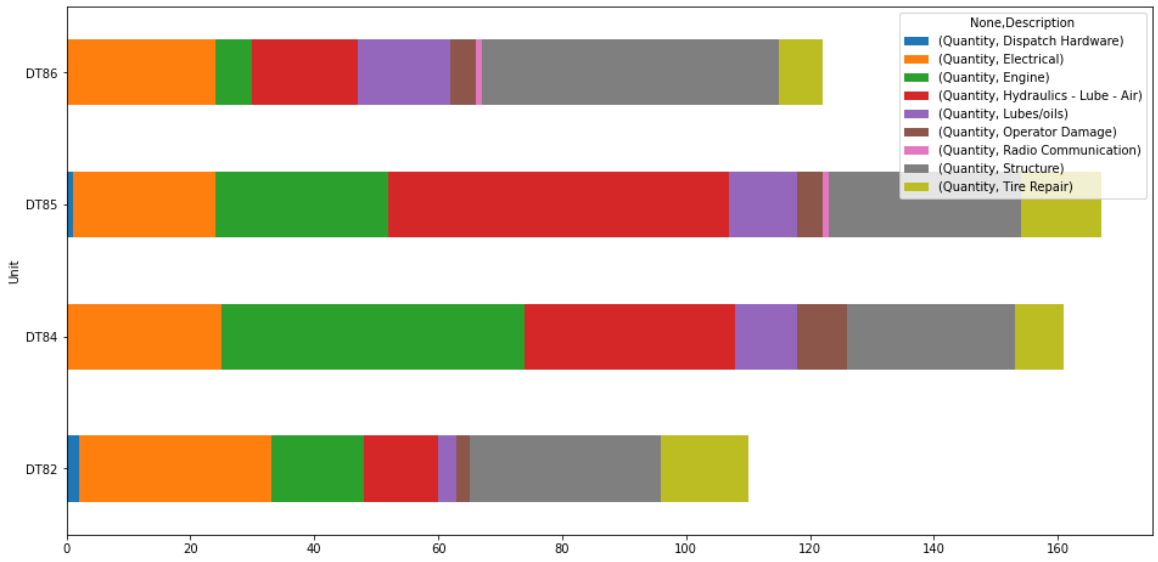

Figure DPE-7: The categories of the unscheduled down events for each machine

Combined Data

The sensor data with the unscheduled down data were combined to observe the trend of failure and even predict when a machine will fail since the sensor data and the unscheduled down data cover the same time interval. The two tables are joined based on the asset and timestamp. The initial labels are normal operation - 0, machine down - 1, deterioration stage (within 1 hour before the machine is down) - 2.

The analysis takes equipment 'DT82' for an initial exploration. There are 224 timestamps where the machine is down (0.96%), 465 timestamps within 1 hour before the machine is down, and 22944 timestamps when the machine is operating normally.

Unscheduled_Down	Asset
0	22944
1	224
2	465

Figure DPE-8: Machine status count

The chart below shows the machine status of DT82 (Figure DPE-9). The deterioration status is usually followed by the broken status. There are several occasions when it does

not follow this pattern, this is likely due to some sensor data not being recorded when the machine is not operating normally.

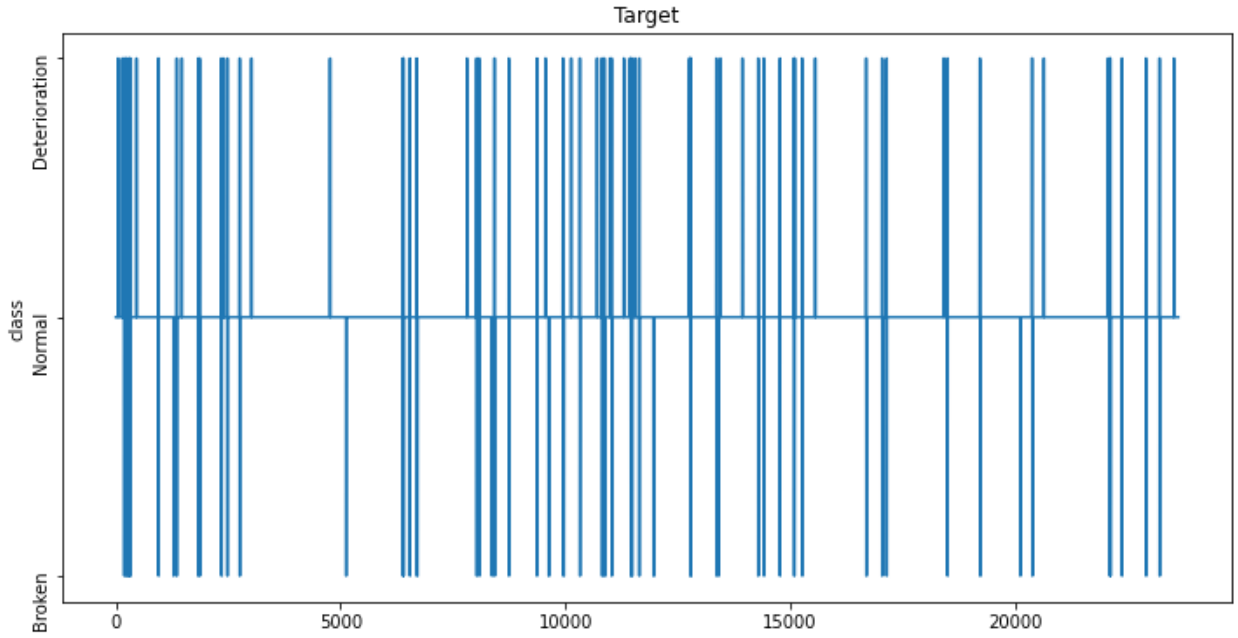

Figure DPE-9: Machine status and timestamp

In the end, if the data were only categorized to 2 labels (normal and broken) for all the equipment. There is also around 0.1% of the time that the machine is down which aligns with the results derived from DT82.

Unscheduled Down	Number of Events
0 (Normal)	85714
1 (Broken)	957

Table DPE-1: Total number of normal vs broken events for all 4 equipments

Improvement Methods and Results

As mentioned in the 'objective and solutioning' section. The first improvement calculates the optimal economic life rather than making a comparison between the repair and replace case. The second improvement predicts the trend of unscheduled MTBF to make the model more general. Please refer to the codes to see how the results and graphs were generated.

1. ***Improvements on the method to calculate the optimal economic life***

The goal of the model is to calculate the total discounted costs derived from operating and maintenance, acquisition and resale value over a period of time to find the optimal replacement age. The solution is taking reference from literature review 3.

Inputs for the model

- A is the acquisition cost of the capital equipment.
- For discrete cost, C_i is the operation and maintenance cost in the i th period from new, assumed to be paid at the end of the period, i = 1, 2,…, n.
- For continuous cost, $c(t)$ is the trend in operation and maintenance cost per unit time of equipment of age t; working age t can be measured in terms of utilization such as, in case of haul trucks, cumulative hours since new
- For discrete benefits, B_i is the production benefits in the i th period from new, assumed to be paid at the end of the period, i = 1, 2,…, n.
- For continuous benefits, $b(t)$ is the trend in production benefits per unit time of equipment of age t; working age t can be measured in terms of utilization such as, in case of haul trucks, cumulative hours since new
- S_i is the resale value of the equipment at the end of the i th period of operation, i = 1, 2,…, n.
- r is the discount factor
- n is the age in periods (such as years) of the equipment when replaced.
- $C(n)$ is the total discounted cost of operating, maintaining, and replacing the equipment (with identical equipment) over a long period, with replacements occurring at intervals of n periods.
- EAC(n) is the equivalent annual cost associated with replacing the equipment at age n periods

Fleet Factors

- For discrete problem, y_i is the utilization value of the xth equipment in a fleet in the i th period from new, assumed as the average utilization throughout the year, i = 1, 2,…, n (in terms of hours used)
- For continuous problem, y(x) is the utilization trend of the xth equipment in a fleet to meet the annual demand (in terms of hours used)
- For discrete problem, HC_i is the operation and maintenance cost per hour in the i th period from new, assumed to be paid at the end of the period, i = 1, 2,…, n.
- N is the fleet size

Technologically Advanced Factors

- n is the number of operating periods during which equipment will be required
- $C_{p,i}$ is the operating and maintenance costs of the present equipment in the i th period from now, payable at time i, i =1,2,...,n
- $S_{p,i}$ is the resale value of the present equipment at the end of i th period from now, i =1,2,...,n
- A_t is the acquisition cost of the technologically superior equipment
- $C_{t,j}$is the operating and maintenance costs of the technologically superior equipment in the j th period after its installation and payable at time j, j =1, 2, …, n
- $B_{t,j}$ is the production benefits of the technologically superior equipment in the j th period after its installation and payable at time j, j =1, 2, …, n
- $S_{t,j}$ is the resale value of the present equipment at the end of j th period from now, j =1,2,...,n
- T is the replacement of the present equipment at the end of T periods of operation, followed by replacement of technologically improved equipment at interval of length n

1. Replace a single equipment with the same model (Discrete)

Same as 3-1, except adding the production benefit into the equation.

$$Optimal\ Economic\ Life\ =\ Min[EAC(n)]\ =\ Min[\frac{\sum_{i=1}^{n}(C_i-B_i)r^i+r^n(A-S_n)}{1-r^n}]\ *\ CRF$$

2. Replace a single equipment with the same model (Continuous)

In the first cycle of operation (m=1), the total discount cost at the end of the operation is:

$$C_1(n)\ =\ \int_0^n(c(t)\ -\ b(t))exp[-\ it]dt\ +\ Ar^n\ -\ S_nr^n = \int_0^n(c(t)\ -\ b(t))exp[-\ it]dt\ +\ r^n(A\ -\ S_n)$$

In an infinite horizon, $C(n)\ = C_1(n)\ + C_2(n)r^n\ + C_3(n)r^{2n}$ +... + $C_n(n)r^{(n-1)n}$ +...

$$C(n)\ = \frac{C_1(n)}{1-r^n} = \frac{\int_0^n(c(t)-b(t))exp[-it]dt+r^n(A-S_n)}{1-r^n}$$

$$Optimal\ Economic\ Life\ =\ Min[EAC(n)]\ =\ Min[\frac{\int_0^n(c(t)-b(t))exp[-it]dt+r^n(A-S_n)}{1-r^n}]\ *\ CRF$$

3. *Replace a fleet of equipment with the same fleet of model (Discrete)*

Work undertaken for the newest N/n equipments (should have the maximum number of available hours in first year) $y_1 * N/n = H_1$

The cost of this will be obtained by considering the average hours used by one truck in its first year

$y_1 * HC_1 = C_1$

The cost for other equipment in subsequent years can be obtained as $C_1, C_2, \ldots, C_n$.

EAC associated with replacement cycle of n year is then

$$Optimal\ Economic\ Life = Min[EAC(n)] = Min[\sum_{i=1}^{n} (C_i - B_i)r^{i-1} + r^n(A - S_n)] * CRF$$

4. *Replace a fleet of equipment with the same fleet of model (Continuous)*

Work undertaken for the newest N/n equipments

$$\int_0^{N/n} y(x)dx = H_1$$

The cost of this will be obtained by considering the average hours used by one truck in its first year

$$\int_0^{H_1/(N/n)} c(t)dt = C_1$$

The cost for other equipment in subsequent years can be obtained as $C_1, C_2, \ldots, C_n$.

EAC associated with replacement cycle of n year is then

$$Optimal\ Economic\ Life = Min[EAC(n)] = Min[\sum_{i=1}^{n} (C_i - B_i)r^{i-1} + r^n(A - S_n)] * CRF$$

5. *Replace single equipment with the technologically advanced model (Discrete)*

$C(T, n) = Cost\ over\ interval\ (0, T) + future\ costs$

$$Optimal\ Economic\ Life = Min[C(T, n)] = Min[\sum_{i=1}^{T} C_{p,i}r^i + r^t(A - S_{p,T}) + (\frac{\sum_{j=1}^{n}(C_{t,j} - B_{t,j})r^j + r^n(A - S_n)}{1 - r^n})r^T]$$

6. *Replace single equipment with the technologically advanced model (Continuous)*

$$Optimal\ Economic\ Life\ =\ C(T,\ n)\ =\ Min[\sum_{i=1}^{T} C_{p,i} r^{i} + r^{t}(A - S_{p,T})\ +\ (\frac{\int_{0}^{n}(c(t)-b(t))exp[-it]dt+r^{n}(A-S_{n})}{1-r^{n}})r^{T}]$$

In summary

Replace with the same equipment model	
Single Equipment	Fleet of equipments
Discrete: $Min[\frac{\sum_{i=1}^{n}(C_{i}-B_{i})r^{i}+r^{n}(A-S_{n})}{1-r^{n}}]\ *\ CRF$ Continuous: $Min[\frac{\int_{0}^{n}(c(t)-b(t))exp[-it]dt+r^{n}(A-S_{n})}{1-r^{n}}]\ *\ CRF$	Discrete: $Min[\sum_{i=1}^{n}(C_{i}-B_{i})r^{i-1}+r^{n}(A-S_{n})]\ *\ CRF$ Where $y_{1}\ *\ HC_{1}=C_{1}$ Continuous: $Min[\sum_{i=1}^{n}(C_{i}-B_{i})r^{i-1}+r^{n}(A-S_{n})]\ *\ CRF$ Where $\int_{0}^{H_{i}/(N/n)} c(t)dt = C_{i}$

Table IM-1: Replace with same equipment model

Replace with technologically advanced equipment (Single Equipment)
Discrete: $Min[\sum_{i=1}^{T} C_{p,i} r^{i} + r^{t}(A - S_{p,T})\ +\ (\frac{\sum_{j=1}^{n}(C_{t,j}-B_{t,j})r^{j}+r^{n}(A-S_{n})}{1-r^{n}})r^{T}]\ *\ CRF$ Continuous: $Min[\sum_{i=1}^{T} C_{p,i} r^{i} + r^{t}(A - S_{p,T})\ +\ (\frac{\int_{0}^{n}(c(t)-b(t))exp[-it]dt+r^{n}(A-S_{n})}{1-r^{n}})r^{T}]\ *\ CRF$

Table IM-2: Replace with technologically advanced equipment

Application (Case Study)

Based on the existing data provided by Kinross, the example falls under the scenario of 'single equipment replacement with discrete cost'.

Assume the following costs and parameters:
Acquisition Cost (A) = $3,824,299, Discount Rate = 0.05

Assume the following O&M cost for the next 10 years in the tables below.

Year	Replacement Interval	MC2%	MC5%	MC7.5%	MC10%	MC25%	Component Replacement Cost	OC	Resale Value[1]
1	Y1	348,990	348,990	348,990	348,990	348,990	0	792765.248	2868224.25
2	Y2	353,622	360,937	367,395	374,211	424,653	171,293	808620.553	2208532.67
3	Y3	358,349	373,512	387,291	402,235	525,538	762,968	824792.964	1744740.81
4	Y4	363,173	386,750	408,802	433,372	660,051	587,093	841288.823	1413240.06
5	Y5	368,095	400,684	432,056	467,969	839,401	212,243	858114.6	1172989.25
6	Y6	373,117	415,352	457,196	506,410	1,078,535	795,518	875276.892	985310.968
7	Y7	378,242	430,791	484,374	549,122	1,397,381	531,443	892782.43	837514.323
8	Y8	383,471	447,044	513,755	596,580	1,822,508	569,625	910638.078	720262.317
9	Y9	388,808	464,151	545,519	649,311	2,389,344	457,003	928850.84	626628.216
10	Y10	394,253	482,159	579,859	707,902	3,145,125	392,843	947427.857	551432.83

Table IM-3: Input Parameters

Year	Replacement Interval	MC2%wInflation	MC10%wInflation	Component Replacement Cost wInflation	OCwInflation
1	Y1	348,990	348,990	0	792,765
2	Y2	360,695	381,695	174,719	824,793
3	Y3	372,827	418,485	793,792	858,115
4	Y4	385,402	459,898	623,028	892,782
5	Y5	398,438	506,544	229,739	928,851
6	Y6	411,951	559,117	878,316	966,376
7	Y7	425,962	618,401	598,491	1,005,418
8	Y8	440,488	685,283	654,320	1,046,037
9	Y9	455,550	760,772	535,452	1,088,297
10	Y10	471,168	846,008	469,484	1,132,264

Table IM-4: Input Parameters Adjusted with 2% Inflation

[1] The resale value from year 1 to year 10, Assume it depreciates around 18% exponentially over the year[10][11][12]

Cost diagrams

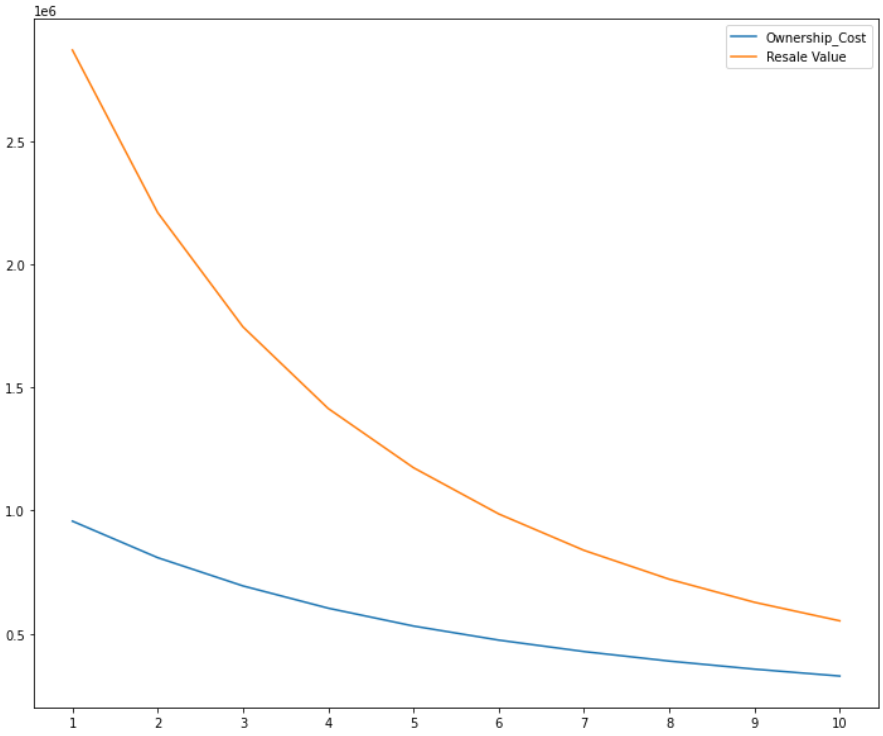

Figure IM-1: Salvage value and ownership cost

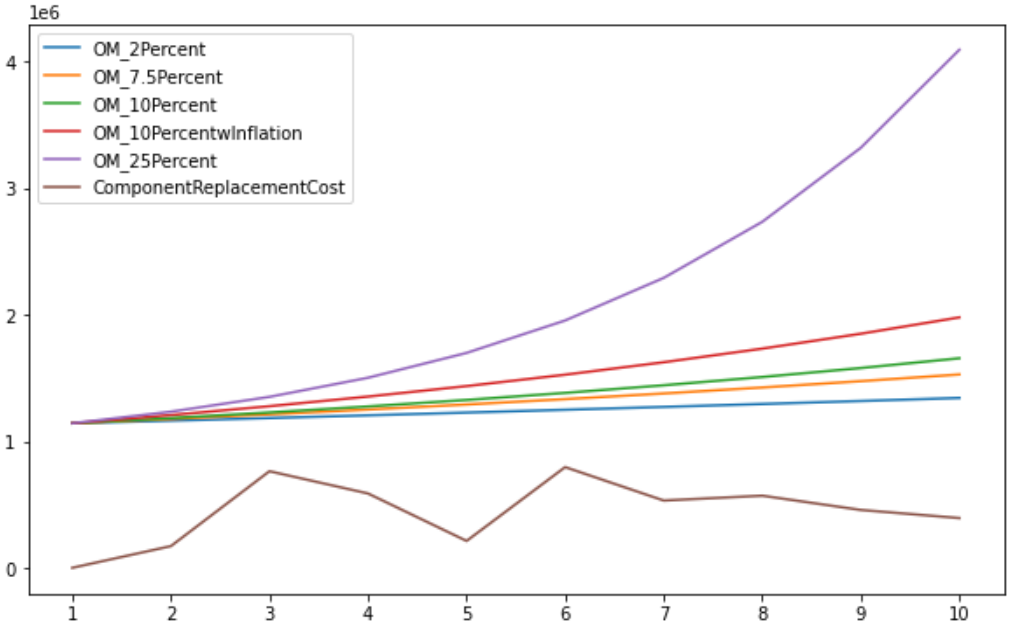

Figure IM-2: Operation and Management Cost

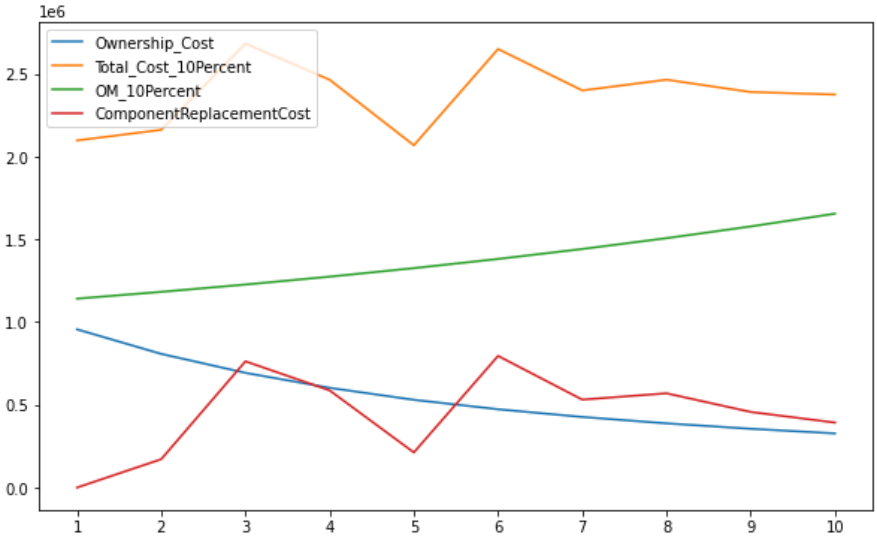

Figure IM-3: Total Cost with no inflation adjustment

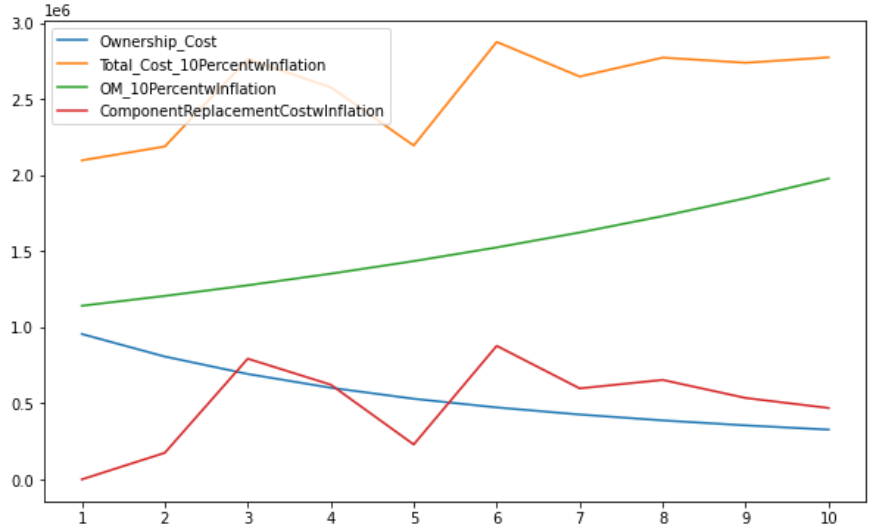

Figure IM-4: Total Cost with inflation adjustment

The client mentioned that the company tends to do over maintenance and hence there is a component replacement cost. The component replacement cost is the sum of costs of all the components that need to be replaced in that year. For example, Engine has an interval of 15,000 hours and that means it needs to be replaced every 3 years assuming the yearly operation time is 5000 hours. Different components have different cost and interval, this part has been explored in the first dataset (Total cost of ownership) in the 'Dataset Preprocessing and Exploration' section. As a result, the total cost of owning the equipment is not the same as for other typical equipment where it is like a convex curve since there is a component replacement cost. In addition, the above charts are for single equipment, the cost maybe more smoothed if the average cost of a fleet of equipment is used.

The total discounted cost is calculated based on the following equation

$$C_1(n) = C_1 r^1 + C_2 r^2 + C_3 r^3 + \ldots + C_n r^n + A r^n - S_n r^n = \sum_{i=1}^{n} C_i r^i + C_n r^n (A - S_n)$$

Without considering the inflation

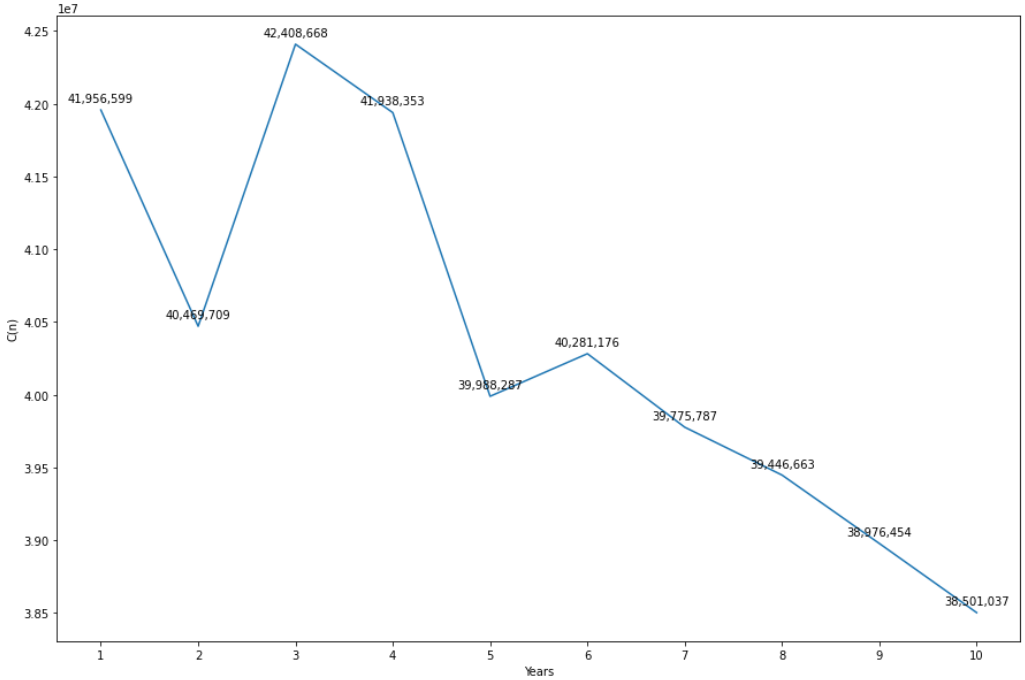

Figure IM-5: Assume a 2% increase in terms of the maintenance cost

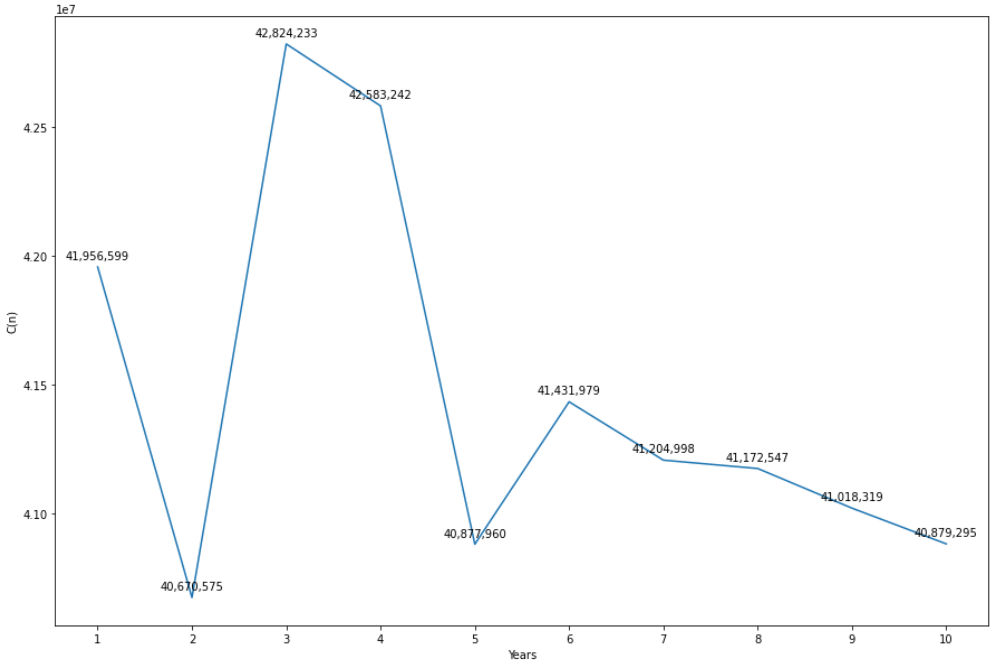

Figure IM-6: Assume a 10% increase in terms of the maintenance cost

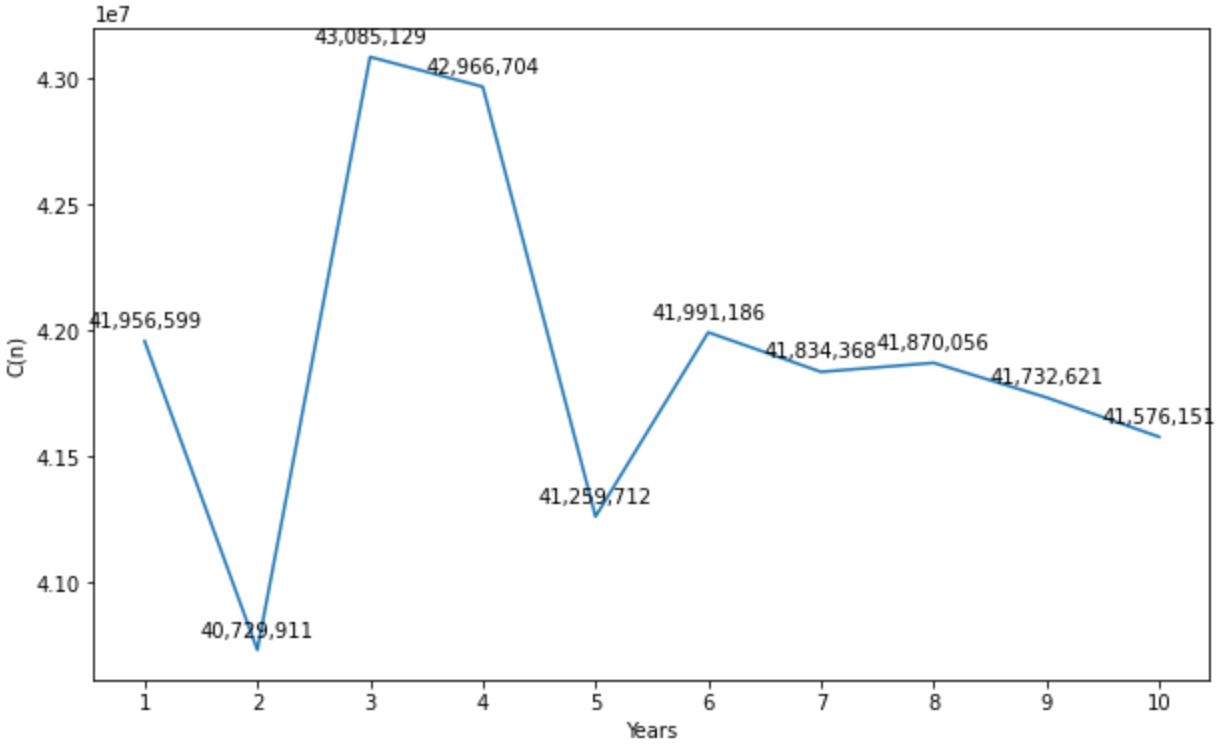

Figure IM-7: Assume a 2% increase in terms of the maintenance cost

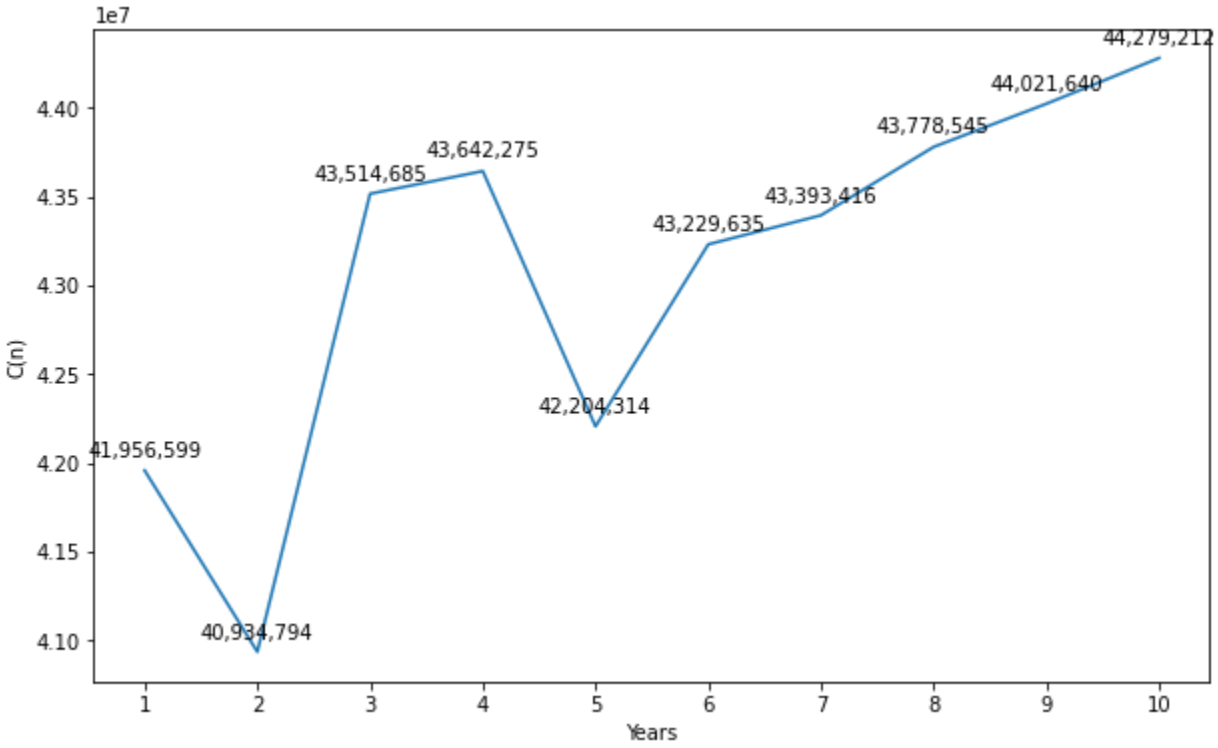

Figure IM-8: Assume a 10% increase in terms of the maintenance cost

Without considering inflation, if the unscheduled MTBF decreases by 2%, there is no need to replace the equipment. However, cost is the lowest at year 2 if 10% decreases in unscheduled maintenance is considered, this is mainly due to a high engine replacement cost at year 3 and time value of money.

Considering the inflation, both scenarios have an optimal replacement time at the end of year 2 for every cycle as the cost is the minimum over an infinite horizon of time. This optimal solution may not be realistic and require further evaluations. The reason is:

- The salvage value is assumed, it might not reflect the actual salvage value. To achieve such cost, the old equipment has to be sold right away at the assumed salvage value as suggested in table IM-3 at every cycle.
- The inflation is considered at 2% each year for all the costs including labor, components, scheduled maintenance, fuel etc., With more accurate inputs, the model may suggest a different result.

2. ***Improvements on the method to calculate the MTBF for equipments in general***

As discussed above in the 'objective and solutioning' section, the second focus is to make the model more general. I decided to tackle the unscheduled MTBF rate to make the model more general. As shown from the sensitivity analysis, with a different % of decrease in terms of the unscheduled MTBF year over year, the replacement decision will be impacted.

Trend Analysis

Starting with the trend analysis, the figure below shows the number of unscheduled broken events over the month. The number of broken events peaked at the end of the year and lowered at the beginning of the year.

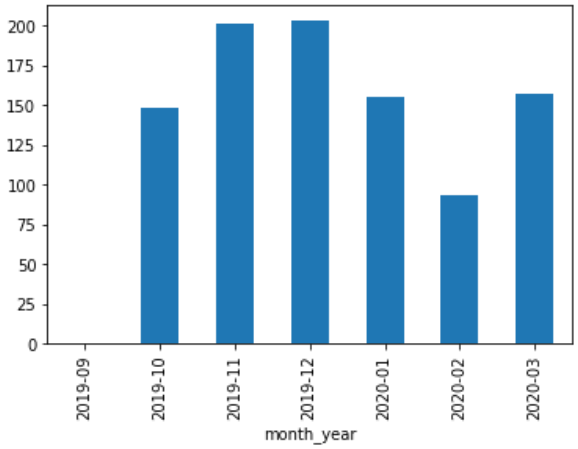

Figure IM-9: Number of unscheduled down events per month

Further breakdown by equipment and calculate the average cumulative hours till breakdown by each machine. The month over month trend of the unscheduled MTBF for each machine looks like the figures below. The ridge regression was applied on top of the bar charts to show the trend.

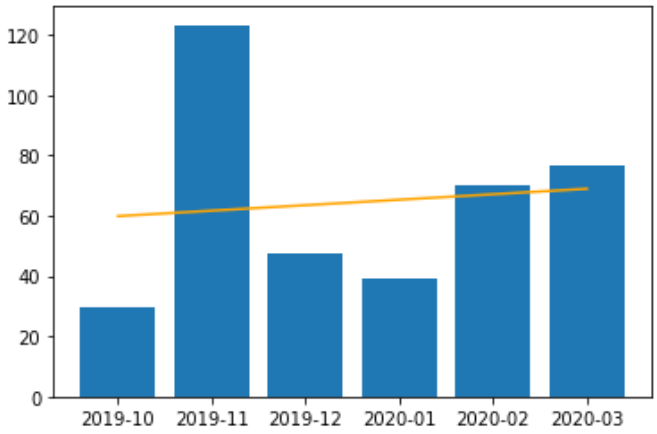

Figure IM-10: Equipment DT-82 Unscheduled MTBF MoM Trend

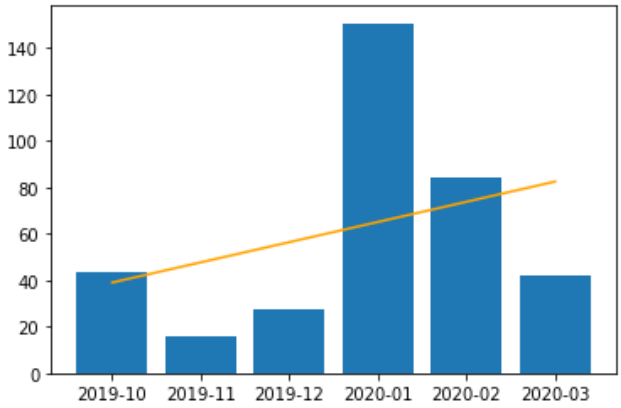

Figure IM-11: Equipment DT-84 Unscheduled MTBF MoM Trend

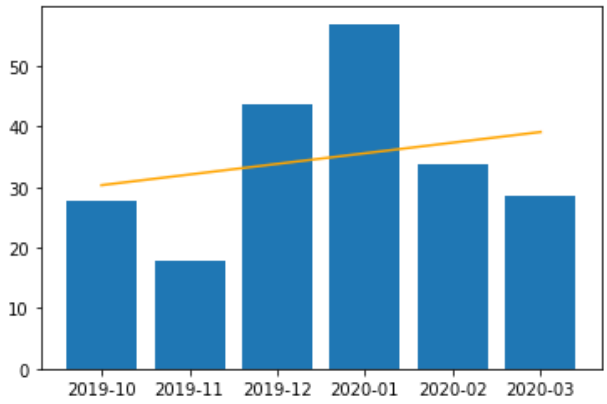

Figure IM-12: Equipment DT-85 MTBF Unscheduled MoM Trend

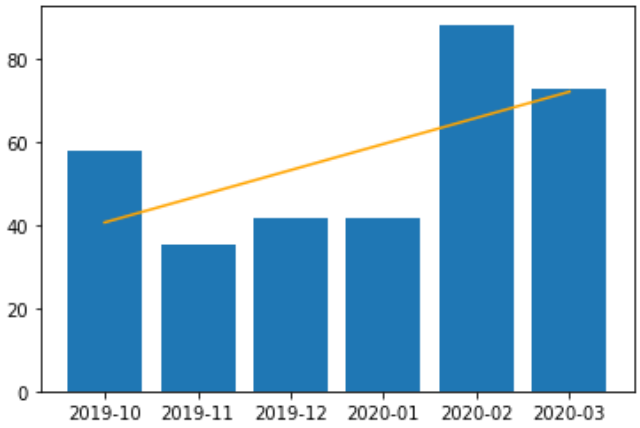

Figure IM-13, Equipment DT-86 Unscheduled MTBF MoM Trend

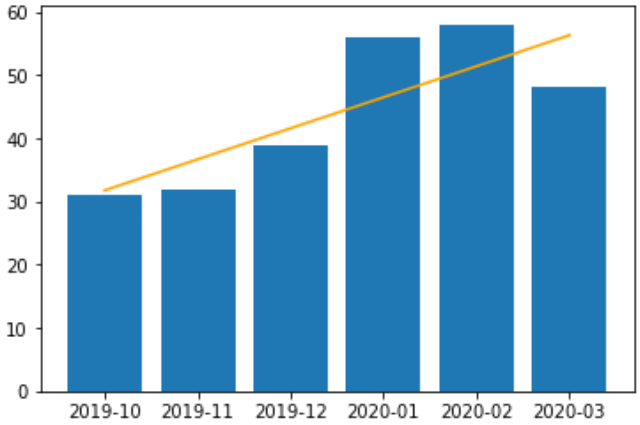

Figure IM-14, Combined Unscheduled MTBF MoM Trend

The time between failure actually has an upward trend which is different than expected. This is most likely due to the limited range of data (only 6 months) . From previous research in the lab, there seems to be a seasonality in terms of the unscheduled MTBF, it usually peaks at the end of the year and lowers after that. This part will be further discussed in the limitation section.

Survival Analysis

Survival analysis is the expected duration of time until one or more events occur. Different models of survival analysis were used in the analysis, one is the Kaplan-Meier Model which is a non-parametric model, the other one is the cox proportional hazard model which is semi-parametric.

Kaplan-Meier Model

The one shown here is the survival curve plotted from the Kaplan-Meier model. The curve illustrates how the survival probabilities change over time. In the first figure below, the x-axis is the total number of service hours. As the service hours increase, the survival probabilities reduce. However, because the data points of total service hours end at around 8700 hours, the probability discontinued and did not go down to 0.

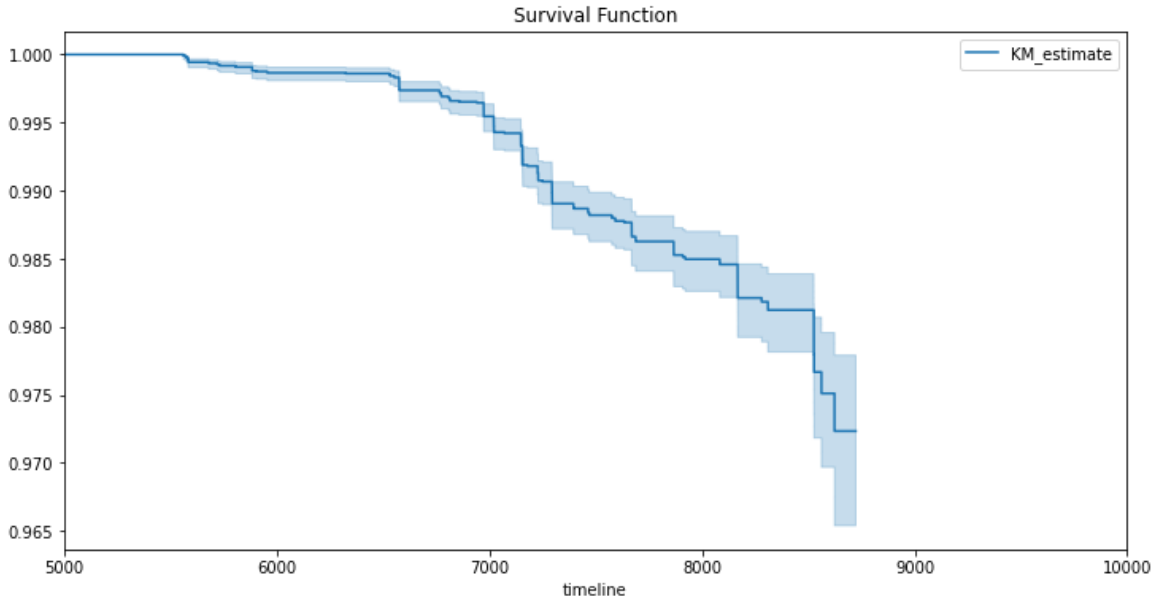

Figure IM-15: Survival Function (Total Service Hours)

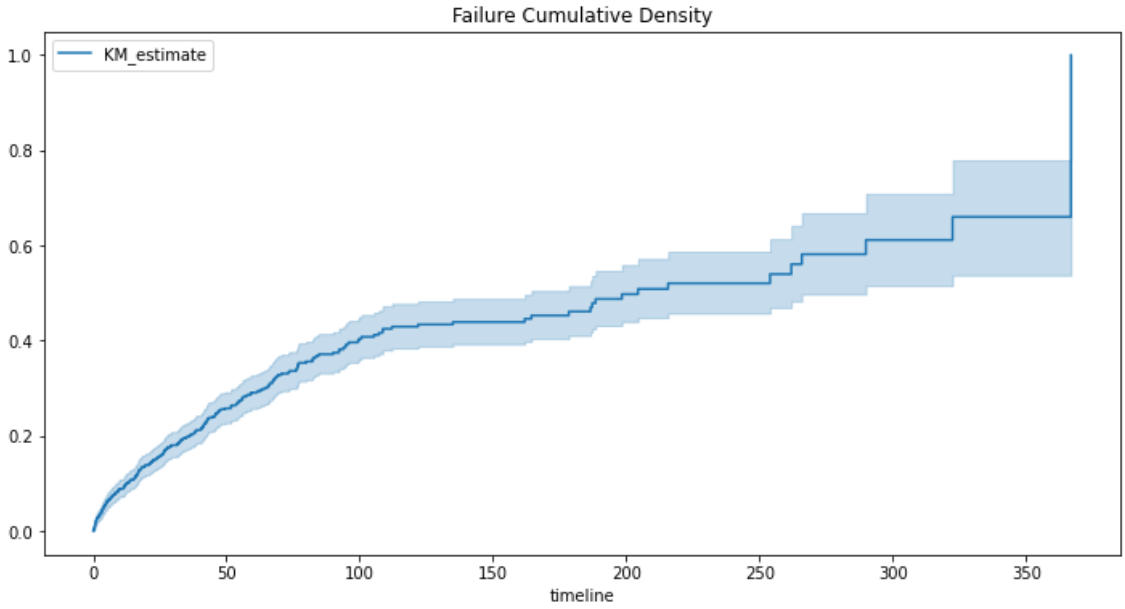

Figure IM-16: Cumulative Failure Function (Cumulative Hours till failure)

Therefore, on the second plot (Figure IM-16), it is the cumulative failure rate by using the cumulative service hours until failure instead of the total service hours. From the graph, at around 350 hours of operation, the probability that the machine breaks down is 1.

There is a greater than 50% probability that the machine will break unscheduled when operated more than 210 hours. This can be used in the previous model to update the maintenance cost. However, it will be great to know the trend of these hours so the number can be updated as the service age increases.

Cox PH Model

The Cox Proportional hazard model is also applied to perform the survival analysis. The first figure (Figure IM-17) shows the coefficients of the variables ranked by the value. The value is also called the hazard ratio, a higher hazard means more at risk of an event occuring. Ignoring the asset feature, it shows that for example, when the engine power derate percentage increases by 1 unit, the baseline hazard of the machine will increase by the exponential value of the coefficient. In contrast, if the pressure increases by 1 unit, the baseline hazard will decrease by exponential value of the coefficient. The second figure (Figure IM-18) shows that the survival varies from equipment to equipment which validates the statement that I made earlier, that different equipment has different unscheduled MTBF.

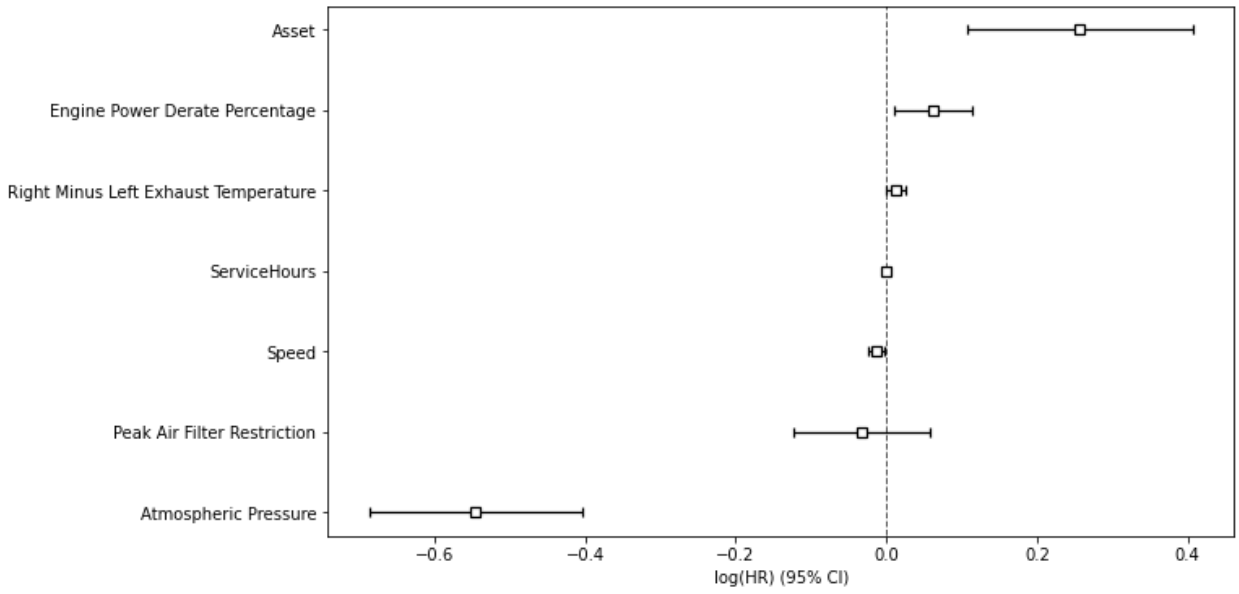

Figure IM-17: Cox PH Coefficients

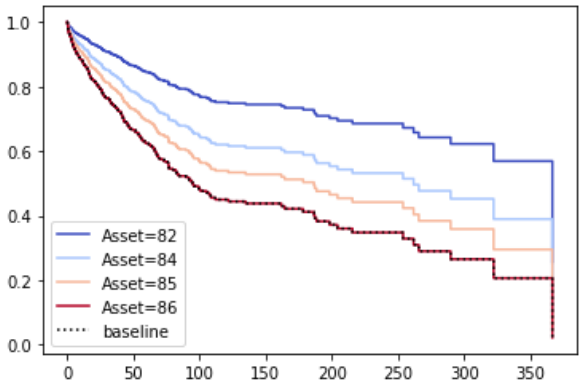

Figure IM-18: Cumulative Failure Function for different equipments

Machine Learning Models to predict the unscheduled down events

Machine learning models were used to predict the downtime based on the features including the sensor data. The idea is if the unscheduled down can be predicted, there might be a better way to calculate and obtain the future unscheduled maintenance cost. The two methods attempted are the LSTM models and XGBoost models.

LSTM Models

In the LSTM method, one equipment - DT82 was used to test out the results. The data splitted to 70% training, 15% validation and 15% test. A simple LSTM model was used to fit the data, it has 42 hidden units and 2 output layers. Initially, The model loss seems satisfactory. However, after plotting out the predicted class with the target. The result is not ideal. It looks like everything is predicted as normal (Figure IM-19 and Figure IM-20). This is mainly because the data is not balanced . After balancing the data using SMOTE, the accuracy goes to 55% after preliminary training (Figure IM-21, Figure IM-22, Figure IM-23, Figure IM-24).

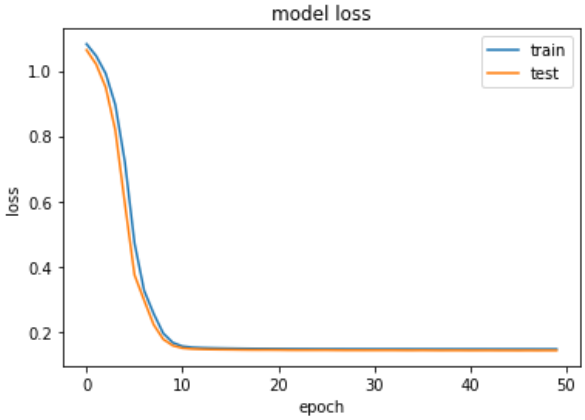

Figure IM-19. LSTM Model Loss before balancing the dataset

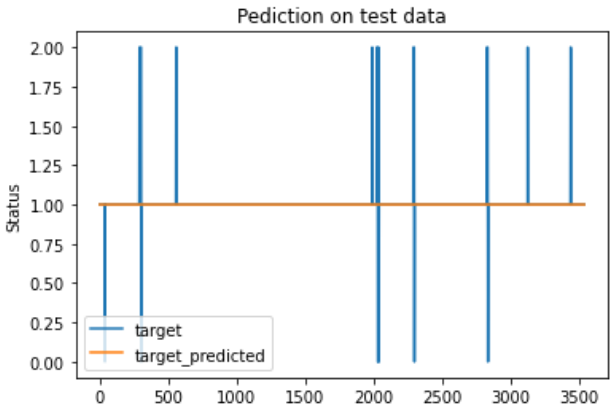

Figure IM-20. LSTM Prediction before balancing the dataset

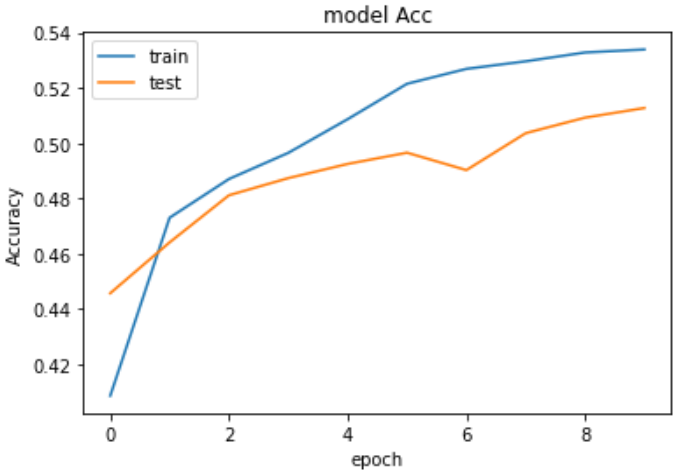

Figure IM-21. LSTM Model Accuracy for balanced data

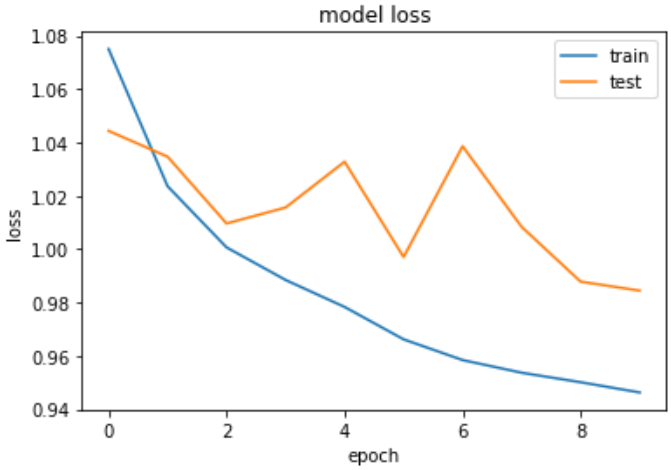

Figure IM-22. LSTM Model loss for balanced data

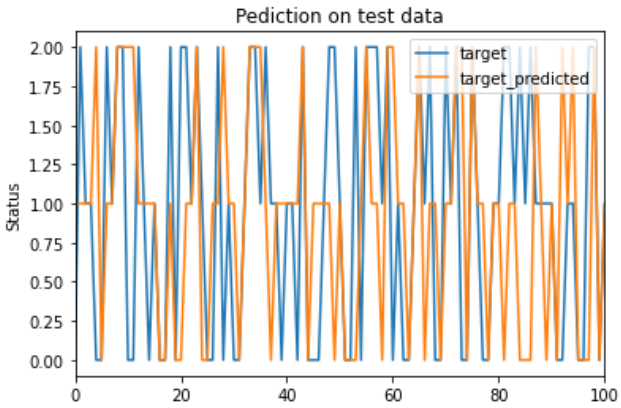

Figure IM-23. LSTM Prediction on balanced data

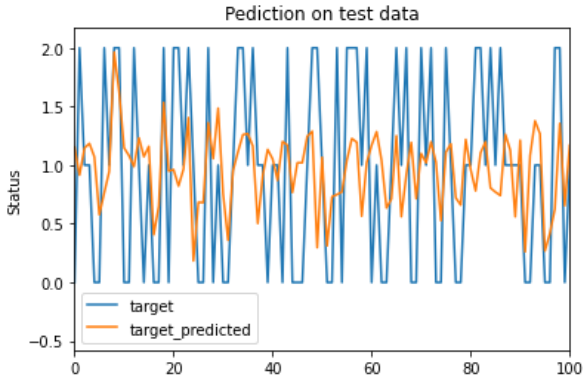

Figure IM-24. LSTM Prediction on balanced data

XGBoost Models

For the XGBoost model, SMOTE was also used to balance the data. Instead of only 1% failure data, 50% of the data are in failure status. The model accuracy is around 83%.

```
Model Report
Accuracy : 0.8348
AUC Score (Balanced): 0.913246
```

Figure IM-25. XGBOOST Model Accuracy

Limitations and Future Directions

Limitations

The purpose of the analysis is not to achieve preventive maintenance or reduce the downtime, rather it is to use the current behavior to find out when it needs to be replaced. Therefore, it is important to know the underlying cost for all types of activity. Many costs

are assumed during the analysis and may not reflect the reality.

For example:

- The salvage value is assumed, it might not reflect the actual salvage value of the equipment. In addition, the company needs to sell the equipment right away so the salvage value can be deducted from the cost.
- The inflation is considered at 2% each year for all the costs including labor, components, scheduled maintenance, fuel etc. With more accurate data on inflation or the cost of different activities and components, the model may suggest a different result.

There are other limitations include:

- Only single equipment data is used
- Discrete cost is only considered at the end of the year, so the decision can be made once a year. It will be great to explore the cost function, so the decision can be made at any time (see below in future directions).
- The date range for the dataset is limited, and hence the trend analysis does not go as expected, the data is not enough to make a conclusion.
- The sensor data is limited, and out of the 4 sensor data, only 2 seems to be useful. (The other 2 sensors are atmospheric pressure and temperature).

Future Directions

- Use cost function and continuous model
- Further exploration on machine learning method to predict the trend and occurrence of unplanned MTBF and determine how to incorporate the result to calculate the maintenance cost
- Consider calculating the total discounted benefits instead of the total discounted cost
- Consider predicting or analyzing the trend for some other adjustable variables.
    - Depreciation rate
    - Production benefits determination
    - Major component interval and the cost
    - Labor cost trend etc.,

Future Data Required

- Fleet cost data instead of single equipment cost data
- Longer sensor data and unscheduled down data (ideally longer than 2 years)
- More sensors in the sensor dataset (More than the 4 we have currently)

Appendix

Cost Associated with Repair and Replacement Decisions

Cost Breakdown

Cost associated with **maintaining and repairing** an equipment	Cost associated with **replacing** an equipment
Planning costs	Planning costs
Cost of repaired parts	Cost of the new unit (Capital cost includes taxes, duties and freight)
Transportation cost to the repair site and back to the mining site (equipments or the whole truck)	Shipping and transportation cost to the site
Operational downtime costs	Setup and assembly cost
Potential environmental cost (Fuel etc.,)	Inspection costs when first acquire a large equipment
Potential operating performance cost[2]	Interest cost
Depreciation	Potential training cost
Cost of labor and operation	Cost of labor and operation

Cost Comparison (✓ represents this method incurs a higher cost)

Cost Type	**Maintaining and repairing** the equipment	**Replacing the equipment**
Planning Costs		✓
Cost of the new unit or component		✓
Transportation cost	Depends	Depends
Operational downtime	✓	
Set up and assembly		✓
Environmental cost	✓	
Operating performance cost	✓	

[2] Assume the replaced equipment will have a better energy saving and performance, the environmental and operating performance cost here is the surplus compare to replace an asset

Interests costs		✓
Depreciation rate	✓	
Training cost	✓	
Cost of labor	✓	

Additional example from the current method

Repair Equipment

		Y1 2022	Y2 2023	Y3 2024	Y4 2025	Y5 2026	Y6 2027	Y7 2028	Y8 2029	Y9 2030	Y10 2031
Current Book Value		1,900,000									
Cash Flow		(1,141,755)	(1,324,995)	(1,929,246)	(1,766,608)	(1,405,692)	(2,003,635)	(1,755,000)	(1,809,434)	(1,713,919)	(1,667,767)
Depreciation		(190,000)	(190,000)	(190,000)	(190,000)	(190,000)	(190,000)	(190,000)	(190,000)	(190,000)	(190,000)
Before Tax Cash Flow		(1,331,755)	(1,514,995)	(2,119,246)	(1,956,608)	(1,595,692)	(2,193,635)	(1,945,000)	(1,999,434)	(1,903,919)	(1,857,767)
Federal Tax Credit @	15%	199,763	227,249	317,887	293,491	239,354	329,045	291,750	299,915	285,588	278,665
Add Back Depreciation		190,000	190,000	190,000	190,000	190,000	190,000	190,000	190,000	190,000	190,000
After Tax Cash Flow		(941,992)	(1,097,746)	(1,611,359)	(1,473,117)	(1,166,339)	(1,674,590)	(1,463,250)	(1,509,519)	(1,428,332)	(1,389,102)
Present Value Factor		100%	95%	91%	86%	82%	78%	75%	71%	68%	64%
NPV of cash flow		(941,992)	(1,045,472)	(1,461,550)	(1,272,534)	(959,550)	(1,312,085)	(1,091,899)	(1,072,787)	(966,751)	(895,428)
Cumulative NPV		(941,992)	(1,987,464)	(3,449,014)	(4,721,548)	(5,681,098)	(6,993,183)	(8,085,082)	(9,157,869)	(10,124,620)	(11,020,048)
Total Net Present Value		(11,020,048)									

Replace Equipment

		Y1 2022	Y2 2023	Y3 2024	Y4 2025	Y5 2026	Y6 2027	Y7 2028	Y8 2029	Y9 2030	Y10 2031
Capital Cost		(3,824,299)									
Salvage Value-Repair Unit Book Value		(20,822)									
Cash Flow		(571,755)	(759,081)	(1,366,655)	(1,206,552)	(847,353)	(1,446,166)	(1,197,520)	(1,251,030)	(1,153,641)	(1,104,625)
Depreciation		(382,430)	(382,430)	(382,430)	(382,430)	(382,430)	(382,430)	(382,430)	(382,430)	(382,430)	(382,430)
Before Tax Cash Flow		(954,185)	(1,141,511)	(1,749,085)	(1,588,982)	(1,229,783)	(1,828,595)	(1,579,950)	(1,633,460)	(1,536,071)	(1,487,055)
Federal Tax Credit @	15%	143,128	171,227	262,363	238,347	184,467	274,289	236,993	245,019	230,411	223,058
Add Back Depreciation		382,430	382,430	382,430	382,430	382,430	382,430	382,430	382,430	382,430	382,430
After Tax Cash Flow		(428,627)	(587,854)	(1,104,292)	(968,204)	(662,886)	(1,171,876)	(960,528)	(1,006,011)	(923,230)	(881,566)
Present Value Factor		100%	95%	91%	86%	82%	78%	75%	71%	68%	64%
NPV of cash flow		(428,627)	(559,861)	(1,001,625)	(836,371)	(545,358)	(918,196)	(716,760)	(714,953)	(624,879)	(568,266)
Cumulative NPV		(4,252,927)	(4,812,788)	(5,814,413)	(6,650,784)	(7,196,142)	(8,114,338)	(8,831,098)	(9,546,052)	(10,170,930)	(10,739,196)
Total Net Present Value		(10,760,018)									

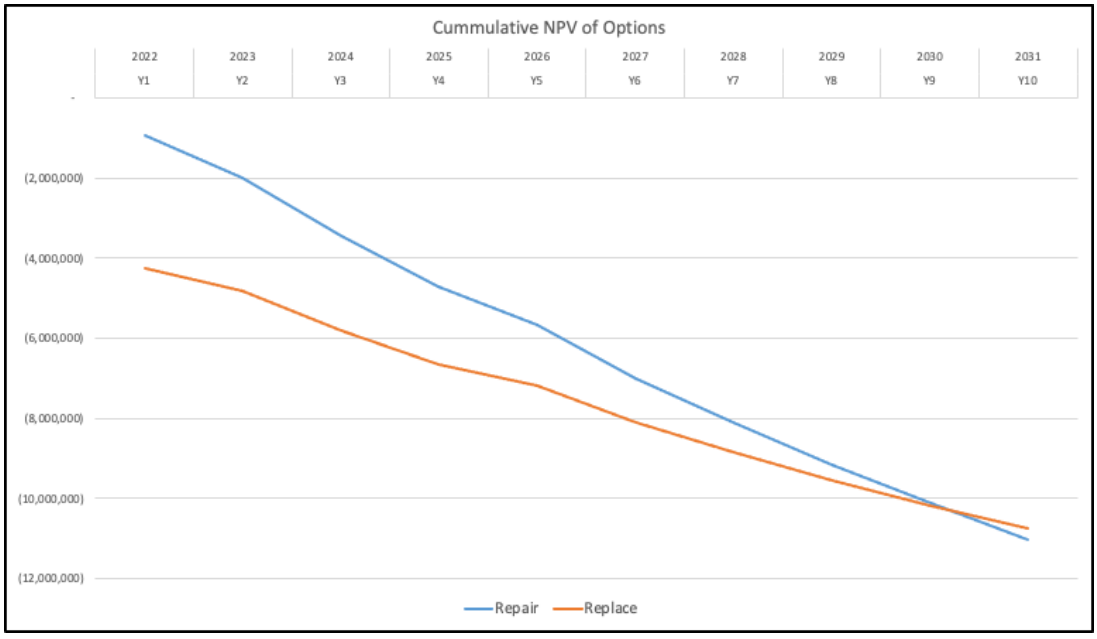

	2022	2023	2024	2025	2026	2027	2028	2029	2030	2031
	Y1	Y2	Y3	Y4	Y5	Y6	Y7	Y8	Y9	Y10
Repair	(941,992)	(1,987,464)	(3,449,014)	(4,721,548)	(5,681,098)	(6,993,183)	(8,085,082)	(9,157,869)	(10,124,620)	(11,020,048)
Replace	(4,252,927)	(4,812,788)	(5,814,413)	(6,650,784)	(7,196,142)	(8,114,338)	(8,831,098)	(9,546,052)	(10,170,930)	(10,739,196)

Code

Sean He - MEng Project.ipynb

Presentation

Sean He - Progress Meeting - Economic Asset Replacement Problem.pptx
Sean He - Progress Meeting 2 - Economic Asset Replacement Problem.pptx
Sean He - Semi-Annual Progress Meeting - Economic Asset Replacement Problem.pptx

Spreadsheets (including data used for code)

Mobile Equipment Repair - Example Demonstration.xlsx

Data used to run the code (in order of when it gets used)
Component_Data.xlsx
MC_OC_Resale_Data.xlsx
Kinross_Sensor_Data_Sample.xlsx
Unscheduled_Down_Data.xlsx
sensor_df_pviot_wIndicator_DT82.csv
sensor_df_pviot_wIndicator_DT84.csv
sensor_df_pviot_wIndicator_DT85.csv
sensor_df_pviot_wIndicator_DT86.csv

Reference

[1] Person. “Implementing Effective Maintenance Strategies for Long Term Production Goals.” Mining Global, 17 May 2020, https://miningglobal.com/supply-chain-and-operations/implementing-effective-maintenance-strategies-long-term-production-goals.
[2] Caron, P. (2021, April 7). 5 Benefits of Better Asset Management in the Mining Industry. Caron Business Solutions. https://www.caronbusiness.com/mining-suite/better-asset-management-mining-industry/
[3] Kinross. (2022). Kinross. http://kinross.com/
[4] Hastings, N. A. J. (2021). Physical Asset Management: With an Introduction to the ISO 55000 Series of Standards (3rd ed.). Springer.
[5]Construction Business Owner Magazine. (2020, February 18). Understanding the Soft Benefits of Replacing Older Equipment. https://www.constructionbusinessowner.com/understanding-soft-benefits-replacing-older-equipment
[6] Cesca, I.G. and Novaes, D.D. (2012). Physical assets replacement: an analytical approach. arXiv preprint arXiv: 1210.3678
[7] Elizna Theron (2016): An integrated framework for the management of strategic physical asset repair/replace decisions
[8] Jardine, & Tsang, A. H. C. (2013). Maintenance, Replacement, and Reliability: Theory and Applications, Second Edition. CRC Press. https://doi.org/10.1201/b14937
[9] Theodore, B. (2020, October 30). CAT 793D Dump Truck Review & Full Specs. Iseekplant. https://blog.iseekplant.com.au/blog/caterpillar-793d-dump-truck-review-specs
[10] BEA GOV. “Table A.—BEA Depreciation Rates, Service Lives, and Declining-Balances Rates” (Accessed 2022, April 12) https://apps.bea.gov/scb/account_articles/national/0597niw/tablea.htm
[11] BMT (2019, Nov 20), Energy policy uncertainty sparks debate on ‘the need for more investment’’ https://www.bmtqs.com.au/bmt-insider/depreciation-for-mining-equipment/
[12] Stats Canada, (2015, Nov 27), Table C.1-7
List of depreciation rates under the new asset code classification — Other machinery and equipment (continued), oil and gas exploration, mining exploration, research and development, and software https://www150.statcan.gc.ca/n1/pub/15-206-x/2015039/t/tblc17-eng.htm